

AD-A279 934



①

**NAVAL POSTGRADUATE SCHOOL
Monterey, California**



THESIS

**DTIC
ELECTE
JUN 07 1994**
S G D

94-16925



13508

**ACOUSTIC POSITIONING OF THE NPS
AUTONOMOUS UNDERWATER VEHICLE (AUV II)
DURING HOVER CONDITIONS**

by

Kevin A. Torsiello

DTIC QUALITY INSPECTED 2

March 1994

Thesis Advisor:

Anthony J. Healey

Approved for public release; distribution is unlimited

94 6 6 041

REPORT DOCUMENTATION PAGE

1a. REPORT SECURITY CLASSIFICATION UNCLASSIFIED		1b. RESTRICTIVE MARKINGS	
2a. SECURITY CLASSIFICATION AUTHORITY		3. DISTRIBUTION /AVAILABILITY OF REPORT Approved for public release; distribution is unlimited	
2b. DECLASSIFICATION/DOWNGRADING SCHEDULE			
4. PERFORMING ORGANIZATION REPORT NUMBER(S)		5. MONITORING ORGANIZATION REPORT NUMBER(S)	
6a. NAME OF PERFORMING ORGANIZATION Naval Postgraduate School	6b. OFFICE SYMBOL (If applicable) 34	7a. NAME OF MONITORING ORGANIZATION Naval Postgraduate School	
6c. ADDRESS (City, State, and ZIP Code) Monterey, CA 93943-5000		7b. ADDRESS (City, State, and ZIP Code) Monterey, CA 93943-5000	
8a. NAME OF FUNDING/SPONSORING ORGANIZATION	8b. OFFICE SYMBOL (If applicable)	9. PROCUREMENT INSTRUMENT IDENTIFICATION NUMBER	
8c. ADDRESS (City, State, and ZIP Code)		10. SOURCE OF FUNDING NUMBERS	
		PROGRAM ELEMENT NO	PROJECT NO
		TASK NO	WORK UNIT ACCESSION NO.
11. TITLE (Include Security Classification) ACOUSTIC POSITIONING OF THE NPS AUTONOMOUS UNDERWATER VEHICLE (AUV II) DURING HOVER CONDITIONS, UNCLASSIFIED			
12. PERSONAL AUTHOR(S) Kevin A. Torsiello			
13a. TYPE OF REPORT Engineer's Thesis	13b. TIME COVERED FROM 3/93 TO 3/94	14. DATE OF REPORT (Year, Month, Day) 1994 March	15. PAGE COUNT 131
16. SUPPLEMENTARY NOTATION The views expressed in this thesis are those of the author and do not reflect the official policy or position of the Department of Defense or the U.S. Government.			
17. COSATI CODES		18. SUBJECT TERMS (Continue on reverse if necessary and identify by block number)	
FIELD	GROUP	SUB-GROUP	
		Autonomous Underwater Vehicle, Acoustic Dynamic Positioning, Marine Vehicle Dynamics, Proportional Derivative Control	
19. ABSTRACT (Continue on reverse if necessary and identify by block number)			
<p>The ability to take position, in a dynamic environment, relative to a local stationary object, is vital to many planned missions for the Naval Postgraduate School's Autonomous Underwater Vehicle (AUV II) project, such as bottom surveying and mine hunting. The AUV II can achieve this ability through the use of its sensors along with stern propulsion motors and tunnel thrusters.</p> <p>The sensors employed by the AUV II include a free directional gyro and independent self-sonar which provide acoustic positioning data without the aid of a transponder net.</p> <p>Described in this thesis are the details of the internal subsystems of the AUV II, and an examination of its positioning ability through the analysis of maneuvering experiments. Commanded motions of yaw, lateral and longitudinal positioning during hover conditions are studied.</p>			
20. DISTRIBUTION/AVAILABILITY OF ABSTRACT <input checked="" type="checkbox"/> UNCLASSIFIED/UNLIMITED <input type="checkbox"/> SAME AS RPT. <input type="checkbox"/> DTIC USERS		21. ABSTRACT SECURITY CLASSIFICATION Unclassified	
22a. NAME OF RESPONSIBLE INDIVIDUAL Anthony J. Healey		22b. TELEPHONE (Include Area Code) 408-656-3381	22c. OFFICE SYMBOL ME/HY

Approved for public release; distribution is unlimited

**ACOUSTIC POSITIONING OF THE NPS
AUTONOMOUS UNDERWATER VEHICLE (AUV II)
DURING HOVER CONDITIONS**

by

**Kevin A. Torsiello
Lieutenant, United States Navy
B. S., University of Connecticut, 1983**

Submitted in partial fulfillment of the
requirements for the degrees of

**MASTER OF SCIENCE IN MECHANICAL ENGINEERING
and
MECHANICAL ENGINEER**

from the

NAVAL POSTGRADUATE SCHOOL

March, 1994

Author:



Kevin A. Torsiello

Approved by:



Anthony J. Healey, Thesis Advisor



**Matthew D. Kelleher, Chairman,
Department of Mechanical Engineering**



**Richard S. Elster
Dean of Instruction**

ABSTRACT

The ability to take position, in a dynamic environment, relative to a local stationary object, is vital to many planned missions for the Naval Postgraduate School's Autonomous Underwater Vehicle (AUV II) project, such as bottom surveying and mine hunting. The AUV II can achieve this ability through the use of its sensors, along with stern propulsion motors and tunnel thrusters.

The sensors employed by the AUV II include a free directional gyro and independent self-sonar which provide acoustic positioning data without the aid of a transponder net.

Described in this thesis are the details of the internal subsystems of the AUV II, and an examination of its positioning ability through the analysis of maneuvering experiments. Commanded motions of yaw, lateral and longitudinal positioning during hover conditions are studied.

Accession For	
NTIS CRA&I	<input checked="" type="checkbox"/>
DTIC TAB	<input type="checkbox"/>
Unannounced	<input type="checkbox"/>
Justification	
By	
Distribution /	
Availability Codes	
Dist	Avail and/or Special
A-1	

TABLE OF CONTENTS

I. INTRODUCTION	1
A. BACKGROUND	1
B. SCOPE OF THESIS.....	2
II. AUV II CONFIGURATION	4
A. SENSORS	7
1. Environment Sensors (Sonar Equipment)	7
a. Profiling Sonar (Tritech ST-1000).....	9
b. Scanning Sonar (Tritech ST-725)	10
c. Depth Sonar (Datasonics PSA-900).....	10
2. Vehicle Sensors	10
a. Gyroscopes.....	11
b. Depth Cell (PSI-Tronix).....	12
c. Vehicle Speed Sensor (Turbo-Probe).....	13
d. Motor RPM Indicator (Hewlett-Packard)	13
B. GESPAC M68020/30 COMPUTER SYSTEM.....	14
1. GESMPU-20 Micro Processor Unit	15
2. GESMFI-1 Multi-Function Interface.....	15
3. GESSIO-1B Serial Input/Output	16
4. GESPIA-3A Peripheral Interface Adapter.....	16
5. GESADA-1 AND GESADA-2 Analog/Digital Interfaces.....	16
6. GESDAC-2B Digital/Analog Converter.....	17
7. GESTIM-1A Multiple Timer Modules	17
C. PROPULSION/MANEUVERING EQUIPMENT.....	17

1. Control Surfaces	18
2. Stern Propulsion.....	18
3. Thrusters.....	19
D. ELECTRICAL POWER EQUIPMENT.....	20
1. 24 Volt Battery Packs (Panasonic).....	21
2. ACON Power Supplies.....	21
3. Calnex Power Supplies.....	22
4. CRYDOM Relays	22
5. Servo Amplifiers (Advanced Motion Controls).....	23
6. Synchro to Digital (S/D) Converter	23
7. Inverter (Motor Inhibitor).....	23
III. EXPERIMENTAL APPARATUS AND PROCEDURE.....	24
A. EQUIPMENT PREPARATION	24
1. AUV II Vehicle	24
2. Lab and Test Facility.....	25
3. Computer Software.....	26
B. EXPERIMENTAL APPARATUS.....	26
C. EXPERIMENTAL PROCEDURE	31
1. Rate Gyro Calibration.....	31
2. Yaw Positioning Experiment.....	37
3. Lateral Positioning Experiment.....	40
4. Longitudinal Positioning Experiment.....	42
IV. EXPERIMENTAL RESULTS.....	47
A. YAW POSITIONING EXPERIMENT.....	47
B. LATERAL POSITIONING EXPERIMENT	53

C.	LONGITUDINAL POSITIONING EXPERIMENT.....	61
D.	THEORETICAL MODEL	72
1.	Theoretical Model Development.....	72
2.	Estimation of the Hydrodynamic Coefficients.....	75
3.	Theoretical Model Results	78
V.	SUMMARY.....	83
A.	CONCLUSIONS.....	83
B.	RECOMMENDATIONS FOR FURTHER STUDY.....	85
APPENDIX A	AUV II CONFIGURATION BLOCK DIAGRAM	87
APPENDIX B	AUV II WIRING LIST.....	89
APPENDIX C	CENTER OF GRAVITY CALCULATION.....	103
APPENDIX D	CENTER OF BUOYANCY CALCULATION.....	105
APPENDIX E	FREE GYRO/SYNCHRO BOARD WIRING DIAGRAM	107
APPENDIX F	KALMAN FILTER SUBPROGRAM	109
APPENDIX G	AUV SIMULATION MODEL	112
	LIST OF REFERENCES.....	116
	INITIAL DISTRIBUTION LIST.....	117

LIST OF TABLES

TABLE 3.1	YAW RATE CALIBRATION: SCALE AND BIAS FACTORS.....	39
TABLE 3.2	LATERAL AND LONGITUDINAL POSITIONING EXPERIMENTS: TEST CONDITIONS.....	43
TABLE 4.1	AUV MODEL: SYMBOLS AND VARIABLES	73
TABLE 4.2	AUV II HYDRODYNAMIC COEFFICIENTS: HOVER CONDITIONS.....	77

LIST OF FIGURES

Figure 2.1	AUV II.....	5
Figure 2.2	AUV II Configuration.....	6
Figure 2.3	Sensor Location (Nosepiece Section).....	8
Figure 3.1	Experimental Set-up.....	27
Figure 3.2	AUV II and Test Tank.....	29
Figure 3.3	AUV II and PC Workstation.....	30
Figure 3.4	Right-Hand Global and Body Fixed Coordinate Systems.....	32
Figure 3.5	Yaw Rate Calibration/Yaw Positioning Experiment.....	34
Figure 3.6	Yaw Rate Calibration: 180 Degree Test (3 Trials).....	36
Figure 3.7	Yaw Rate Calibration: 30 Degree Test.....	38
Figure 3.8	Lateral Positioning Experiment.....	41
Figure 3.9	Longitudinal Positioning Experiment.....	44
Figure 4.1	Yaw Position Experiment: 90 Degree Test.....	49
Figure 4.2	Yaw Position Experiment: 90, 180, 360 Degree Tests.....	50
Figure 4.3	Yaw Position Experiment: 360 Degree Test, with Disturbances.....	52
Figure 4.4	Lateral Position Experiment: Test 1.....	54
Figure 4.5	Lateral Position Experiment: Test 1 (Thruster Voltage/Yaw Position).....	55
Figure 4.6	Lateral Position Experiment: Test 2.....	57
Figure 4.7	Lateral Position Experiment: Test 3.....	58
Figure 4.8	Lateral Position Experiment: Test 4.....	59

Figure 4.9	Lateral Position Experiment: Test 5.....	60
Figure 4.10	Longitudinal Position Experiment: Test 1	62
Figure 4.10	Longitudinal Position Experiment: Test 1 (continued).....	63
Figure 4.11	Longitudinal Position Experiment: Test 2	65
Figure 4.12	Longitudinal Position Experiment: Test 3	66
Figure 4.13	Longitudinal Position Experiment: Test 4	67
Figure 4.14	Longitudinal Position Experiment: Test 5	68
Figure 4.15	Longitudinal Position Experiment: Test 6	69
Figure 4.16	Longitudinal Position Experiment: Test 7	71
Figure 4.17	AUV Model: Yaw Position Experiment.....	79
Figure 4.18	AUV Model: Lateral Position Experiment (Test 3).....	80
Figure 4.19	AUV Model: Longitudinal Position Experiment (Test 7).....	82

ACKNOWLEDGMENTS

I would like to express my most sincere gratitude to the following people:

LCDR Craig Bateman, Lcdr Mary Zurowski, LT Barb Shea and CPT Pat Kanewski, for among many things, your friendship and help with preparing the lab and test facility.

LCDR Dave Gordon, for your help with the word processing.

Charles Crow, Jim Selby, Mardo Blanco, Tom McCord and Glenda Coleman, Mechanical Engineering Department, Naval Postgraduate School, for your outstanding technical skills and material assistance.

Jim Scofield and Tom Christian, Mechanical Engineering Department, Naval Postgraduate School, for your expertise and many hours of dedication to this project.

Dr. Anthony Healey, my thesis advisor, and Dave Marco, Mechanical Engineering Department, Naval Postgraduate School, for your patience, time, inspiration, friendship and generous assistance in helping me complete this thesis.

The Naval Postgraduate School, Direct Research Fund, for the financial support of this project.

Prof. Charles N. Calvano, CAPT, USN (Ret), Walter A. Ericson, CAPT, USN (Ret), Richard E. Pearsall, CAPT, USN (Ret) and David E. Woodbury, CAPT, USN (Ret), for your help and guidance, and to the United States Navy,

especially the Engineering Duty Community, for providing me with this, among many career opportunities.

And most importantly, to my parents, for a lifetime of support and encouragement.

Thank you. Thank you very much.



I. INTRODUCTION

This chapter provides a discussion of the background information and outlines of the scope of study for this thesis.

A. BACKGROUND

The applications of Remotely Operated Vehicles (ROVs) and Autonomous Underwater Vehicles (AUVs) are subjects of increasing widespread interest by both civilian and military organizations.

The operation of ROVs is traditionally accomplished by the use of a physical tether, through which electrical power, control and sensory data are transferred between the vehicle and a surface ship. An ROV therefore, is under the continuous control of a human operator (pilot), and is dependent on and tethered to the host platform.

An AUV on the contrary, operates independently of any physical or electrical tether, and requires little to no intervention from an outside activity. This level of autonomous operation permits a greater scope of mission capabilities, and as such, is the subject of numerous research projects encompassed in the Autonomous Underwater Vehicle project at the Naval Postgraduate School, in Monterey, California, at the Monterey Bay Aquarium Research Institute, MIT Sea Grant, Charles Stark Drake Laboratories, Woods Hole Oceanographic Institute, Florida Atlantic University and the Naval Undersea Warfare Center, Newport, Rhode Island, amongst others.

Future missions planned for the AUV project include environmental surveying, search and mine hunting missions. Vital to the accomplishment of these types of missions, is the capability for the vehicle to position itself in the vicinity of a stationary object or change its position with respect to an object, within a dynamic environment.

The ability to accurately maneuver itself, at relatively high speeds, within a confined environment, has been demonstrated by the second generation design of the NPS AUV (AUV II) (Warner, 1991). The ability to achieve accurate dynamic positioning, during hover conditions, based on the vehicle's own acoustic data input, has been made possible, only recently, through several configuration changes to the AUV II. These configuration changes include the addition of a high frequency profiling self-sonar, and horizontal and vertical tunnel thrusters.

The profiling sonar installed in the AUV II, provides acoustic environmental and positioning data without the use of external signals or transponder networks. The performance of the sonar has been tested and verified by previous experimentation (Ingold, 1991).

The design and performance testing of the tunnel thrusters have been verified and documented by Good (1989), Cody (1992) and Brown (1993).

B. SCOPE OF THESIS

The objective of this thesis is to experimentally examine the capability of the NPS AUV II to achieve accurate acoustic positioning, during hover conditions. It is the contention of this work that both lateral and longitudinal

position of the vehicle can be maintained using high frequency onboard sonar returns without the use of a transponder net. Furthermore, that without ocean current disturbances, the precision of the positioning is limited only by the precision of the sonar and the threshold of operation of the propulsors, and stable motion is achievable.

Chapter II provides documentation of the major design and configuration changes incorporated into the AUV, which provide the capability for the vehicle to accomplish the hover positioning experiments.

Chapter III includes a description of the test facility, laboratory and equipment set-up used for the experiments. The procedures for the positioning experiments are also discussed.

The results of the positioning experiments are provided in Chapter IV, along with the development of a theoretical model and its comparison to the experimental data.

A summary of conclusions and recommendations for further study is discussed in Chapter V.

II. AUV II CONFIGURATION

Since the time of its original design (Good, 1989) and successful waterborne demonstration (Warner, 1991), several design and configuration concepts have been the subject of research surrounding the AUV project at NPS, resulting in numerous published theses. The result thus far has produced the current configuration of the AUV II, pictured in Figure 2.1.

This chapter provides a description of the major equipment groups which comprise the current configuration of the AUV. Each section discusses the nominal operating characteristics and ratings as applicable, and refers to figures within the text, or diagrams and the wiring list which are included in the appendices. The following equipment groups are discussed:

1. Sensors (Environment and Vehicle).
2. GESPAC M68020/30 Computer System.
3. Propulsion and Maneuvering Equipment.
4. Electrical Power Equipment.

A simplified block diagram of these major equipment groups is provided in Appendix A. This diagram shows the basic system power paths and the computer data transfer paths between the components.

The wiring list for the AUV II is provided in Appendix B.

Figure 2.2 shows the placement of the major equipment components in the AUV. As discussed in Good (1989), the propulsion and maneuvering equipment (control fins, tunnel thrusters and stern propulsion motors) is

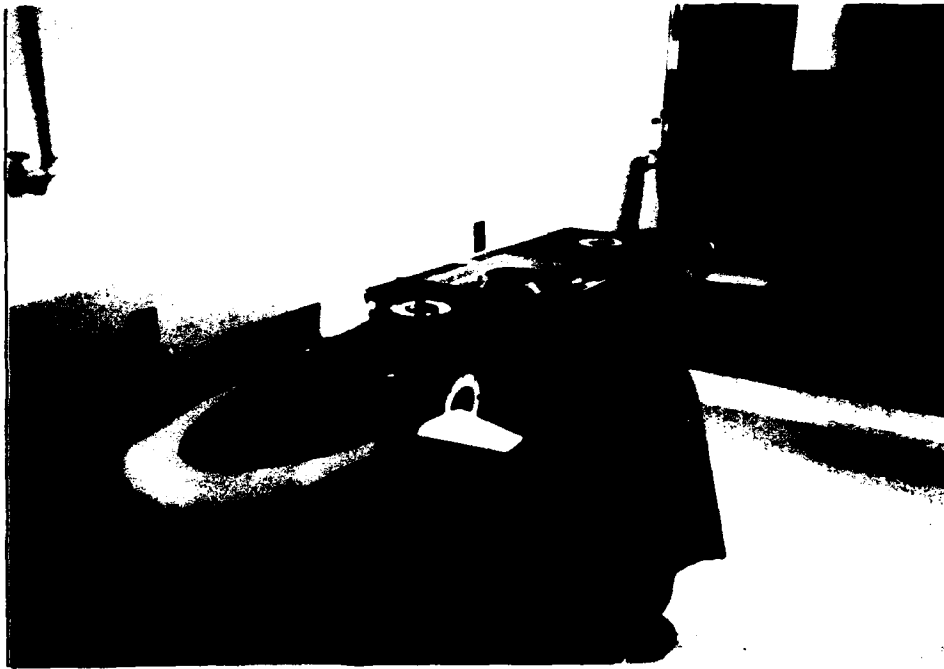
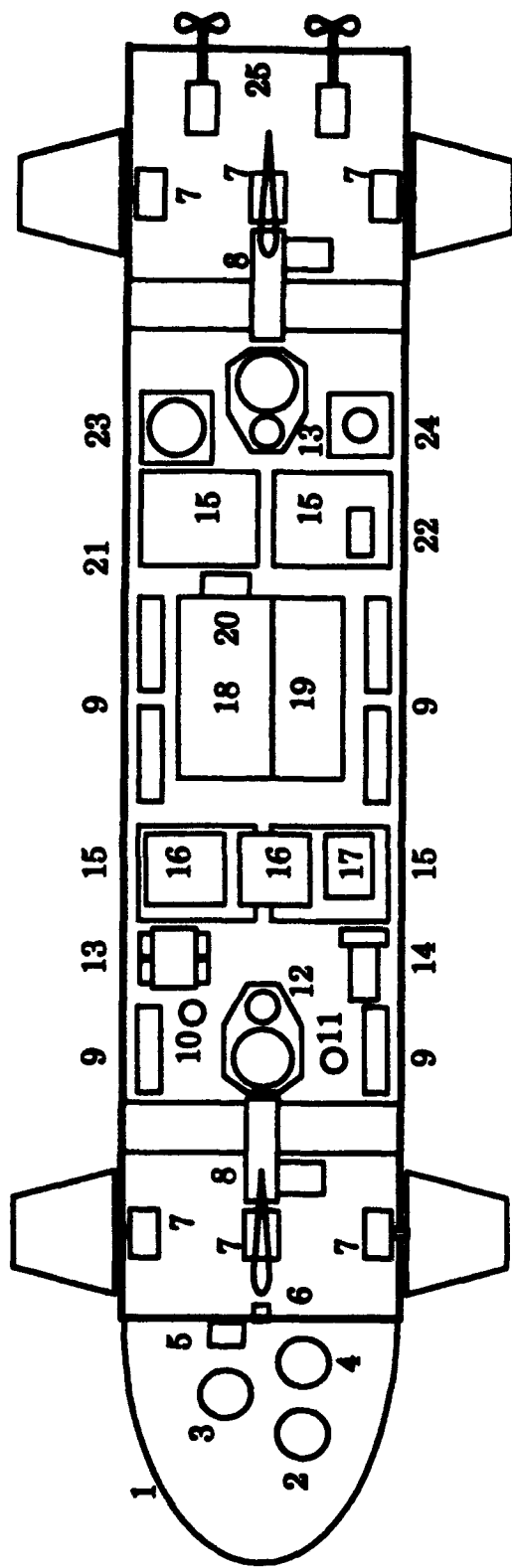


Figure 2.1 AUV II



- | | | |
|---------------------------|--|---|
| 1 Nosepiece (Flooded) | 10 Power/Run Plug | 18 GESPAC (Execution Processor) OS-9 |
| 2 ST-1000 | 11 Serial Port Connector | 19 GESPAC (Tactical Processor) DOS |
| 3 Datasonics | 12 Vertical Thruster | 20 Synchro/Digital Converter |
| 4 ST-725 | 13 Rate Gyro | 21 Pressure Hull (Air charged to 1 psi) |
| 5 Flow Meter | 14 Vertical Gyro | 22 Inverter (Motor Inhibiter) |
| 6 Depth Cell | 15 12 VDC Battery | 23 Free Directional Gyro |
| 7 Control Fin Servo Motor | 16 ACON Power Supply | 24 400 Hz Power Supply |
| 8 Horizontal Thruster | 17 Calnex Power Supplies/
CRYDOM Relays | 25 Stern Propulsion Motors |

Figure 2.2 AUV II Configuration

arranged in the vehicle, to achieve the most efficient maneuvering capabilities. The remainder of the equipment is located to achieve the most favorable volume and weight distribution, and to minimize the length of the wire runs. The batteries therefore, are centrally located in order to keep the center of gravity close to the center of the vehicle body. The computer is located at the center of the vehicle body, with the served equipment located as close as possible to the computer.

Calculations of the centers of gravity and buoyancy are provided in Appendices C and D.

A. SENSORS

The sensor systems incorporated into the AUV II provide the necessary input data, for both environment conditions and vehicle motion, to achieve autonomous vehicle operation and control.

1. Environment Sensors (Sonar Equipment)

The sonar suite consists of three types of sonar transducers with primary functions being horizontal environmental surveying (profiling), target imaging (scanning) and bottom surveying (depth measuring). The three types of sonar used for these functions, are respectively; the Tritech ST-1000 and ST-725 sonar and the Datasonics PSA-900 altimeter. Placement of the transducers, in the (flooded) nosepiece section of the AUV is shown in Figure 2.3.

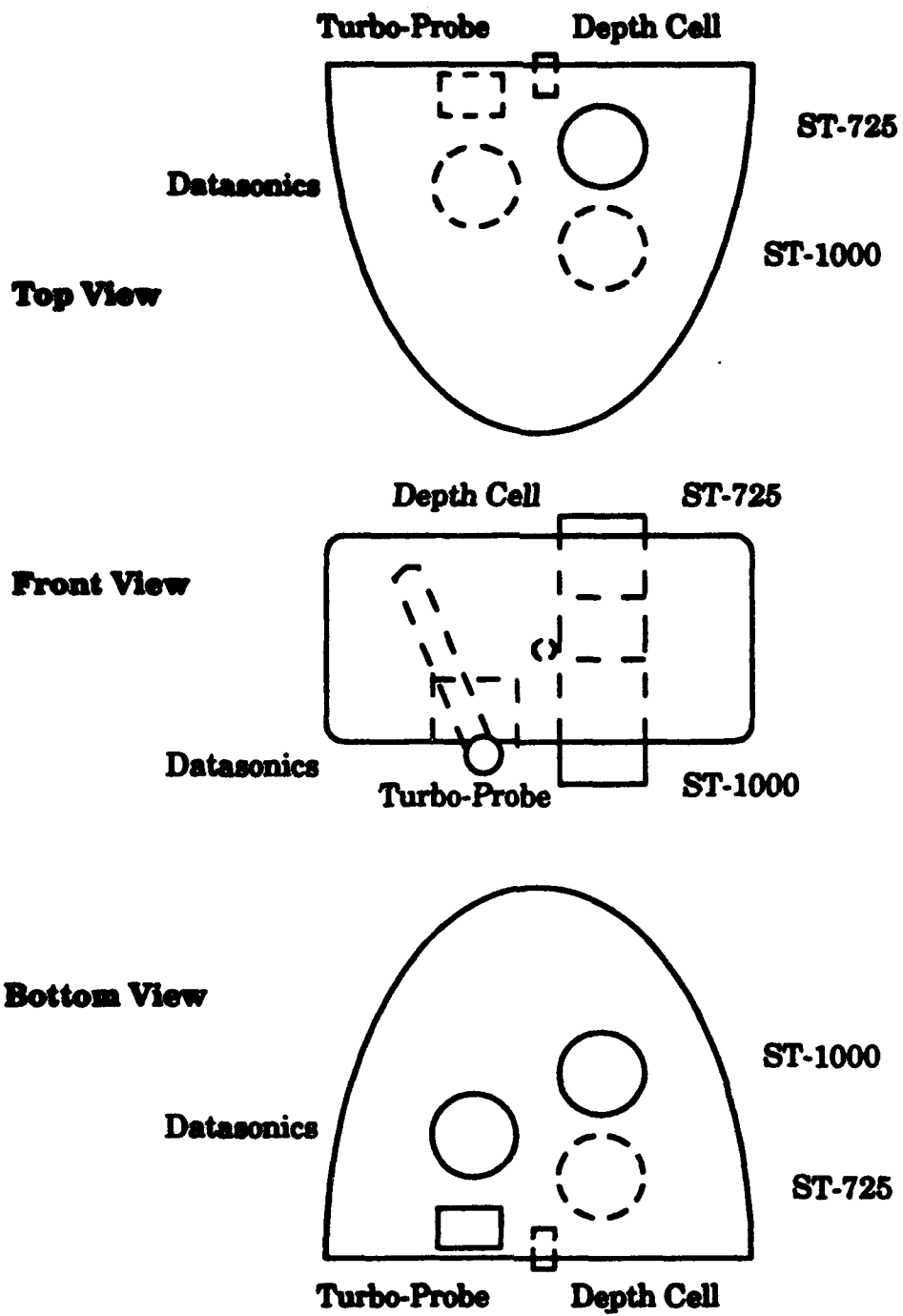


Figure 2.3 Sensor Location (Nosepiece Section)

a. Profiling Sonar (Tritech ST-1000)

The profiler is the model ST-1000 sonar, manufactured by Tritech International, Ltd. This unit is a compact system, operated by a PC compatible computer and is integrated with the ST-725 scanning sonar.

The ST-1000 sonar head operates at a frequency of 1250 kilohertz (1000 kilohertz, nominal), with a one degree conical beam. It requires 24 to 28 volts (DC) power at 800 miliamps, and can be operated at depths up to 4900 feet, over eight selectable ranges between three and 160 feet.

The ST-1000 can be operated in two modes; Sector Profiling or Sector Sonar Scanning. The Profiling mode provides 360 degree coverage, where the delay time to the first echo is sensed and returned to the device serial port connector. The Scanning mode is continuous, and can be used for horizontal sector scan, or for vertical left or right side direction coverage. In this mode, the intensity of the returning echoes are sensed as a function of delay time and returned to the device serial port connector as a string of values, one in each of 64 range pixels. At larger total ranges, full range is divided into 128 range pixels. For the shorter ranges, a sonar pixel will be 9.3 centimeters long by 1.8 degrees wide. Intensities are scaled from one to 15, where 15 represents the highest strength.

The ST-1000 sonar head is mounted vertically, in the AUV, protruding through the bottom of the nosepiece.

b. Scanning Sonar (Tritech ST-725)

The scanning sonar is the ST-725, also manufactured by Tritech. It operates at a frequency of 725 kilohertz with a one degree by 24 degree fan beam.

The ST-725 sonar head is mounted aft of the ST-1000, but protruding through the top of the nosepiece.

c. Depth Sonar (Datasonics PSA-900)

The depth sonar is the Model PSA-900 Sonar Altimeter, manufactured by Datasonics, Inc. It is microprocessor controlled.

The Datasonics operates at a frequency of 210 kilohertz, with a ten degree conical beam. It requires 15 to 28 volts (DC) at 100 miliamps and can be operated at depths up to 6500 feet, at ranges up to 90 feet.

The Datasonics transducer is installed as described in Good (1989), with a plastic cone, mounted in the nosepiece. Only one Datasonics transducer is used here, as opposed to the original configuration, and it is mounted facing downward, aimed through the bottom of the nosepiece.

2. Vehicle Sensors

The vehicle sensor components provide the input data for the position and motion of the AUV.

a. Gyroscopes

Three types of gyros were used to measure the vehicle's angular position and roll, pitch and yaw rates. All three types are manufactured by Humphrey, Inc.

(1) *Free Gyro.* The free gyro measures the yaw angle of the vehicle. The Model FG23-7102-1 is a two-degree-of-freedom unit which references its own case frame.

Its inner and outer gimbals have 360 degree and negative to positive 85 degree motion, which require 26 volts (AC), 400 Hertz input. The pickoff is an outer gimbal syncro control transmitter which outputs 11.8 volts (AC). The gimbals have a remote caging/uncaging device which requires 28 volts (DC) input.

The gyro motor requires 115 volts (AC), 400 Hertz, and spins at approximately 24,000 revolutions per minute. The Model PS27-0101-1 power supply provides the 400 Hertz (26 and 115 volts (AC)) input to the gyro.

The free gyro is located aft in the midbody section of the AUV. The wiring diagram for the free gyro is provided in Appendix C.

(2) *Vertical Gyro.* The vertical gyro measures the pitch and roll angles of the vehicle. The Model VG34-0301-2 is a two-degree-of-freedom unit with both axes slaved to local gravity.

It's inner and outer gimbals have 360 degree (roll) and negative to positive 80 degree (pitch) motion. The pickoff is a plastic

potentiometer, which outputs negative ten to positive ten volts (DC). Required input is 28 volts (DC).

The vertical gyro is located forward in the midbody section of the AUV. Since the vehicle body is rigid, gyro placement was a matter of arrangement rather than a matter of required location within the body.

(3) *Rate Gyros.* The rate gyros measure the roll, pitch and yaw rates of the vehicle. Each component of the Model RG02-2324-1 has single-degree-of-freedom motion along its designated axis, and is torsion spring mounted to produce gimbal displacements proportional to angular rate inputs.

Required input is 28 volts (DC). The pickoffs are resistance potentiometers which produce output voltages of negative ten to positive ten volts (DC). Maximum rates are 360, 90 and 90 degrees per second for roll, pitch and yaw.

The rate gyros are located forward in the midbody section of the AUV.

b. Depth Cell (PSI-Tronix)

Vehicle depth is measured using a differential pressure transducer manufactured by PSI-Tronix, Inc.

The PWC series (S11-131) is a strain gage based transducer which operates from zero to 15 pounds per square inch (depth to approximately 34 feet), referenced to one atmosphere. It requires 12 to 18 volts (DC) supply and outputs zero to ten volts (DC).

The probe for the depth cell is located in the nosepiece section of the vehicle in the aft bulkhead, in order to permit contact with the water at the vehicle's depth, with minimal flow.

c. Vehicle Speed Sensor (Turbo-Probe)

The vehicle speed through the water is measured by a Turbo-Probe turbine flow meter, manufactured by Flow Technology, Inc.

The transducer is an axial rotor element, mounted at the end of a strut. The strut houses an electromagnetic pickoff assembly which generates electrical pulses of a frequency proportional to the rotor speed and flow velocity. The flow meter has an operating range of one tenth to six feet per second.

The flow meter is used in conjunction with the LFA-307 Range Extending Amplifier, also manufactured by Flow Technology. This amplifier is used for signal conditioning to insure good linearity at low flow velocities.

The flow meter is mounted in the nosepiece section of the AUV with the rotor element protruding through the bottom of the nosepiece.

d. Motor RPM Indicator (Hewlett-Packard)

Hewlett-Packard Model HEDS-5000 series optical encoders are used to measure motor speed.

These encoders are configured with a lensed LED source, an integrated circuit (IC) with detectors and output circuitry, and a code wheel which rotates between the emitter and detector IC. Rotation of the code wheel generates a pulsed input which the IC circuitry processes to produce a digital

pulsed output. Rotation speed is measured in terms of the pulse count per unit time, or the time width of successive pulses. The encoders require a supply voltage of one half to seven volts (DC) input and operate up to 30,000 revolutions per minute.

Each thruster and stern propulsion motor is configured with an encoder attached to its shaft.

B. GESPAC M68020/30 COMPUTER SYSTEM

The function of providing real time control of the AUV II is accomplished through the use the GESPAC M68020/30 series computer system and various input/output control cards.

The OS-9 Operating System is used in the GESPAC. It provides real time, multi-tasking capability. C language is the source code. It is independent from the input/output devices.

The software package PC Bridge (trademark of GESPAC, Inc.), is used to communicate between the GESPAC and an external IBM PC for the purposes of file transfer. As the processor system is an embedded real time processor, it operates on a single board without the benefit of an associated hard disc for storage of memory modules. Only operating system modules are "burned" into EPROM, thus run modules that form the vehicle control functions at run time must be loaded from an external computer into the embedded processor.

The major components of the embedded computer system are positioned in a twelve card cage, located in the midbody section of the vehicle. Communication with the GESPAC is accomplished through an RS-232 serial

communications port, located on the top of the vehicle, through a watertight connector and a sufficiently long, lightweight watertight cable.

The following sections give a brief description of the major components of this system. The paths for data input/output between the components are shown in the block diagram of Appendix A.

1. GESMPU-20 Micro Processor Unit

The GESMPU-20 module uses a 32 bit 68020 microprocessor built into a single board. The microprocessor uses a non-multiplexed G96 bus with 32 bits of address and 32 bits of data. The board runs at 25 megahertz and has an associated two megabytes of CMOS Dynamic RAM, on an adjacent card. Its power requirement is positive five volts (DC).

The GESMPU-20, through its device drivers and execution level real time control software, compiled into executable modules, controls all computer functions in the AUV.

2. GESMFI-1 Multi-Function Interface

The GESMFI-1 is a universal interface module with two RS-232 serial ports, two, eight-bit parallel ports and three 16-bit timers. The module runs with either one megahertz or two megahertz synchronous timing and has 50 bytes of CMOS RAM. The power requirements are positive five and negative to positive 12 volts (DC).

The GESMFI-1 interfaces with the 14-bit Synchro to Digital converter, which operates on the data from the free gyro. The MFI card

provides the embedded processor with a digital data value of zero to 16384 (2^{14}), corresponding to one revolution (360 degrees) of the yaw angle gyro.

3. GESSIO-1B Serial Input/Output

The GESSIO-1B dual interface module provides two RS-232 capable asynchronous serial ports. The power requirements are positive five and negative to positive 12 volts (DC).

The GESSIO-1B provides the interface for the ST-725 and ST-1000 sonar transducers.

4. GESPIA-3A Peripheral Interface Adapter

The GESPIA-3A has two parallel 16-bit input/output ports and four 16-bit timers. The power requirement is positive five volts (DC).

This module provides the interface for the free gyro cage/uncage command and status signals. It also provides an input for the Datasonics sonar transducer, the CRYDOM relays and the Callex power supplies. It controls the Transistor-Transistor Logic (TTL) which provides the switching signals for the relay/power supply system.

5. GESADA-1 AND GESADA-2 Analog/Digital Interfaces

The GESADA-1 and GESADA-2 modules provide analog to digital (A/D) and digital to analog (D/A) functions. The GESADA-1 module has a 16 channel, ten-bit A/D input section and a four channel, ten-bit D/A output section. The GESADA-2 module has a 16 channel, ten-bit A/D input section. Both modules require positive five and negative to positive 12 volts (DC).

The GESADA-1 module interfaces the outputs from the Diagnostics module. The GESADA-2 module interfaces the inputs from the vertical and rate gyros, the depth cell and the Datasonics transducer.

6. GESDAC-2B Digital/Analog Converter

The GESDAC-2B module provides an 8 channel, 12-bit D/A output. Its power requirement is positive five volts (DC).

This module interfaces the inputs to the propulsion and thruster motor servo amps.

7. GESTIM-1A Multiple Timer Modules

The GESTIM-1A modules provide the System Timing Control (STC) functions. Each module has five, 16-bit channels and a real time clock/calendar function. The power requirement is positive five volts (DC).

Five GESTIM-1A timing modules are used in the AUV which coordinate the signals between the tachometer sources (thruster and stern propulsion motor speed indicators, flow meter and control surface servo motors).

C. PROPULSION/MANEUVERING EQUIPMENT

The propulsion and maneuvering systems are comprised of three groups of equipment; control surfaces, stern propulsion and thrusters.

1. Control Surfaces

The development of the design of the control surfaces is presented in Good (1989). The shape used for the AUV II application is the NACA 0015 foil section.

Two cruciform arrangements of control surfaces are used; one arrangement forward and one aft, on the midbody section of the AUV. This arrangement provides highly efficient maneuvering capability in both the horizontal and vertical planes as evidenced by previous waterborne testing of the AUV (Healey and Marco, 1992).

The control surfaces are positioned through the use of radio controlled aircraft servo motors. Airtronics Model 94510 servos are installed, one for each control surface. These motors have a maximum torque rating of 110 ounces-inches (6.875 pound-inches), and a response time of one half second for a zero to 90 degree movement.

2. Stern Propulsion

The AUV II is configured with a conventional twin screw propulsion system. Detailed development of the design is provided in Good (1989).

A commercially purchased running gear hardware kit, manufactured by Gato/Balao, Inc., is installed. The kit consists of two brass propellers, stainless steel shafts and three inch brass stuffing tubes. Two, four blade, four inch diameter propellers are installed, each capable of providing approximately five pounds of thrust at full load (Saunders, 1990, Coty, 1992).

Electric DC servo motors are used for the stern propulsion units. The PITMO DC Model 14202 series motor, manufactured by Pittman, Inc., has a stall torque of 106 ounce-inches, a no load speed of 3820 revolutions per minute and a peak power draw of 333 Watts. Operating at 24 volts (DC), the motor has a no load current rating of 0.230 amps.

3. Thrusters

The AUV II is configured with four tunnel thrusters which provide the capability for slow speed maneuvering, hovering and station keeping. The thrusters are mounted in pairs, one mounted horizontally, one vertically; each pair is mounted forward and aft, in the midbody section of the AUV.

Each thruster assembly consisted of a DC servo motor, a reduction gear and housing assembly, a propeller assembly and thruster tunnels.

The servo motors used for the thrusters are the same as those used for the stern propulsion units described above; PITMO DC Model 14202 series.

The reduction gear is a single stage, single reduction spur gear configuration. The pinion and gear are made of Delrin (trademark of Winfred M. Berg Company). Both the pinion and gear have a pitch of 24 teeth per inch. The pinion has 45 teeth and a pitch diameter of 1.875 inches, and the gear has 90 teeth and a pitch diameter of 3.750 inches. The resulting reduction ratio provided is two to one. The gear is configured as a ring gear and is fitted around the propeller and hub assembly. The reduction gears are assembled into an aluminum housing to which the thruster servo motors are mounted.
(Cody, 1992)

The propeller and hub assembly is made of brass. The propeller is three inches in diameter, and has four blades mounted at 45 degrees. The blade angle is constant along its length, and the blade has zero camber which permits equal thrust in both forward and reverse directions of rotation. The propeller and hub assembly is mounted on a stainless steel shaft and the thrust/journal bearings are made of Teflon. (Cody, 1992)

Aluminum struts, mounted in the thruster tunnels, support the propeller shaft, oriented axially in the thruster housing. The tunnels have an inside diameter of three inches, and are mounted in two sections on either side of the thruster housings, placing the thruster housings at the midpoints of the tunnels. The horizontal tunnels are 16.5 inches and the vertical tunnels are ten inches in length, corresponding to the width and height of the AUV.

The modeling and performance analysis of the thruster assemblies have been the subject of several theses, including Good (1989), Cody (1992) and Brown (1993).

D. ELECTRICAL POWER EQUIPMENT

The objective of the original design considerations for the power requirements of the AUV II was to provide adequate energy onboard which would support all vehicle functions for at least an hour of completely autonomous operation. The installed electrical system provides enough power to run the vehicle's onboard computer, sonar and electronics systems in addition to power for mobility.

This section describes the major components of the electrical power system.

1. 24 Volt Battery Packs (Panasonic)

Two 24 volt (DC) battery packs provide the main power source for the AUV. Each battery pack is made up of two, 12 volt (DC) Panasonic Model LCL12V38P rechargeable, sealed lead-acid batteries connected in series. The batteries weigh 31.5 pounds, and have nominal capacities of 34.0 amp-hours (ten hour rate) and 38.0 amp-hours (20 hour rate).

The series battery packs provide 24 volts (DC) power to the following equipment:

- 1. Rate gyros.**
- 2. Vertical gyro.**
- 3. 400 Hertz power supply for the free gyro.**
- 4. ACON computer power supplies.**
- 5. CRYDOM relays.**
- 6. Calex power supplies.**
- 7. Six, PMW servo amplifiers (thruster and stern propulsion motors).**
- 8. Tachometer sources (thruster and stern propulsion motor speed indicators, Turbo-probe).**

The battery packs are located in the midbody section of the AUV, one forward and one aft of the GESPAC computer cage.

2. ACON Power Supplies

Two ACON Model R100T2405-12TS inverter/power supplies are installed to provide power to the computer systems. The two power supplies

are independent and provide positive five and negative to positive 12 volts (DC).

The power supplies are mounted in the midbody section above the forward battery pack.

3. Calox Power Supplies

The Calox Models 12S15, 48S15 and 12S5 power supplies provide positive five and negative to positive 15 volts (DC) for the following equipment:

1. Reference source for the rate gyros and vertical gyro (+/-15 volts (DC)).
2. Datasonics sonar (+15 volts (DC)).
3. Depth cell (+15 volts (DC)).
4. GESTIM-1A timer cards (+15 volts (DC)).
5. Control surface servo motors (+5 volts (DC)).
6. CRYDOM relays (+5 volts (DC)).

The power supplies are mounted in the midbody section above the forward battery pack.

4. CRYDOM Relays

The CRYDOM Model 6300 relays provide the voltage switching using TTL logic input from the GESPIA-3A modules. Power is supplied to the following components:

1. Tritech sonar (ST-1000 and ST-725) (+24 volts (DC)).
2. Cage/uncage voltage for the free gyro (ground path).

5. Servo Amplifiers (Advanced Motion Controls)

Motor speed for the thruster and stern propulsion motors is controlled through the use of Advanced Motion Controls PWM Model 30AD8DD servo amplifiers. One amplifier is used for each motor. The PWM servo amplifier uses a zero to ten volt control signal to modulate the pulse width of a 24 volt, five to 45 kilohertz (load dependent) output signal to the motor. Direction of the motor is controlled by changing the polarity of the control signal.

The servo amplifiers are located in the midbody section of the AUV, mounted on the port and starboard bulkheads.

6. Synchro to Digital (S/D) Converter

The Synchro to Digital Converter is a 14-bit device designed at the Naval Postgraduate School. It uses an Analog Devices card which converts the phase components of the free gyro output signal to digital data.

The S/D converter is located in the midbody section and is mounted on the aft end of the GESPAC computer card cage. The wiring diagram for the S/D converter/free gyro is provided in Appendix C.

7. Inverter (Motor Inhibitor)

A signal inverter is installed between the GESPIA-3A module and the servo amps to prevent energizing the thruster or stern propulsion motors during computer system start-ups.

The inverter is located in the midbody section and is mounted above the aft battery pack.

III. EXPERIMENTAL APPARATUS AND PROCEDURE

This chapter provides a description of the equipment and procedures used to conduct the hover positioning experiments for the AUV II.

Background information is discussed concerning the preparation of the AUV II vehicle, the lab and support facilities and the test equipment, followed by an outline of the procedures used for the experiments and data collection.

A. EQUIPMENT PREPARATION

The equipment used for the hover positioning experiments are categorized into three groups; the AUV II vehicle, the test facility and the programmed software code.

1. AUV II Vehicle

Over the course of the thirty months since the vehicle completed its last waterborne tests, numerous configuration changes have been incorporated into the AUV, the results of which were presented in Chapter II. Many man-hours were consumed, involving the expertise of the Mechanical Engineering Department machine shop personnel, electronics technicians, staff, ... and a few students.

New equipment groups installed in the AUV include sonar, gyros, power supplies, speed sensors and computer systems, however, the equipment which provide the means to accomplish the objective of this thesis are the thrusters. The location of the horizontal thrusters, forward and aft of the

vehicle's center of gravity permit rotation and lateral translation, while the vehicle is hovering.

The final design concept for the thrusters was completed and a prototype assembly was manufactured and satisfactorily tested (Cody, 1992). The three remaining thruster assemblies were then constructed and the four units installed in the AUV.

2. Lab and Test Facility

The test facility for the AUV project is located in building 230 of the Naval Postgraduate School Annex. The facility houses a 18,000 gallon capacity test tank which measures 20 by 20 by 6 feet. Other equipment include a filtration and recirculation system, hoist, catwalk and external computers.

The external computers include an IBM PC clone 486 with a VGA graphics monitor, a clone 286 PC and the GESPAC Development System, which is a replication of the in-vehicle system with a hard drive, C code cross-compiler and PC Bridge software for transferring compiled modules of code to and from the vehicle.

In preparation for the hovering experiments the interior of the tank was painted with white epoxy, and a 2.5 foot square grid pattern was laid out along the bottom and sides of the tank. This permitted good visibility of the vehicle, and provided a reference for vehicle pre-positioning and motion observation, during testing. A catwalk was installed across the top of the tank for vehicle launch and recovery, and experiment observation.

3. Computer Software

In order to support the basic operating functions of the AUV in addition to executing the positioning experiments, numerous software programs were written and installed in the onboard GESPAC and external control computer systems. The development of the software programs is the subject of a doctoral dissertation, currently in progress by David B. Marco.

Some of the AUV operations supported by the software include the following:

1. AUV system start-up.
2. Free gyro caging/uncaging.
3. Gyro zeroing functions.
4. Sonar operations.
5. Sensor data input functions (A/D).
6. Command positions for motion experiments.
7. Control law functions for each operating mode of behavior.
8. Command data output functions (D/A).
9. Data storage for analyses.

It should be noted that independent software modules for debugging subsystem operations are not only desirable, but essential to the calibration and verification of vehicle functions.

B. EXPERIMENTAL APPARATUS

The equipment arrangement for the hovering motion experiments is shown in Figure 3.1.

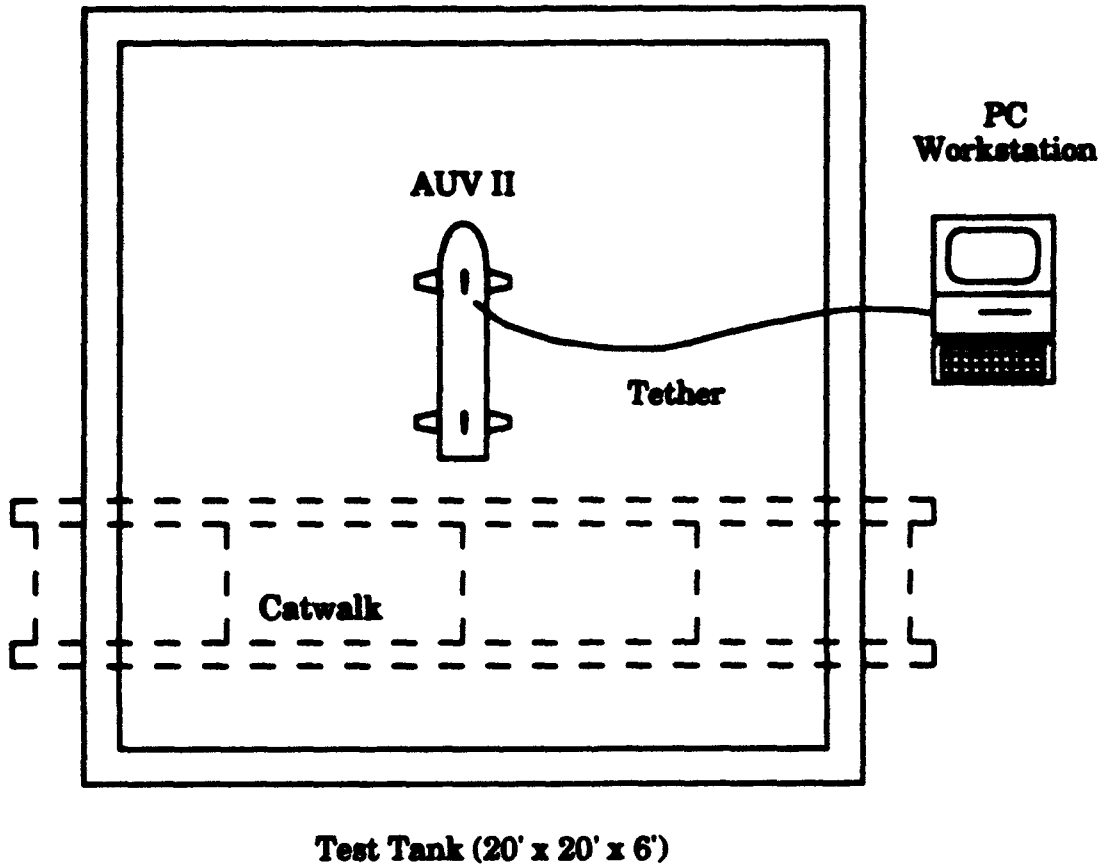


Figure 3.1 Experimental Set-up

For the purposes of conducting these experiments, an electronic tether was attached to the onboard GESPAC computer via the RS-232 connection. This provided a direct path for file and data exchange between the GESPAC computer and the external PC workstation running PC Bridge software.

The vehicle is lifted into the test tank via the hoist, and positioned for the start of each experiment by observers on the catwalk. The observers remain stationed on the catwalk throughout the tests to recover the vehicle or prevent damage should an equipment casualty occur.

The vehicle is operated externally through the PC workstation, however the serial link is used only for file and data transfer. Motion commands are built into the run program through screen entry, but once entered, the vehicle is completely independent of any further commands for the operation. Data files recorded for each experiment are down-loaded to the PC workstation.

The AUV II vehicle, test tank and PC workstation are pictured in Figures 3.2 and 3.3.

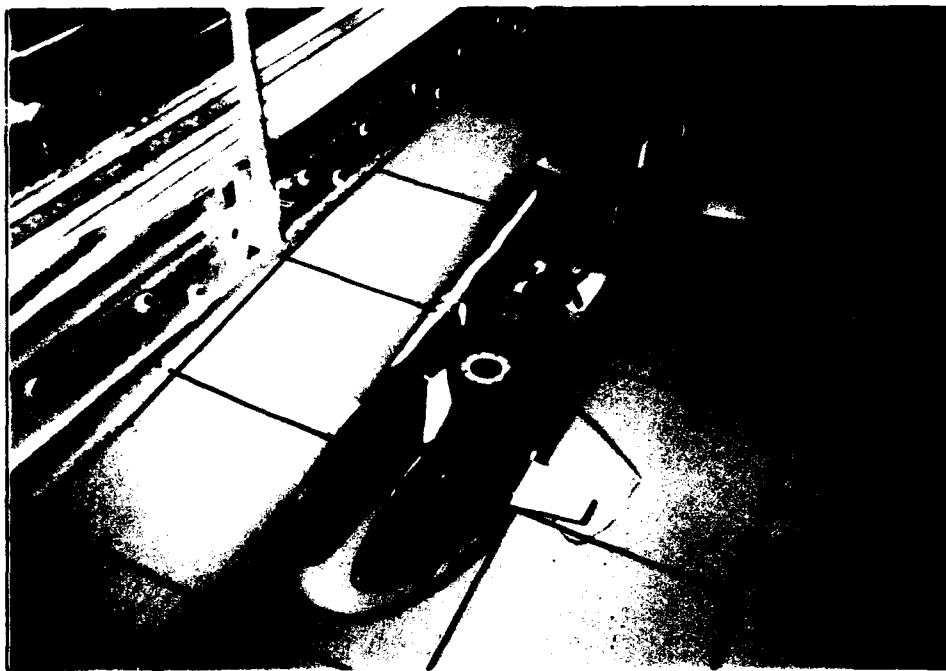
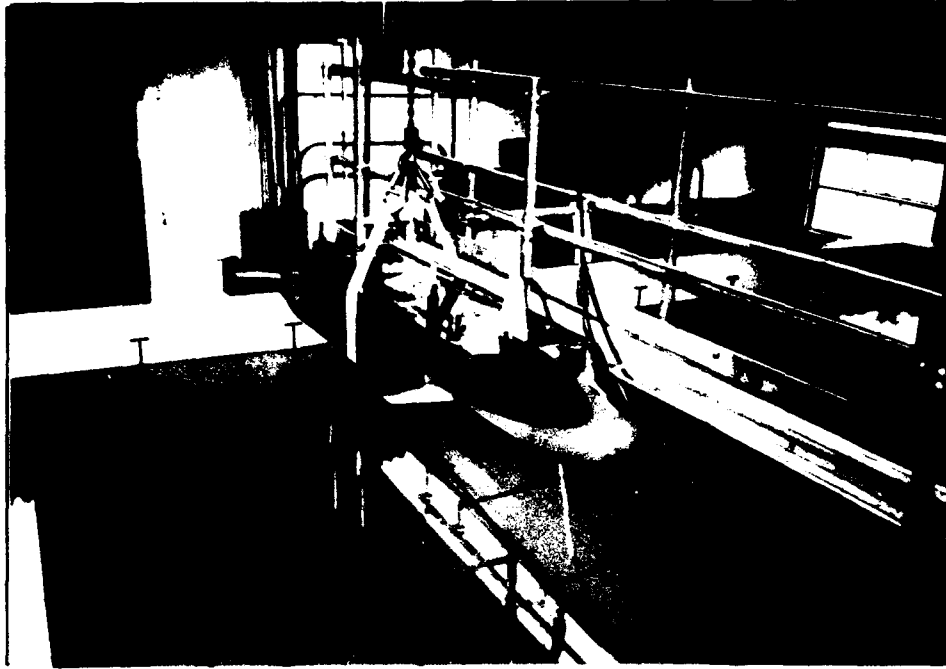


Figure 3.2 AUV II and Test Tank



Figure 3.3 AUV II and PC Workstation

C. EXPERIMENTAL PROCEDURE

This section describes the procedures used to calibrate the test equipment and outlines the three types of hover positioning experiments, including data collection.

1. Rate Gyro Calibration

Calibration of the rate gyro was required due to a new power supply being used for its input. The new power supply also produced a change in the range of output voltages from the gyro.

It was anticipated that both a scale factor and a bias error would be electronically introduced into the gyro output.

An additional bias error was expected as a result of the zeroing procedure to be used at the start of the experiments. During this procedure, the vehicle is held as motionless as possible in the tank. As the experiment starts, before any control motion begins, a segment of the run code reads the sensors, taking initial position readings of the vehicle relative to the environment. Average values of positions and rates are calculated and used as zero points for the following test rate and position measurements. Unless the vehicle is perfectly motionless (which is impossible in this test facility), there will be some rate bias introduced, however it was expected that this would be small.

Referencing the right-hand global and body fixed coordinate systems, as shown in Figure 3.4, the scale factor (SF) and bias factor (BF) errors are modeled by the following equation:

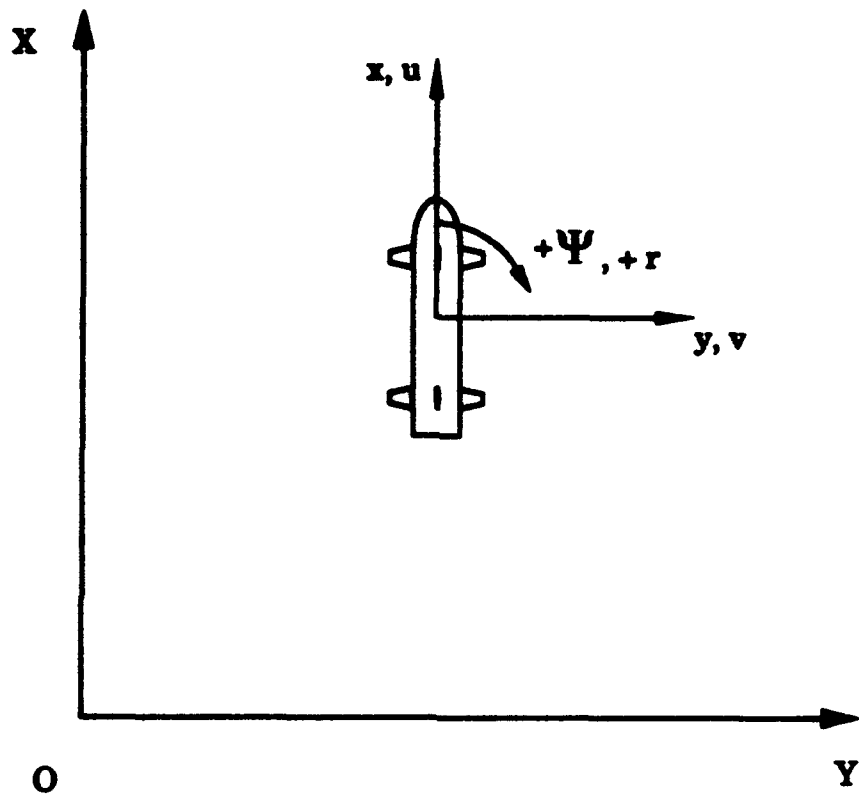


Figure 3.4 Right-Hand Global and Body Fixed Coordinate Systems

$$r_{\text{exper}} = (D[\Psi_{\text{exper}}] - BF) + SF$$

where it was considered that the precision of the heading gyro (drift rate less than six degrees per hour) was such that

$$D[\Psi_{\text{exper}}] = r_{\text{true}}$$

The experimental yaw rate can then be corrected by the following equation:

$$r_{\text{true}} = r_{\text{exper}} \times SF + BF$$

The true yaw rate could then be found by correlating the experimental yaw rate data to the derivative of the yaw position data using a first order least squares fit.

Since the vehicle, when placed in the tank, essentially behaved as an ideal rate table, it was decided to use the vehicle's own motion under a yaw position command to calibrate the rate gyro. This motion is shown in Figure 3.5. Inputs from the free gyro were used to determine the vehicle's yaw position.

The control laws for the yaw position commands were derived on the basis that the commanded moment is directly proportional to the differential thrust between the forward and aft lateral thrusters, where the thrusters are used in opposite directions. Additionally, the thruster force is proportional to the square of the applied motor voltage (using the absolute value to account for direction).

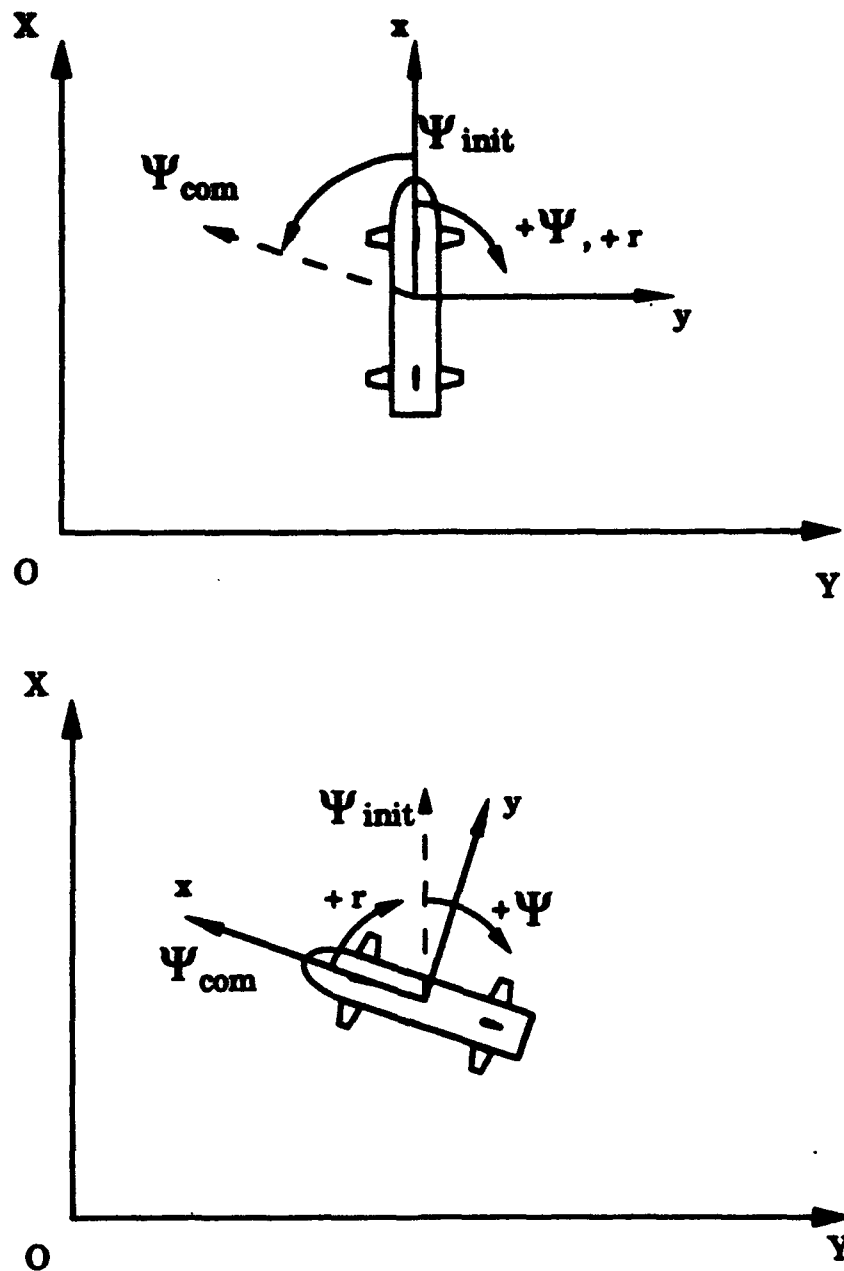


Figure 3.5 Yaw Rate Calibration/Yaw Positioning Experiment

$$M_{\text{com}} \propto (F_{\text{Fwd Thrust}} - F_{\text{AR Thrust}})$$

$$F_{\text{Fwd Thrust (Yaw)}} = -F_{\text{AR Thrust (Yaw)}}$$

$$F_{\text{Thrust}} \propto V_{\text{Thrust}} |V_{\text{Thrust}}|$$

However, in order to keep the control effort linear, the position commands were generated using proportional derivative control laws for the thruster voltages. Based on the equations above, the control laws for the forward and aft thruster voltages are as follows:

$$V_{\text{Fwd Thrust}} = -K_{\Psi}(\Psi - \Psi_{\text{com}}) - K_r(r - r_{\text{com}})$$

$$V_{\text{AR Thrust}} = K_{\Psi}(\Psi - \Psi_{\text{com}}) + K_r(r - r_{\text{com}})$$

$$K_r = K_{\Psi} \times T_{d\Psi}$$

The control law gains were selected heuristically, estimating that a full voltage control effort (24 volts) would be used for a yaw position error of $\pi/8$ (22.5 degrees), with a nominal time constant of one second. These estimates resulted in the following control law gains for yaw positioning:

$$K_{\Psi} = 60$$

$$T_{d\Psi} = 1$$

The position commands were given for yaw angles of (negative) 30, 60, 90, 180 and 360 degrees (relative to a starting position). Three trials were completed for each commanded position angle.

The data recorded included yaw position, yaw rate and forward and aft thruster voltage inputs as functions of time. Figure 3.6 presents the yaw position versus time and the yaw rate versus time curves for the three, 180

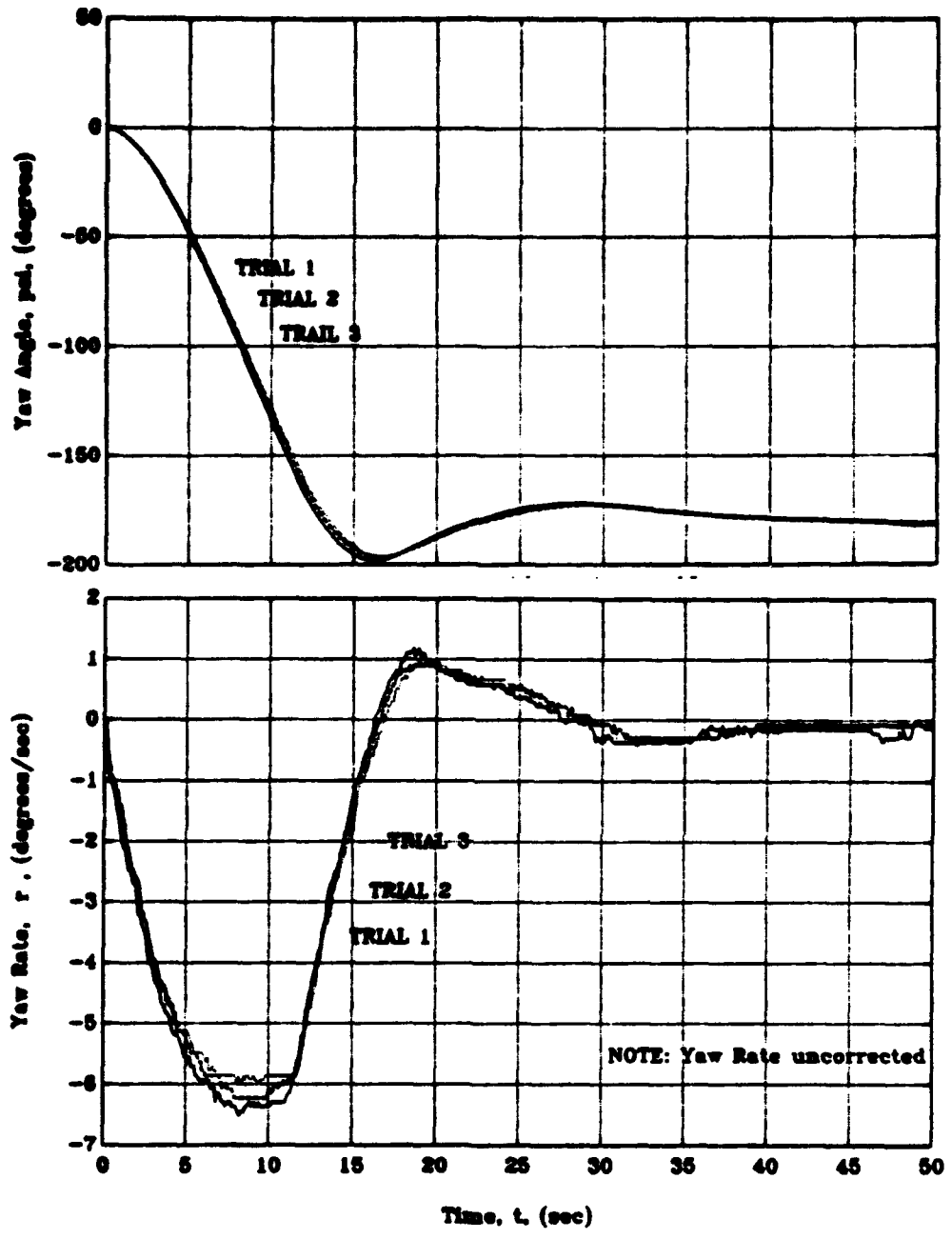


Figure 3.6 Yaw Rate Calibration: 180 Degree Test (3 Trials)

degree tests. (Note that the yaw rate curve is uncorrected.) It is shown in this figure that good repeatability was achieved.

A first order, least squares fit was used to obtain the scale factor and bias factor between the measured yaw rate data and the derivative of the yaw position data. Starting with the first 30 degree test, a scale factor of 3.2709, and a bias factor of 0.0043 were obtained. Figure 3.7 presents these results. This figure shows that an accurate fit was obtained.

For comparison, the measured yaw position data was compared to the integral of the corrected yaw rate data. These results are also presented in Figure 3.7. Fairly good agreement was achieved.

Using the same procedure, the scale and bias factors were obtained for the remaining tests. The results are presented in Table 3.1. From the results, it was observed that the scale factor varied slightly, however a nominal value of 3.00 would not produce a great error in any of the tests. The variation in the bias was small and appeared to be random.

Based on these results, it was felt that the yaw position data was more reliable and all subsequent yaw rate data would be corrected using the same procedure.

2. Yaw Positioning Experiment

As discussed in the previous section, the yaw positioning experiment was used for the rate gyro calibration.

Inputs from the free gyro were used to determine the vehicle's yaw position. The position commands were given for yaw angles of (negative) 30,

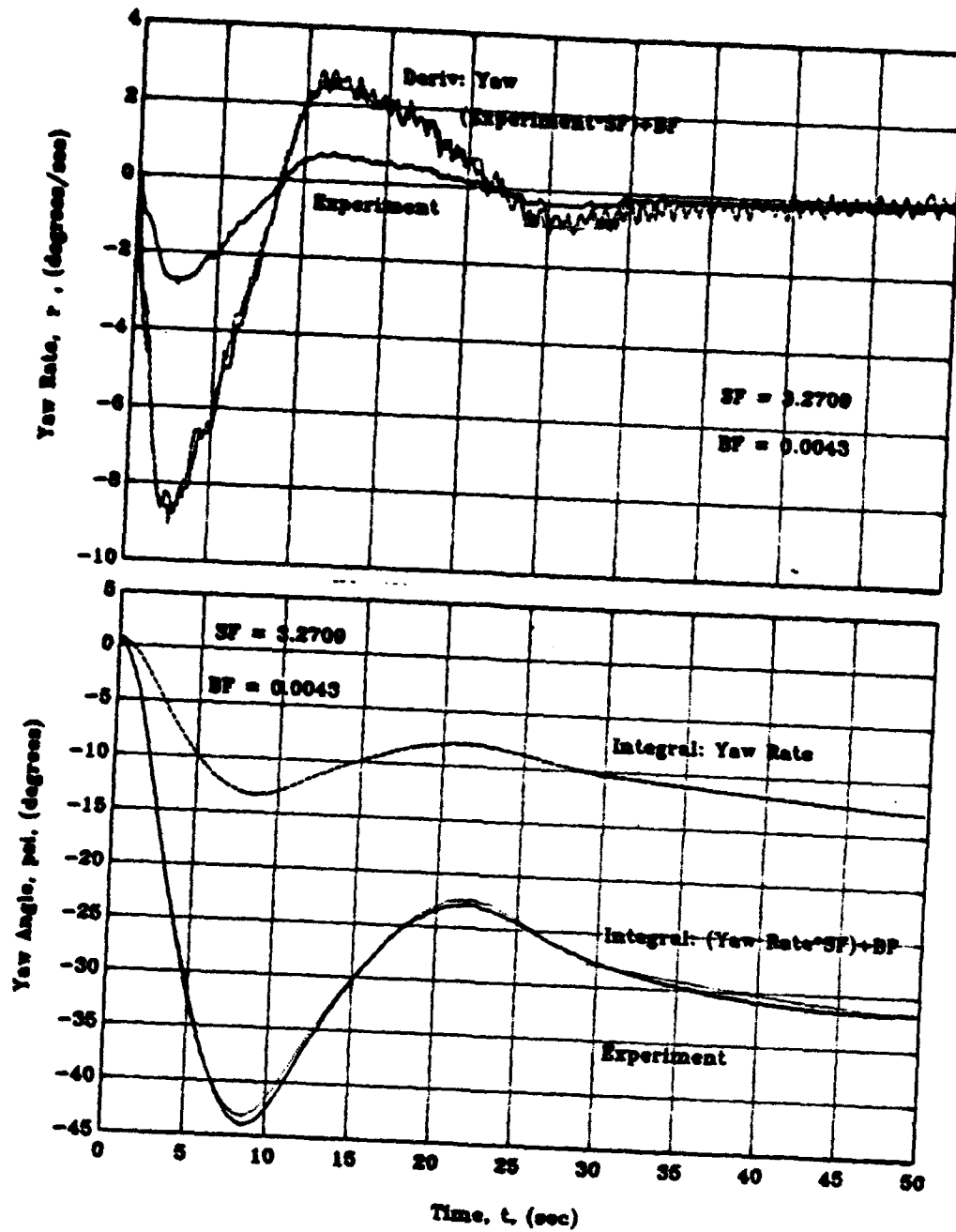


Figure 3.7 Yaw Rate Calibration: 30 Degree Test

TABLE 3.1 YAW RATE CALIBRATION: SCALE AND BIAS FACTORS

TEST	TRIAL	SCALE FACTOR (SF)	BIAS FACTOR (BF)
30 DEGREE	1	3.2709	0.0043
	2	3.2980	0.0055
	3	3.2662	0.0017
60 DEGREE	1	3.0059	0.0013
	2	3.0257	-0.0011
	3	3.0209	0.0025
90 DEGREE	1	2.9529	0.0004
	2	2.9699	-0.0034
	3	2.9375	0.0010
180 DEGREE	1	2.8387	0.0031
	2	2.8592	0.0008
	3	2.8799	0.0010
360 DEGREE	1	2.8208	0.0015
	2	2.8727	0.0004
	3	2.8470	0.0046

60, 90, 180 and 360 degrees, using a proportional derivative control law. The data obtained for the calibration tests was used to analyze the yaw positioning capability of the AUV.

3. Lateral Positioning Experiment

The motion for the lateral positioning experiment is shown in Figure 3.8. In addition to inputs from the free gyro, inputs from the profiling sonar were used to determine the vehicle's lateral position with respect to the tank wall.

The control laws for the lateral positioning commands incorporated the combined behavior modes of yaw and lateral motion. For the yaw motion, the control effort is generated in the same way as discussed for the yaw positioning experiment. For the lateral motion however, the forward and aft lateral thrusters are used in the same direction.

$$F_{\text{Fwd Thrust (Lat)}} = F_{\text{Aft Thrust (Lat)}}$$

$$F_{\text{Thrust}} \propto V_{\text{Thrust}} |V_{\text{Thrust}}|$$

Therefore, for a linear control effort, accounting for both behavior modes, the lateral position commands for the thruster voltages are given using the following proportional derivative control laws:

$$V_{\text{Fwd Thrust}} = -K_{\psi}(\Psi - \Psi_{\text{com}}) - K_r(r - r_{\text{com}}) - K_Y(Y - Y_{\text{com}}) - K_v(\dot{Y} - \dot{Y}_{\text{com}})$$

$$V_{\text{Aft Thrust}} = K_{\psi}(\Psi - \Psi_{\text{com}}) + K_r(r - r_{\text{com}}) - K_Y(Y - Y_{\text{com}}) - K_v(\dot{Y} - \dot{Y}_{\text{com}})$$

$$K_r = K_{\psi} \times T_{d\psi}$$

$$K_v = K_Y \times T_{dY}$$

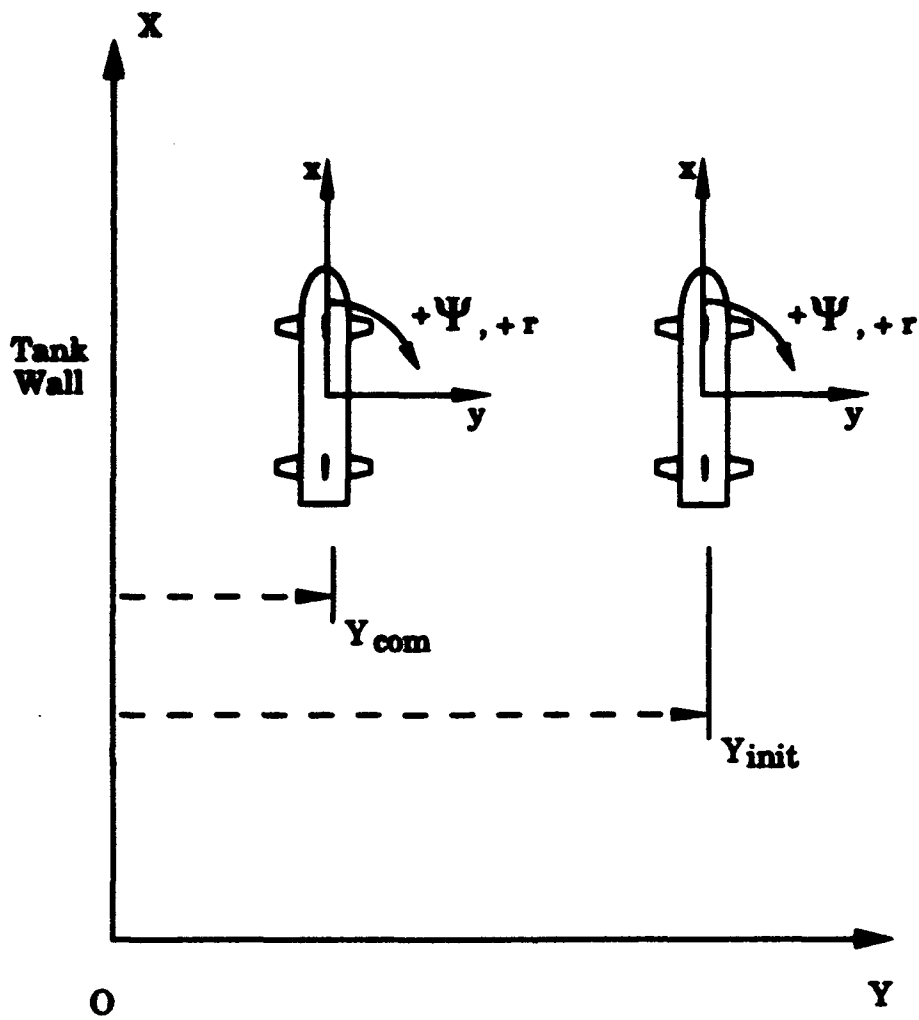


Figure 3.8 Lateral Positioning Experiment

Table 3.2 lists the test conditions for the lateral positioning experiment. The control law gains were varied in order to examine the coupling effects between the lateral and yaw motions. The effects of changes in the range of motion were examined by varying the initial and commanded positions to cover small and large changes in position. A commanded yaw position of zero degrees was given for all tests.

Data collected included range (global Y direction) to the wall, sway velocity, yaw position, yaw rate, and forward and aft thruster voltage as functions of time.

The sway velocity data was obtained by extracting an estimate of the derivative of the lateral range data from the sonar, using a Kalman filter subprogram. The smooth velocity estimate was used for the velocity error feedback. The filter also provided a smooth position estimate which was used for the position error feedback. The subprogram for the Kalman filter, in C source code, is provide in Appendix F.

4. Longitudinal Positioning Experiment

The motion for the longitudinal positioning experiment is shown in Figure 3.9. In addition to inputs from the free gyro, inputs from the profiling sonar were used to determine the vehicle's position with respect to the tank wall, ahead.

The control laws for the longitudinal positioning commands account for the behavior modes of yaw and longitudinal motion, however these modes are controlled separately through use of the thrusters and the stern propulsion

**TABLE 3.2 LATERAL AND LONGITUDINAL POSITIONING
EXPERIMENTS: TEST CONDITIONS**

LATERAL POSITIONING EXPERIMENT: TEST CONDITIONS

TEST	Ky	Tdy	Kpsi	Tdpsi	Yinit	Ycom	PSIcom
1	7	2	60	1	5.0	3.5	0.0
2	10	3	80	1	9.4	4.0	0.0
3	12	3	80	1	9.0	4.0	0.0
4	12	3	60	1	9.0	3.0	0.0
5	10	3	80	1	16.0	4.0	0.0

LONGITUDINAL POSITIONING EXPERIMENT: TEST CONDITIONS

TEST	SONAR GAIN	Kx	Tdx	Kpsi	Tdpsi	Xinit	Xcom	PSIcom
1	13	10	3	60	1	12.0	7.5	0.0
2	13	10	3	60	1	12.0	5.0	0.0
3	9	10	3	60	1	12.0	5.0	0.0
4	5	10	3	60	1	12.0	5.0	0.0
5	5	10	3	60	1	11.6	5.0	0.0
6	5	10	4	60	1	7.0	2.5	0.0
7	5	10	4	60	1	12.0	3.0	0.0

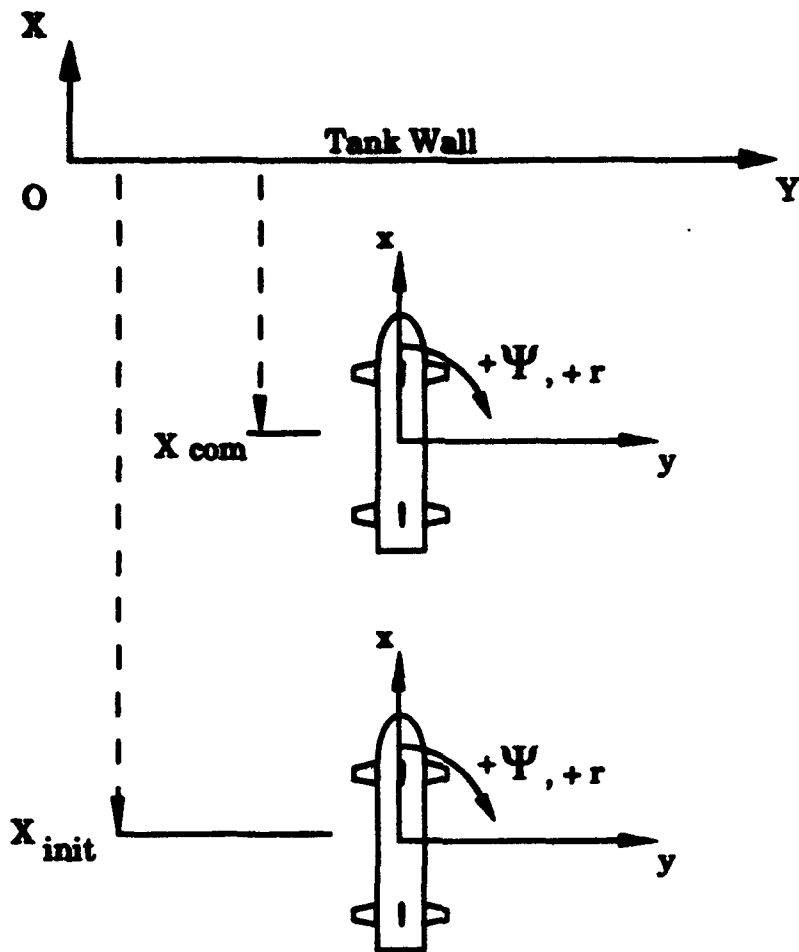


Figure 3.9 Longitudinal Positioning Experiment

motors. Similar to the thrusters for lateral motion, the stern propulsion motors are used in the same direction.

$$F_{\text{Port Prop}} = F_{\text{Starb Prop}}$$

$$F_{\text{Prop}} \propto V_{\text{Prop}} |V_{\text{Prop}}|$$

Therefore, a linear control effort is achieved, by generating the longitudinal position commands using the following proportional derivative control law for the stern propulsion motor voltages:

$$V_{\text{Stern Prop}} = K_X (X - X_{\text{com}}) + K_u (\dot{X} - \dot{X}_{\text{com}})$$

$$K_u = K_X \times T_{dX}$$

In addition, as for the yaw positioning experiment, position commands for thruster voltages were given using the following control laws:

$$V_{\text{Fwd Thrust}} = -K_\Psi (\Psi - \Psi_{\text{com}}) - K_r (r - r_{\text{com}})$$

$$V_{\text{Aft Thrust}} = K_\Psi (\Psi - \Psi_{\text{com}}) + K_r (r - r_{\text{com}})$$

$$K_r = K_\Psi \times T_{d\Psi}$$

Table 3.2 lists the test conditions for the longitudinal positioning experiment. The sonar gains were varied in order to examine the effects on the stability of the position data. The sonar gains shown are equivalent to the percentages of the total transmission power of the transducer. The thruster voltage control law gains for yaw position were set at 60 and one (proportional and derivative, respectively), and a commanded position of zero degrees was given.

The lateral and yaw motion coupling effects were examined along with the effects of changes in the range of motion.

Data collected included range (global X direction) to the wall, surge velocity, yaw position, yaw rate, and forward and aft thruster, as well as stern propulsion motor voltages as functions of time.

The surge velocity data was obtained, similarly to the lateral positioning experiment, through the use of the Kalman filter subprogram.

IV. EXPERIMENTAL RESULTS

The purpose of this chapter is to document trends in the experimental data collected for the AUV positioning experiments. Each type of motion studied (yaw, lateral and longitudinal), is addressed separately, and specific observations are made with respect to the dynamics of the motion, ability to achieve the commanded final position, commanded thruster and stern propulsion voltages and where applicable, the effects of changes in control law gains, sonar gains and the range of motion.

The results of the positioning experiments are then compared to a theoretical model.

A. YAW POSITIONING EXPERIMENT

As described in Chapter III, yaw positioning experiments were used for the rate gyro calibration. Inputs from the free gyro were used to determine the vehicle's yaw position. Position commands were given using proportional derivative control laws, for thruster voltages. The position commands were given for yaw angles of (negative) 30, 60, 90, 180 and 360 degrees (relative to a starting position).

The data obtained for the calibration tests was used to analyze the yaw positioning capability of the AUV. The data recorded included yaw position, yaw rate and forward and aft thruster voltage inputs as functions of time.

Figure 4.1 shows the yaw position, yaw rate and thruster voltages for the 90 degree test. The yaw position curve shows the motion response expected from a proportional derivative control law. During the initial stage of motion, the vehicle did not quite reach a constant turning rate as seen by an inflection point at approximately six seconds. With a steady state error band of approximately seven degrees, a single overshoot is observed due to inertial forces initially dominating the motion. Drag forces, proportional to the square of the yaw rate then became dominant, and the motion of the vehicle was heavily damped to an accurate steady state position.

The yaw rate curve shows consistent results with peak turning rates occurring at approximately six and 13.5 seconds.

The thruster voltage curve shows the forward and aft thrusters were employed in equal and opposite directions. Also note that saturation had occurred until approximately six seconds, which as previously mentioned, was not long enough to reach a constant turning rate.

The effects of the magnitude of the commanded turn are shown in Figure 4.2. The yaw position curves show that the vehicle had reached a constant, peak turning rate at approximately seven seconds, for the 180 and 360 degree tests. Consistent dynamic results are shown with single overshoots followed by heavily damped approaches to accurate steady state positions.

The yaw rate curves show the constant turning rates for the 180 and 360 degree tests. The differences in the values of the rates is due to experimental repeatability. The average peak turning rate was observed to be approximately 16.0 degrees per second.

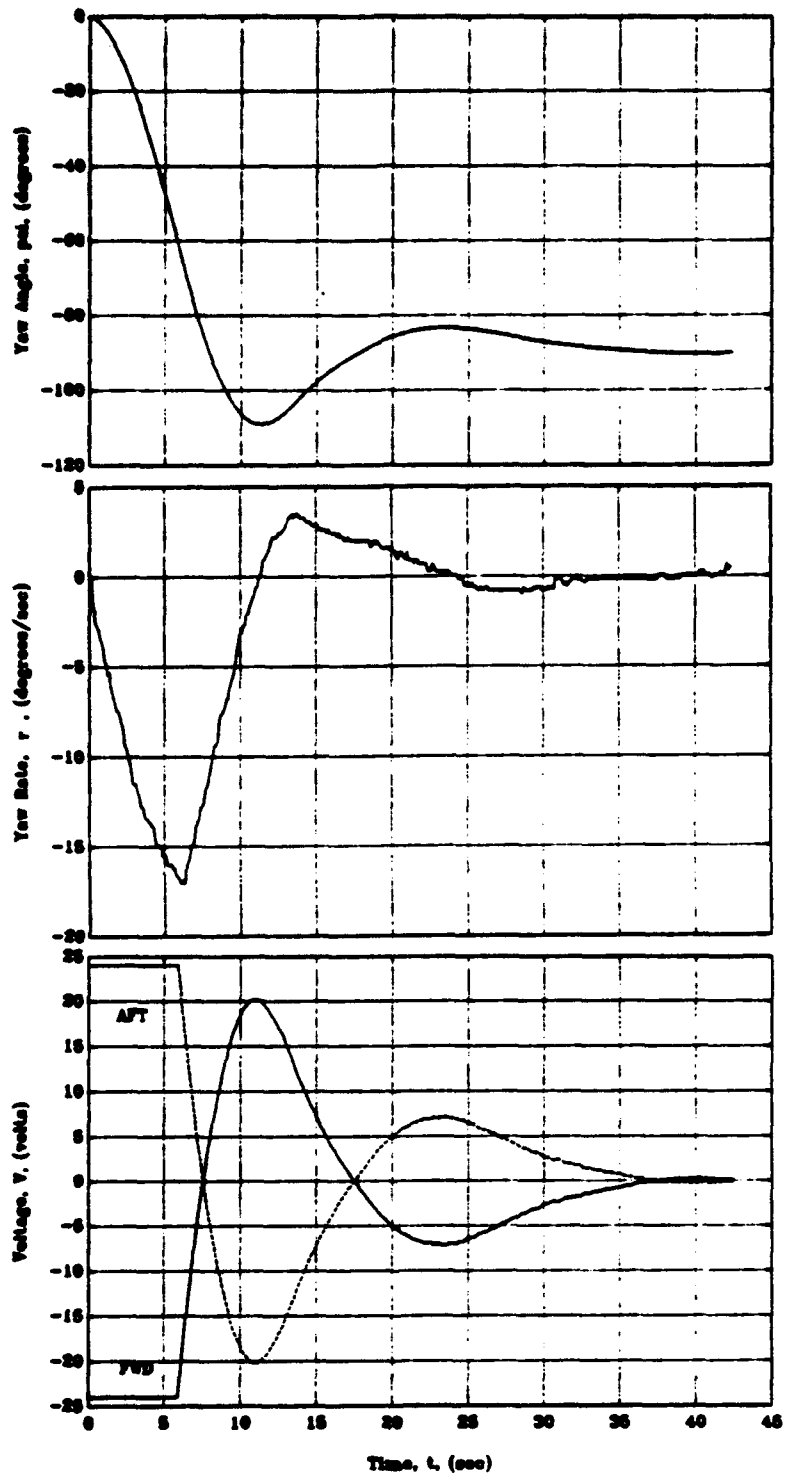


Figure 4.1 Yaw Position Experiment: 90 Degree Test

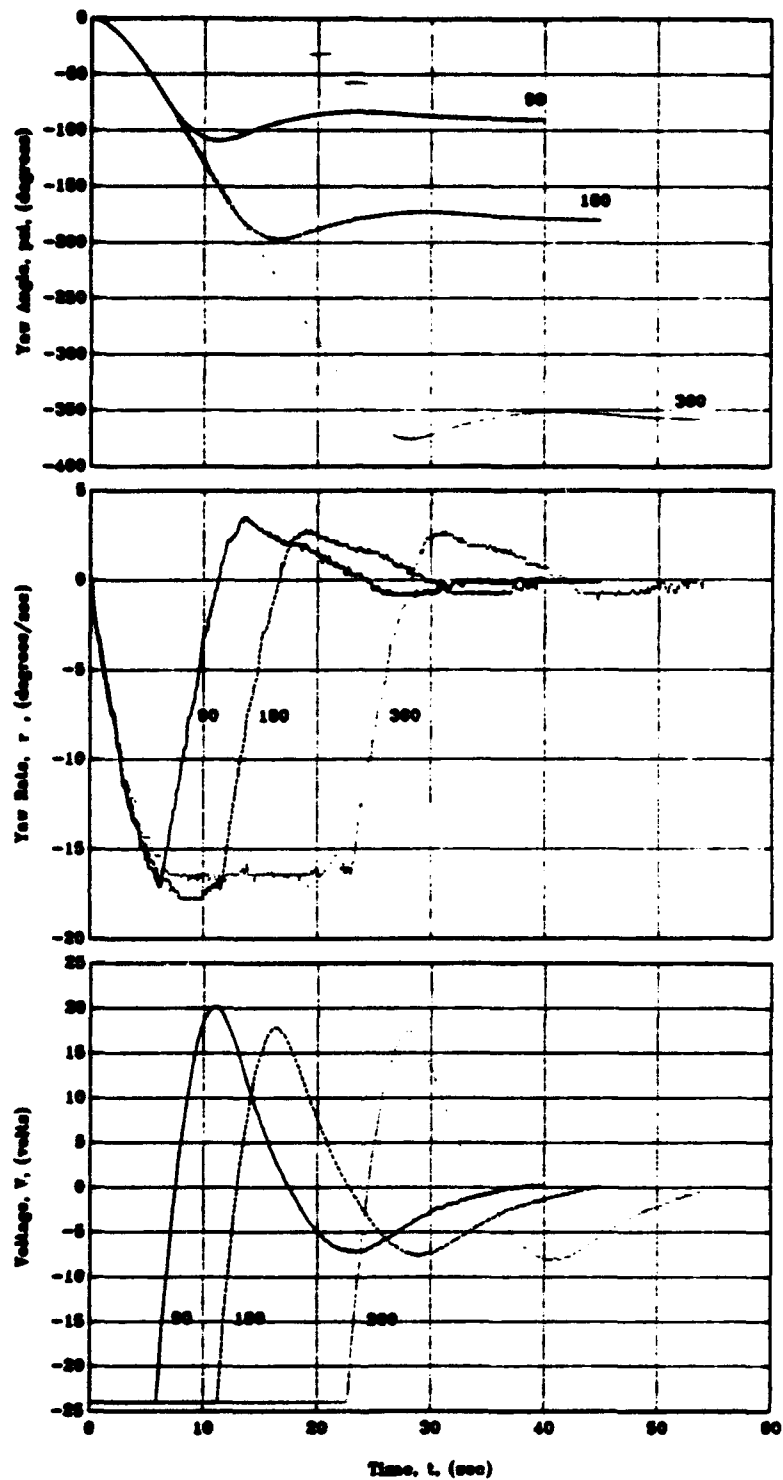


Figure 4.2 Yaw Position Experiment: 90, 180 and 360 Degree Tests

While the error is small, the final steady state yaw position was not exact in all cases. As discussed in Cody (1992), a small voltage threshold exists for the thruster motors, due to mechanical friction in the motor and reduction gear housing (stiction), which prevents very small corrections in position. This condition, to varying extents exists in all of the thruster assemblies as well as the stern propulsion assemblies.

The thruster voltage curves show the different time periods of saturation for the three tests. The differences in the peak voltages are due to the differences in the combined effects of the position error and the turning rate from which the proportional derivative control law determines the control effort. As previously mentioned, the final steady state voltage was not always zero volts due to thruster stiction.

The vehicle's ability to recover a commanded position, given a disturbance is shown in Figure 4.3. Once the vehicle reached the commanded position, it was given two manual disturbances in the direction of the overshoot. In both cases, the commanded position was quickly recovered. The thruster curve shows that saturation occurred for both recovery efforts.

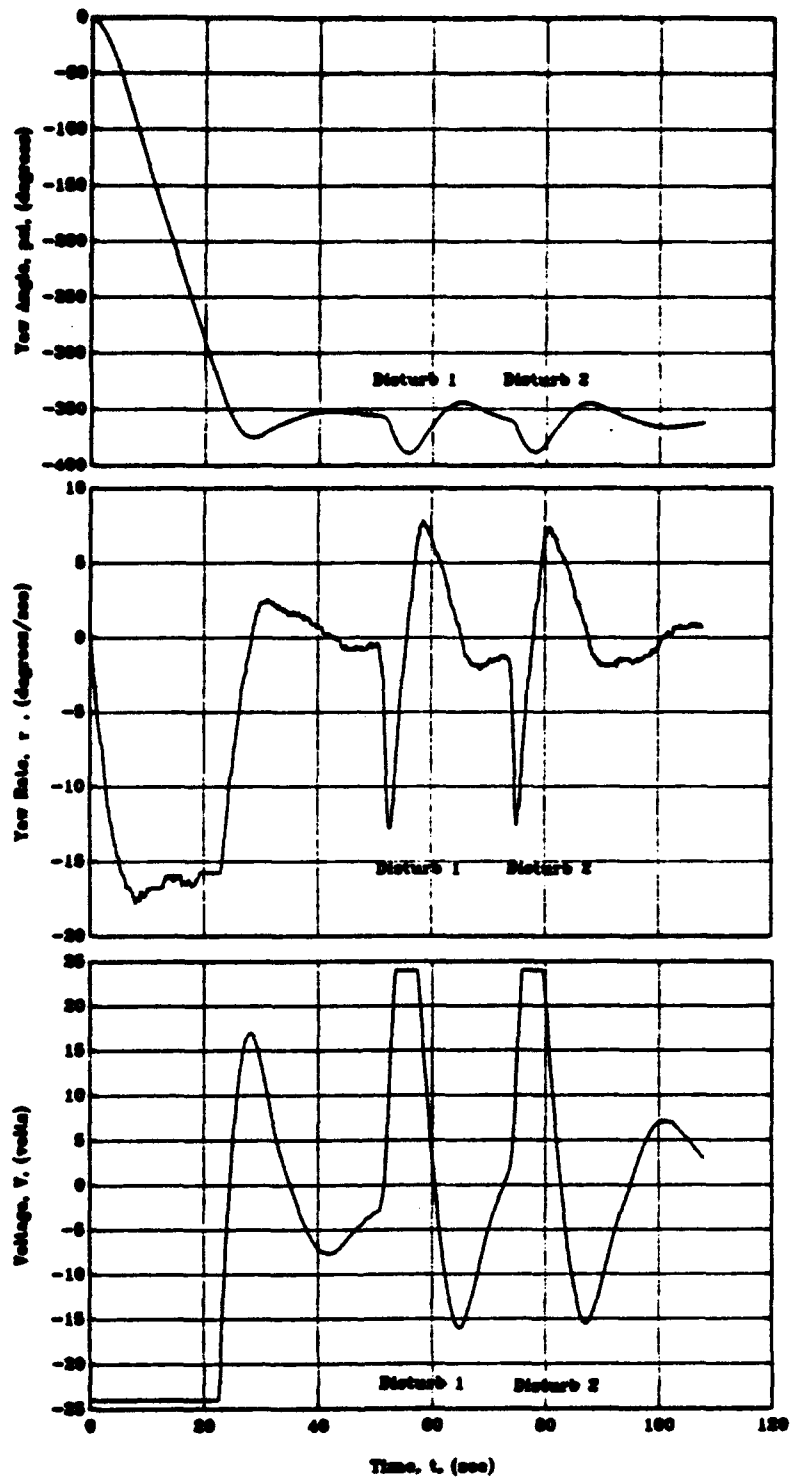


Figure 4.3 Yaw Position Experiment: 360 Degree Test, with Disturbances

B. LATERAL POSITIONING EXPERIMENT

The procedure for the lateral positioning experiment was described in Chapter III. Inputs from the free gyro and the profiling sonar were used to determine the vehicle's lateral position with respect to the tank wall. Position commands for the thruster voltages were given using proportional derivative control laws.

The test conditions for the lateral positioning experiment are shown in Table 3.2. The data collected included range (global Y direction) to the wall, sway velocity, yaw position, yaw rate, and forward and aft thruster voltage as functions of time.

Figure 4.4 shows the results for Test 1. The range curve shows a single overshoot approach to an accurate steady state commanded position for a modest positioning command as expected for the proportional derivative control. Consistent with the results for the yaw positioning experiment, error in the final steady state position achieved is due to thruster stiction. A noticeable amount of noise is present in the range signal and is emphasized in the velocity curve.

The yaw position curve shows very small deviations from the commanded zero degree position. For clarity, the negative value of the forward thruster voltage was plotted for the thruster voltage curve. Neither thruster reached saturation for this small range of motion, however the relative dominance of the yaw position error to the control effort can be seen in the difference between the voltage curves. This difference is shown in Figure 4.5, where the yaw position curve is also plotted for comparison.

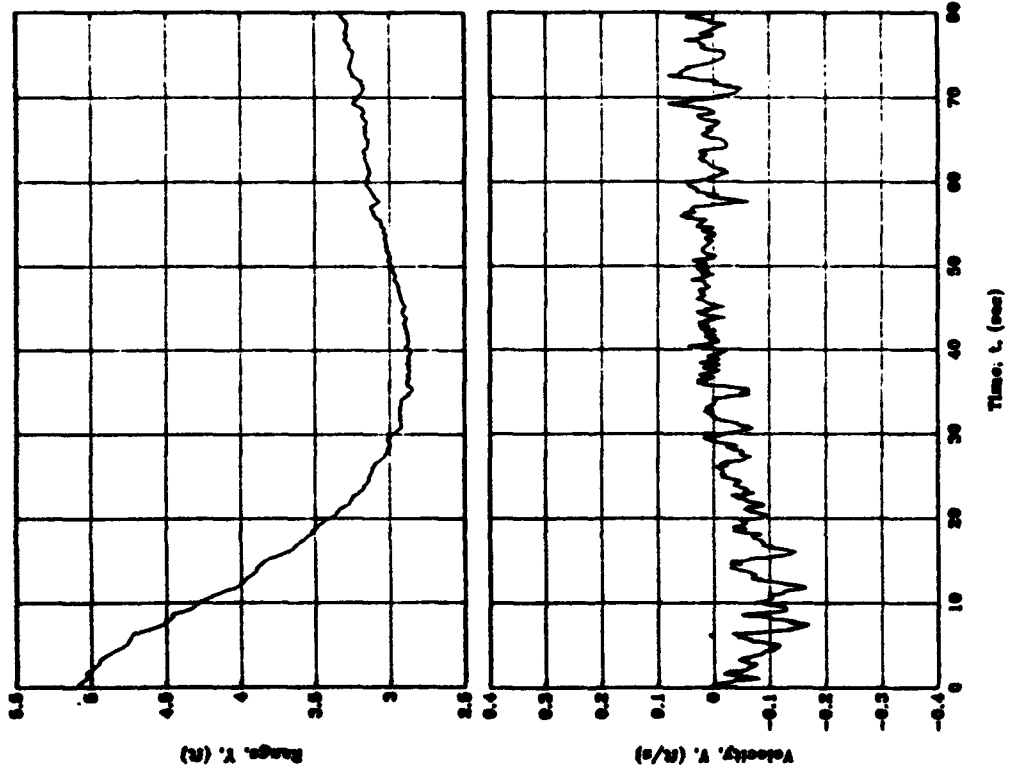
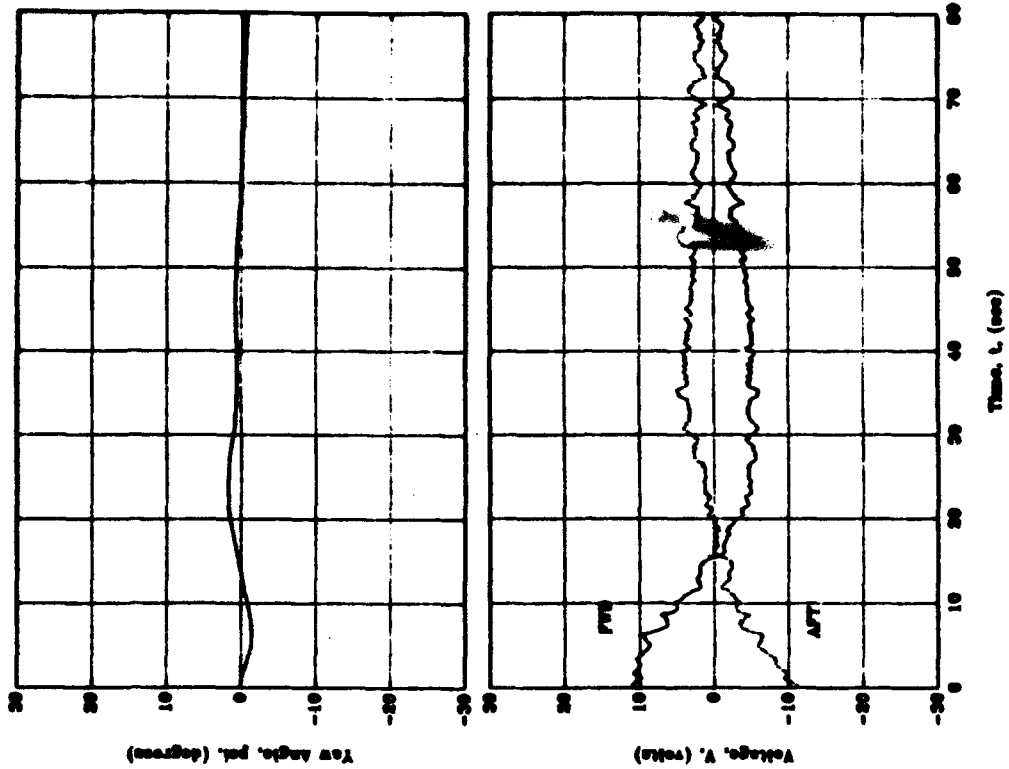
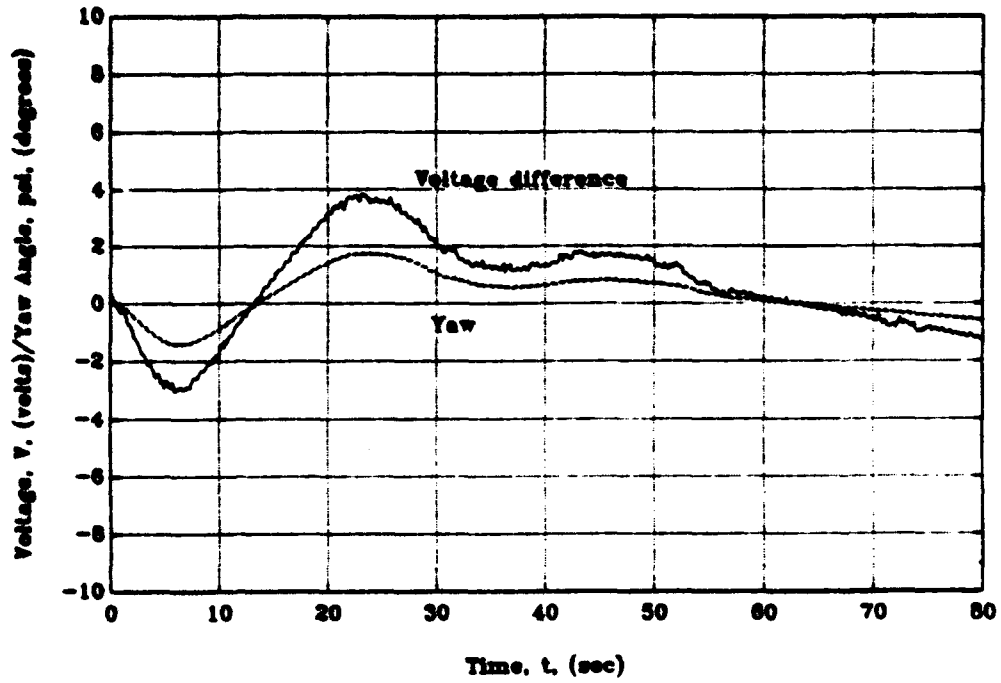


Figure 4.4 Lateral Position Experiment: Test 1



**Figure 4.5 Lateral Position Experiment: Test 1
(Thruster Voltage /Yaw Position)**

For Test 2, a greater range of motion was commanded, and the control law gains were increased. The yaw position curve of Figure 4.6 shows the characteristic approach to the commanded position with slightly less noise, until 70 seconds where the sonar return went unstable. This instability at close range, was attributed to a high sonar gain. The effects of reducing the sonar gains were examined during the longitudinal positioning experiment.

With the increased control law gains, coupling of the two motion control modes of yaw and sway was emphasized, as shown by the yaw position curve. Proportional derivative control does not compensate for this effect, and the result was a disturbance effect created by one mode working against the other.

The thruster voltage curve shows that both thrusters reached saturation. The aft thruster was reduced sooner due to the decrease in yaw position caused by the smaller horizontal cross-section area of the vehicle's stern.

Further increase of the lateral position control law gains showed little reduction in the response time to achieve the commanded position in Test 3, however the yaw position was stabilized as shown in Figure 4.7.

Test 4 demonstrated that a softer vehicle response, in yaw position, resulted from reducing the yaw position control gains, as shown in Figure 4.8. In this test, greater sway induced yaw motion was developed.

A greater range of motion was attempted for Test 5, and as Figure 4.9 shows, the thrusters were saturated for a greater period of time resulting in reduced vehicle control in yaw position.

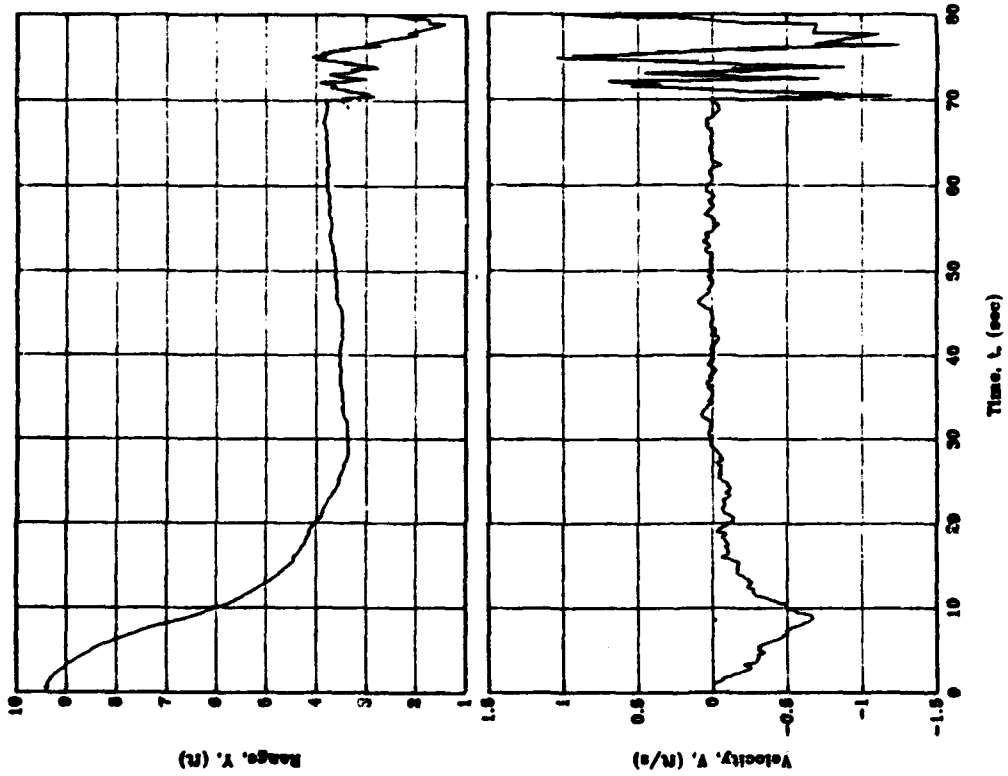
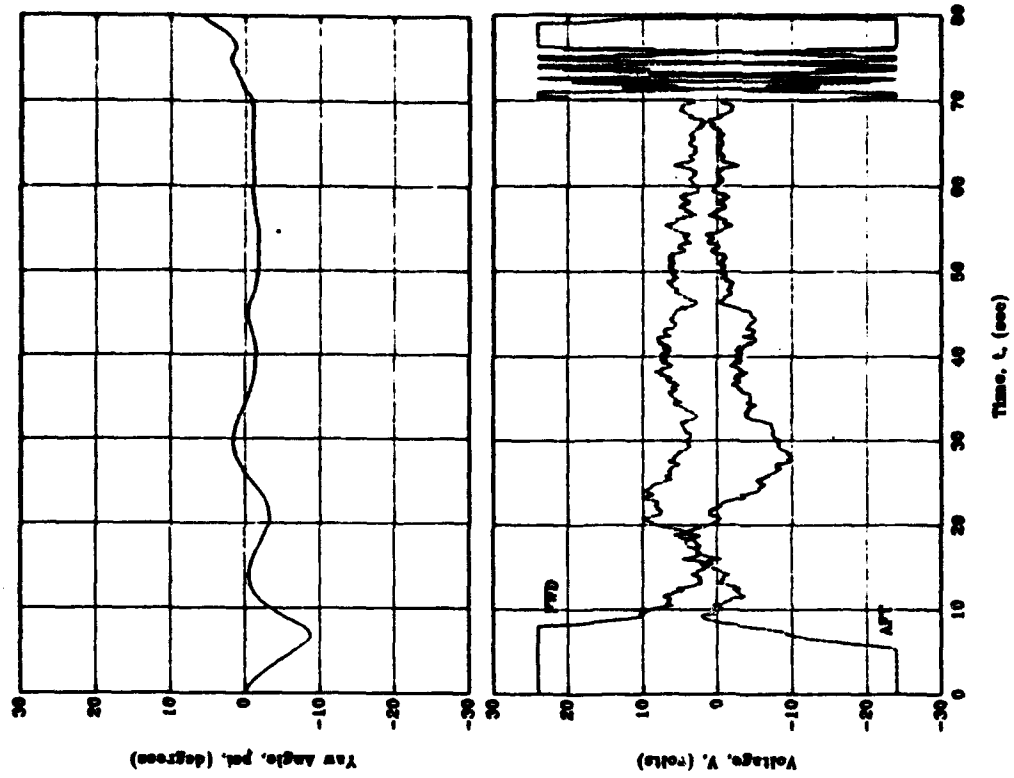


Figure 4.6 Lateral Position Experiment: Test 2

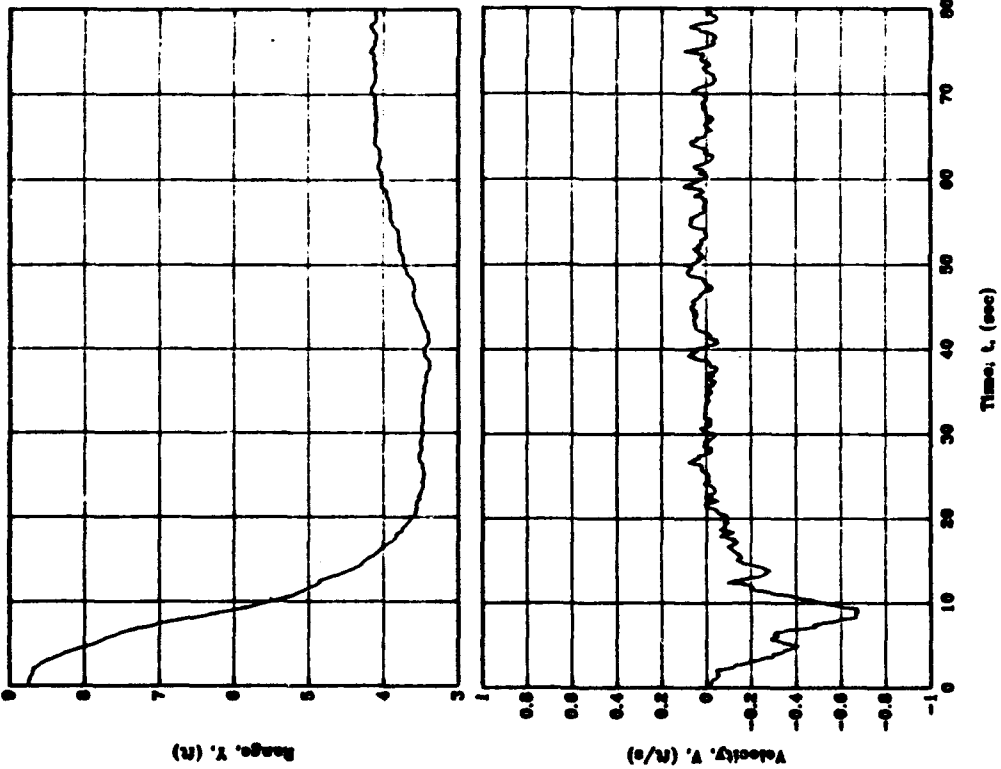
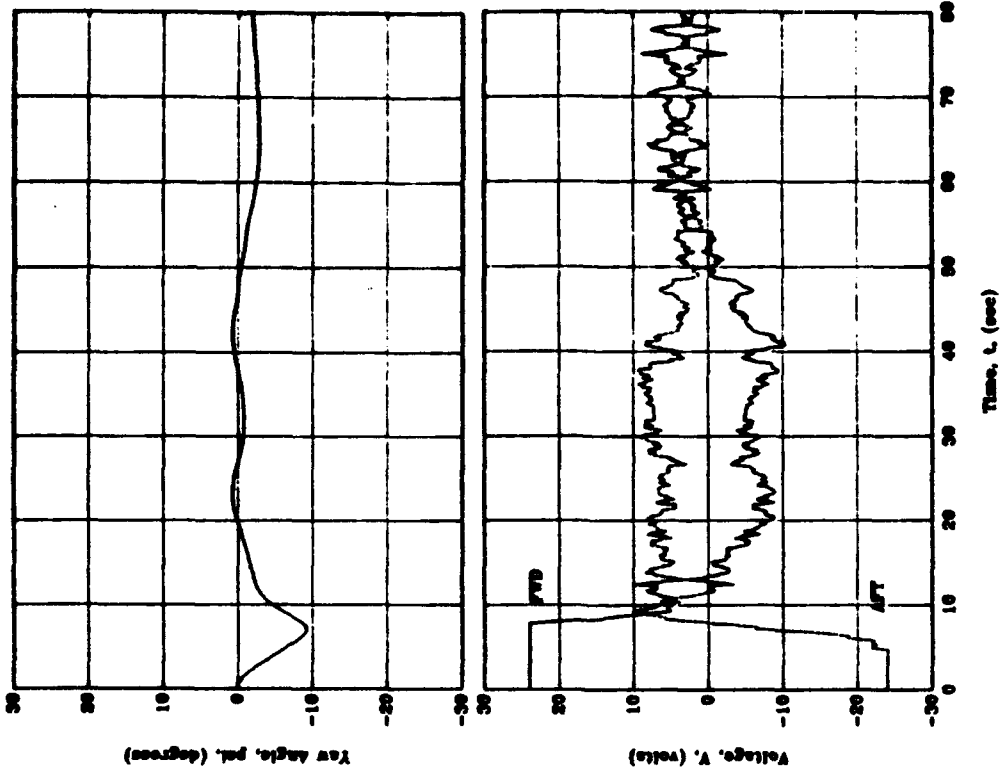


Figure 4.7 Lateral Position Experiment: Test 3

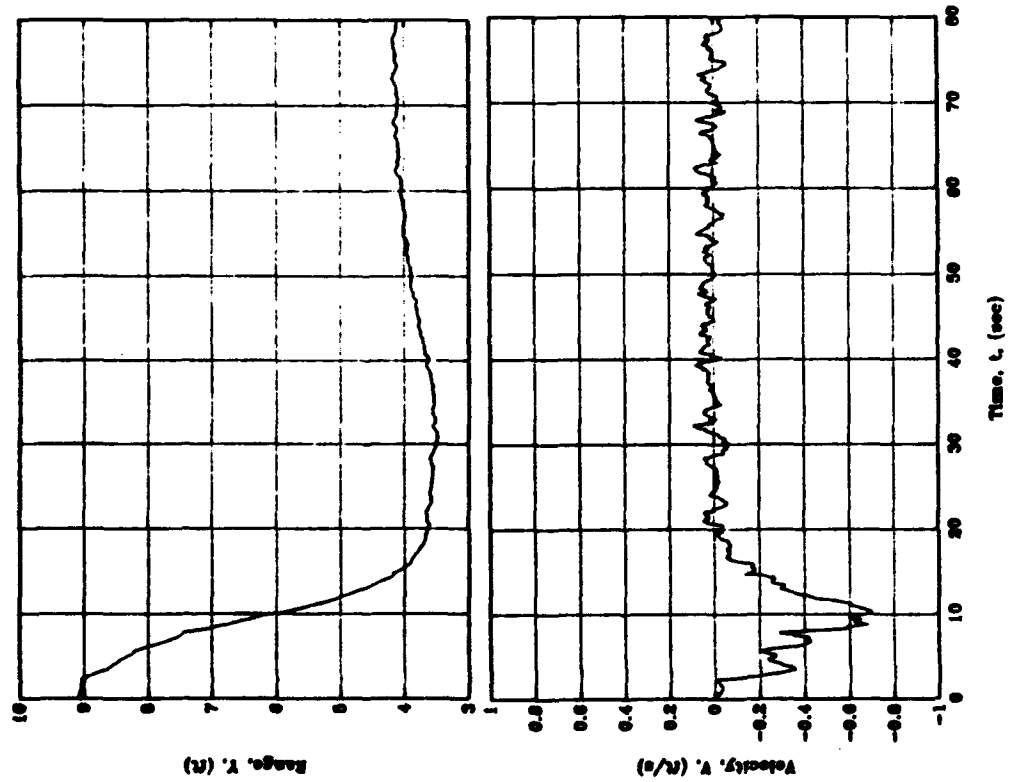
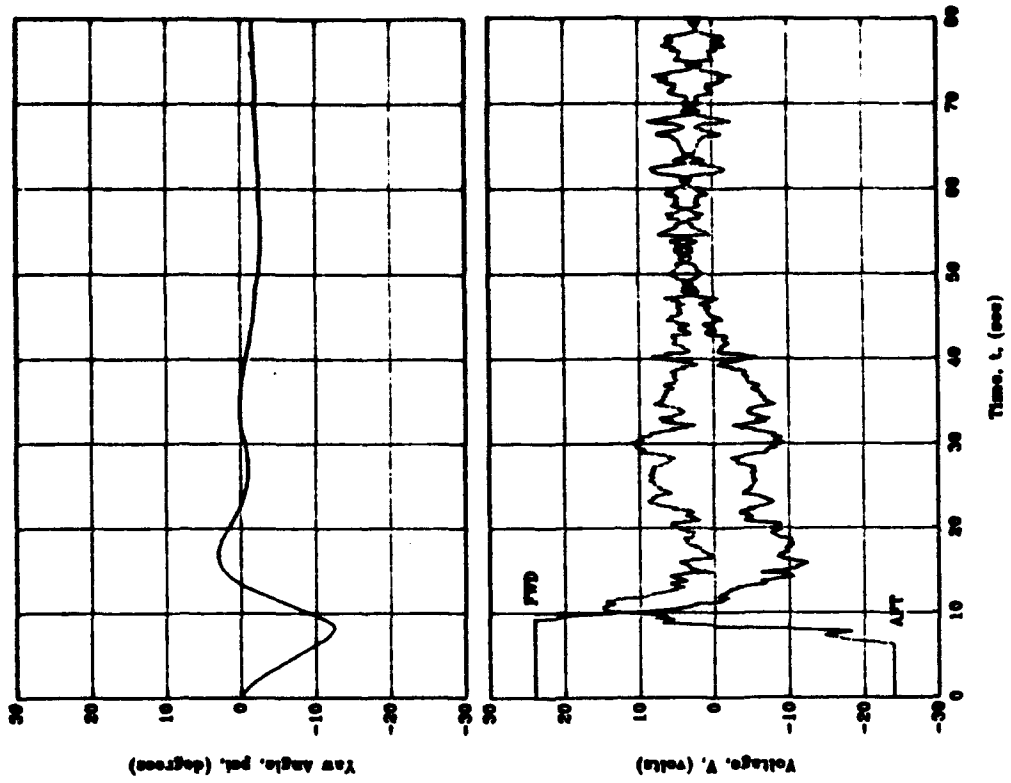


Figure 4.8 Lateral Position Experiment: Test 4

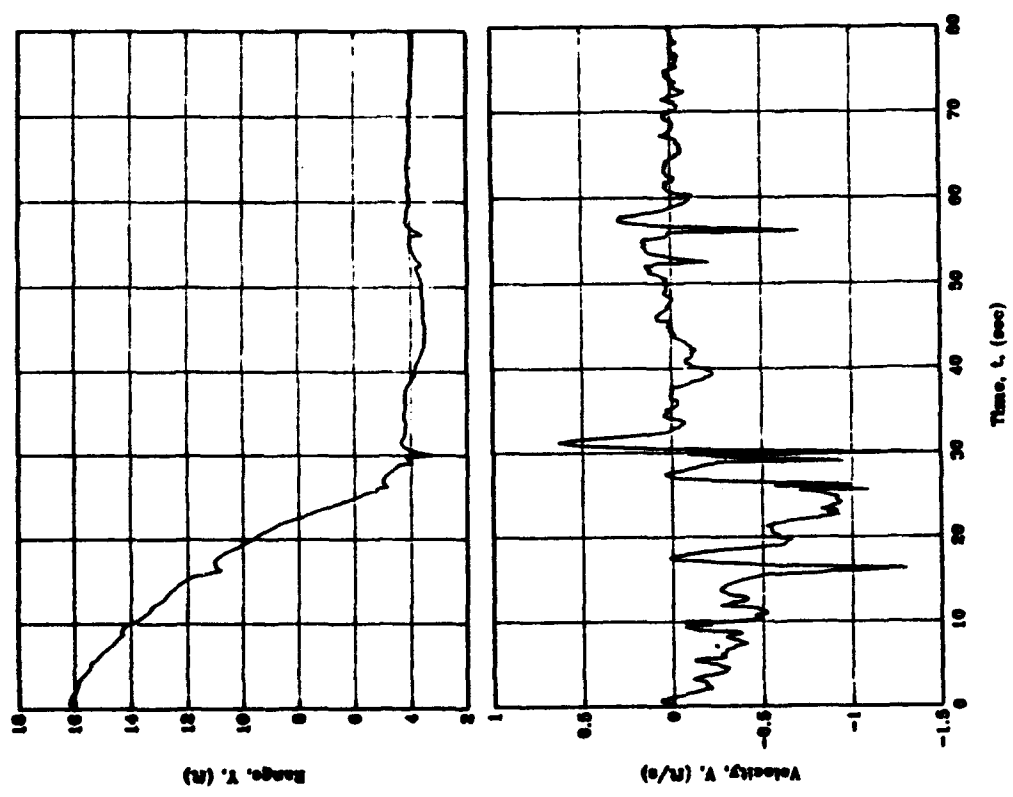
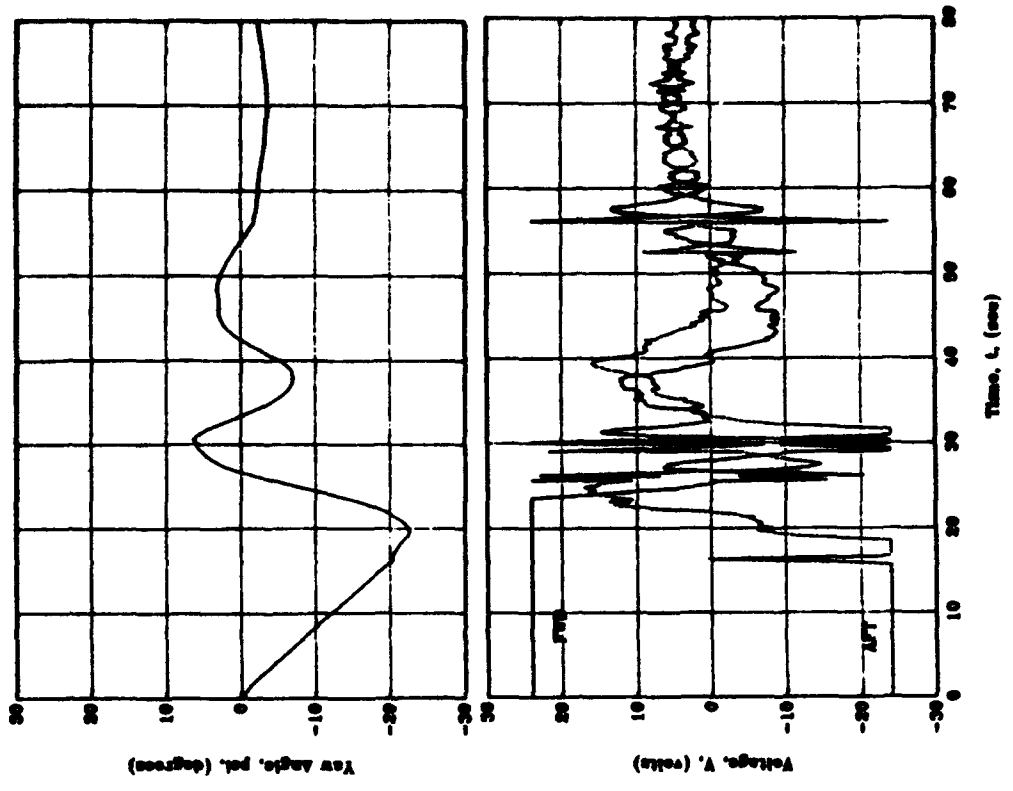


Figure 4.9 Lateral Position Experiment: Test 5

C. LONGITUDINAL POSITIONING EXPERIMENT

Chapter III described the procedure for the longitudinal positioning experiment. Inputs from the free gyro and the profiling sonar were used to determine the vehicle's longitudinal position with respect to the tank wall. Position commands for the stern propulsion and thruster voltages were given using proportional derivative control laws.

The test conditions for the longitudinal positioning experiment are shown in Table 3.2. The data collected included range (global X direction) to the wall, surge velocity, yaw position, yaw rate, forward and aft thruster voltage and stern propulsion motor voltage as functions of time.

The dynamic characteristics of the motion for Test 1 were consistent with the proportional derivative control as shown in Figure 4.10. A single overshoot was observed, with a highly damped approach to the commanded steady state position. The stiction effects were observed in the stern propulsion assemblies, which resulted in a small steady state position error in the longitudinal position.

The velocity curve reflects a greater amount of signal noise as the sonar reaches a position closer to the wall.

The yaw position curve reflects the motion induced by the stern propulsion motors operating independently with different levels of stiction.

The thruster voltage curve shows that small thruster control efforts were generated to correct the yaw motion. Although identical voltage signals were generated for both stern propulsion motors, the negative value of the right propulsion motor was plotted for clarity. Saturation was observed for both

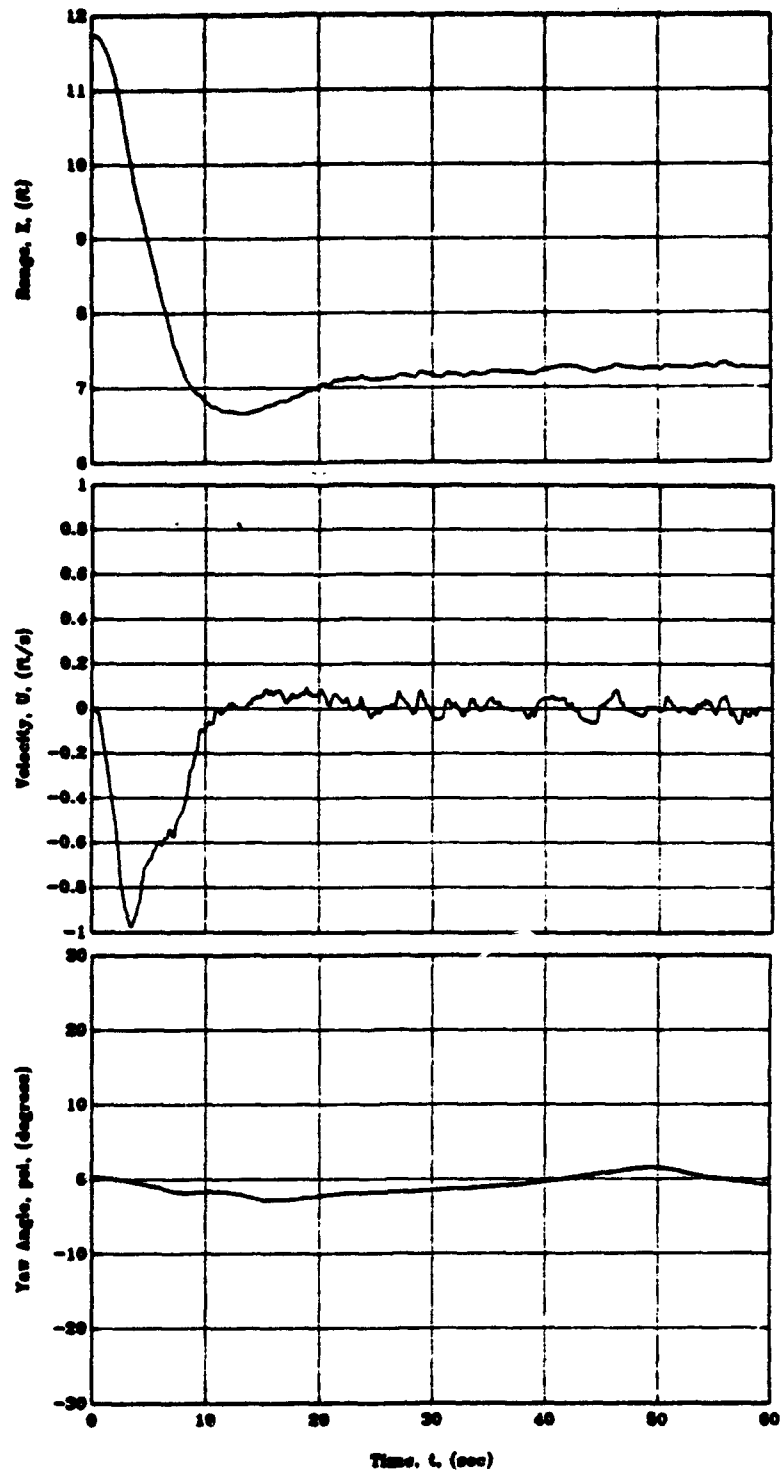


Figure 4.10 Longitudinal Position Experiment: Test 1

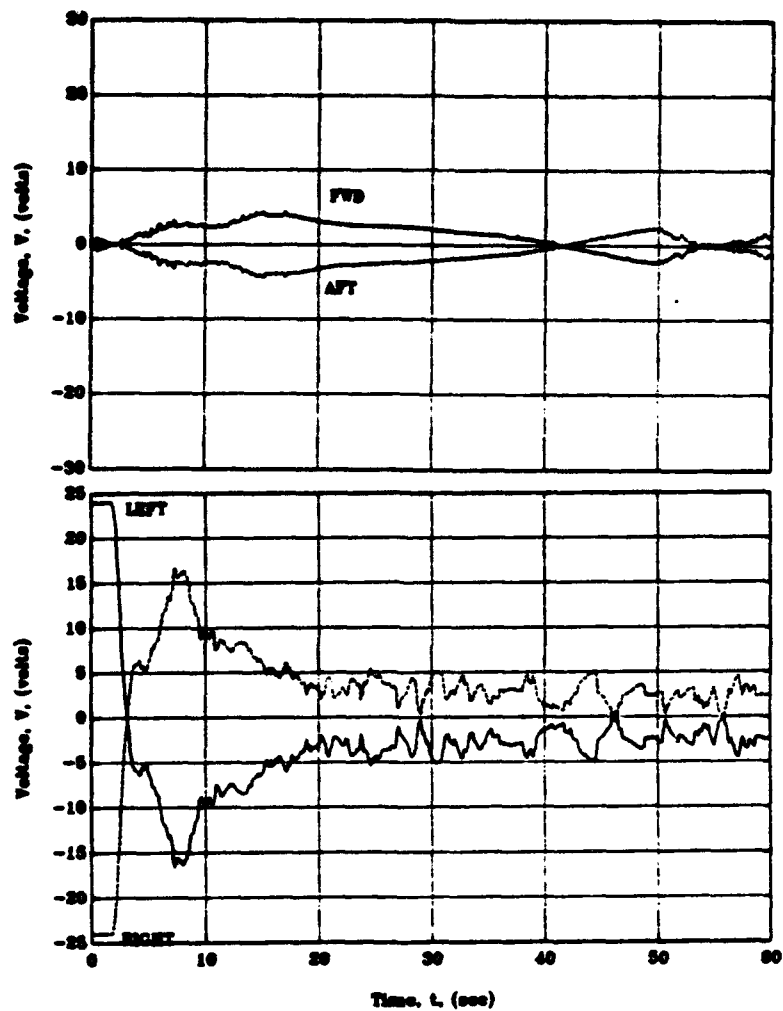


Figure 4.10 Longitudinal Position Experiment: Test 1 (continued)

motors followed by direction reversals to achieve the commanded steady state position.

For Test 2, a final commanded position closer to the tank wall (5.0 feet) was attempted. As shown in Figure 4.11, the stern propulsion motors were saturated for a greater period of time and a higher surge velocity was reached which resulted in greater, reversing effort.

Additionally, as the sonar spent a greater amount of time in closer proximity to the wall, the range input became unstable. This effect produced a greater amount of noise in the lateral range and surge velocity plot.

The same commanded position was attempted for Test 3, however a lower sonar gain was used (9 vice 13). Figure 4.12 shows that the same motion resulted with less noise produced in the range and velocity signals.

For Test 4, the sonar gain was reduced further (to 5), however very little improvements in the motion or the noise levels were observed, as shown in Figure 4.13.

Figure 4.14, for Test 5 demonstrates the repeatability with the same results as Test 4.

A very aggressive approach to the wall was attempted for Test 6 using a commanded position of 2.5 feet. Figure 4.15 shows that frequent voltage adjustments were generated to the stern propulsion motors which resulted in slight oscillations in longitudinal position and velocity as the vehicle approached the steady state position.

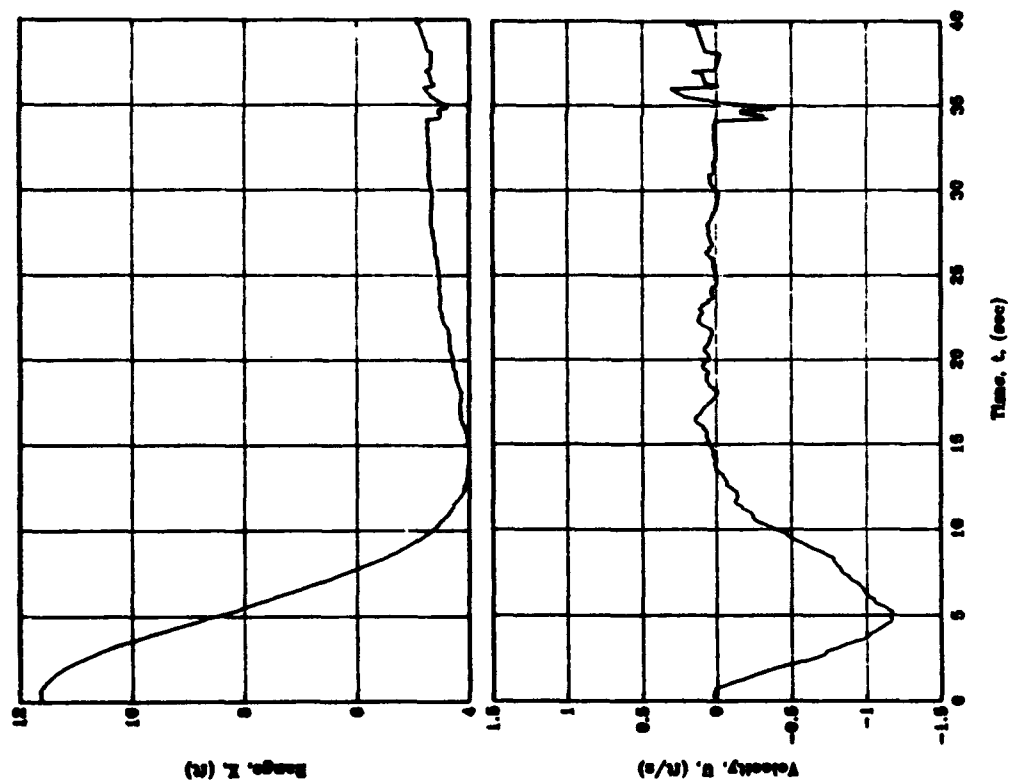
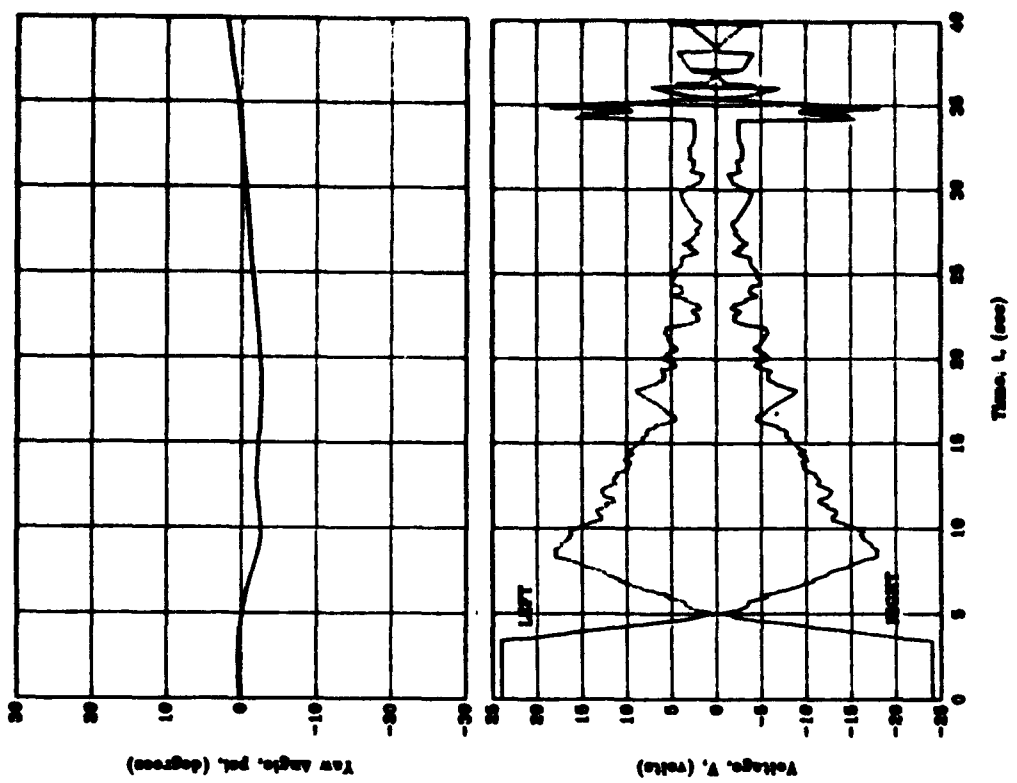


Figure 4.11 Longitudinal Position Experiment: Test 2

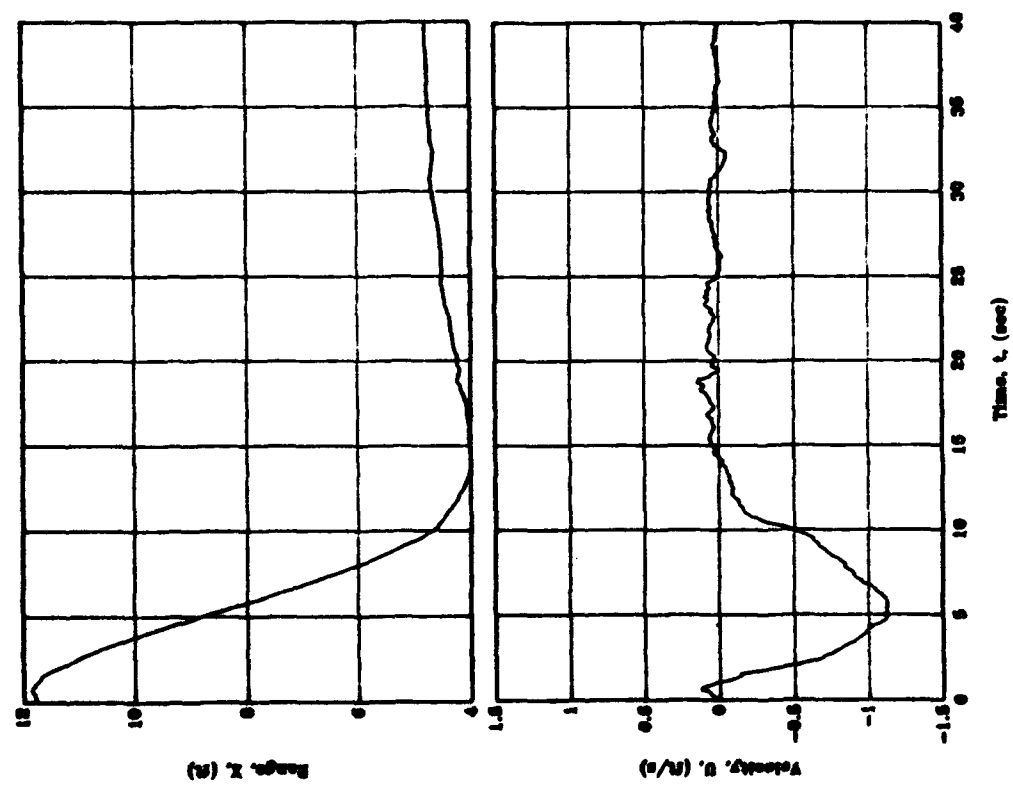
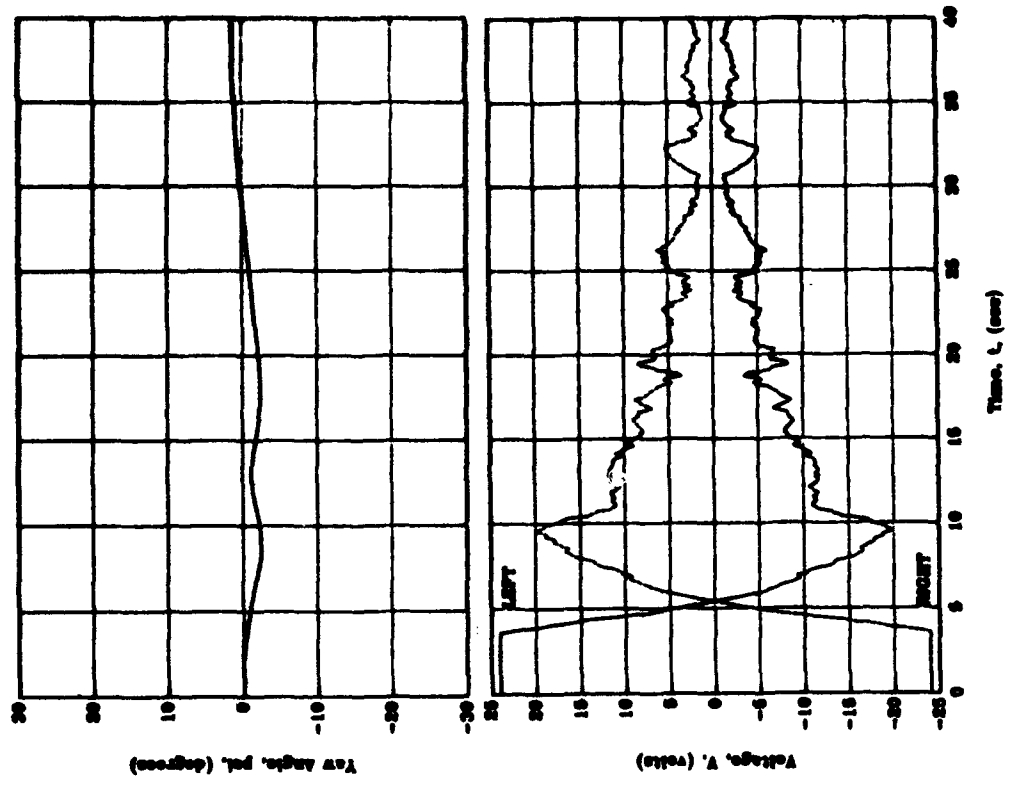


Figure 4.12 Longitudinal Position Experiment: Test 3

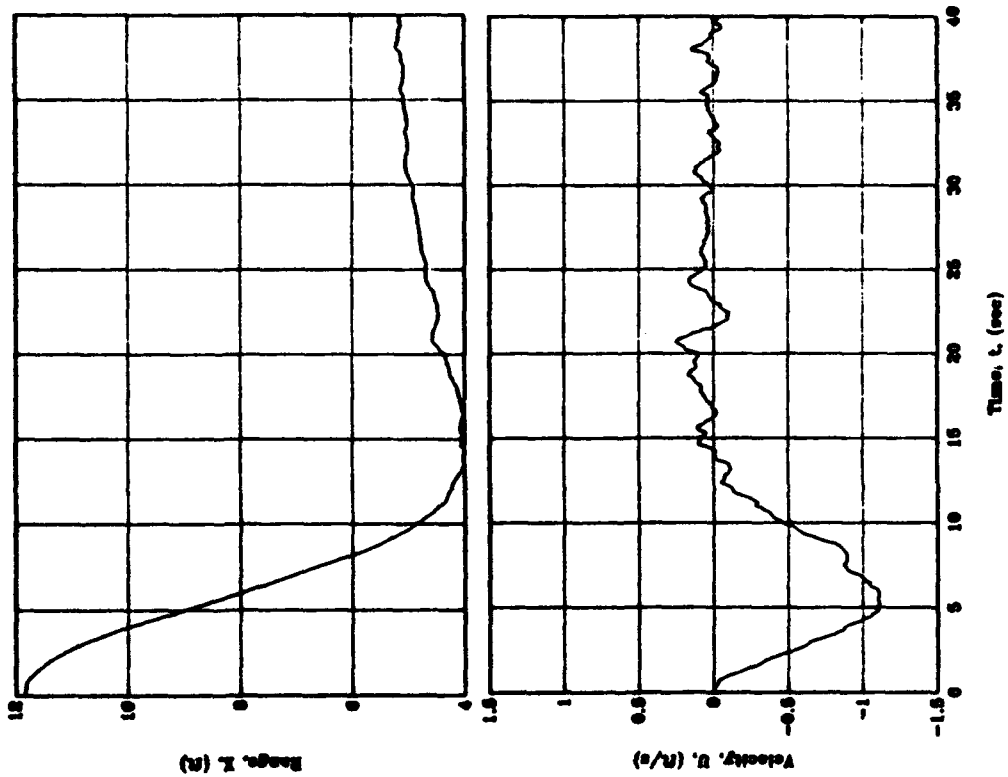
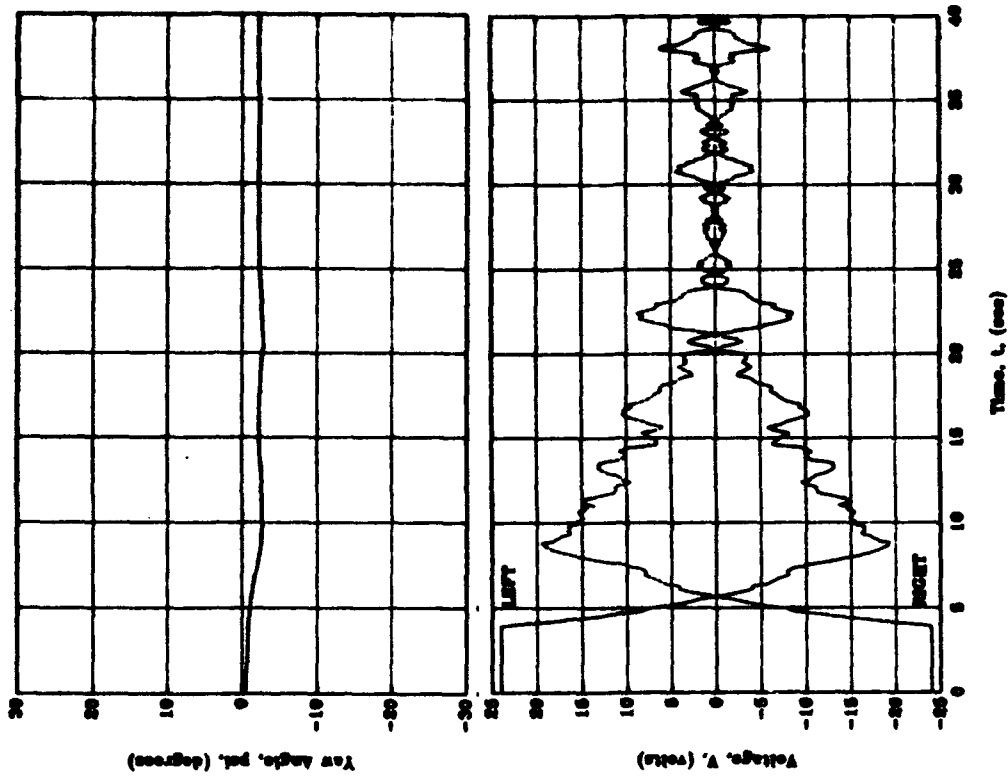


Figure 4.13 Longitudinal Position Experiment: Test 4

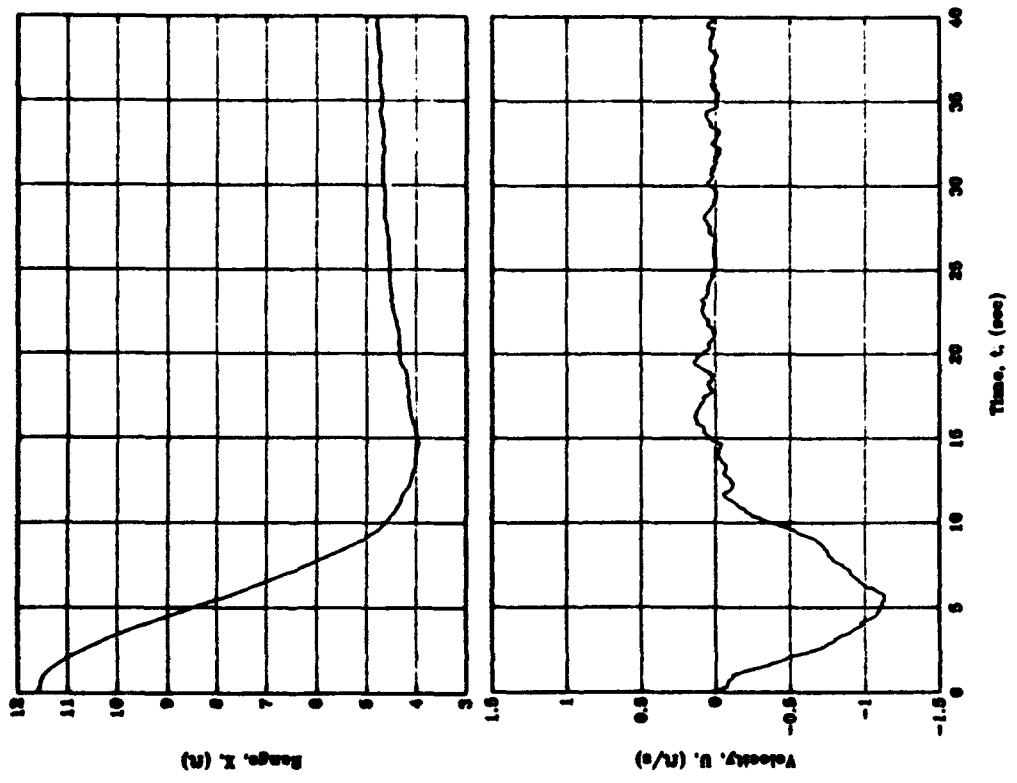
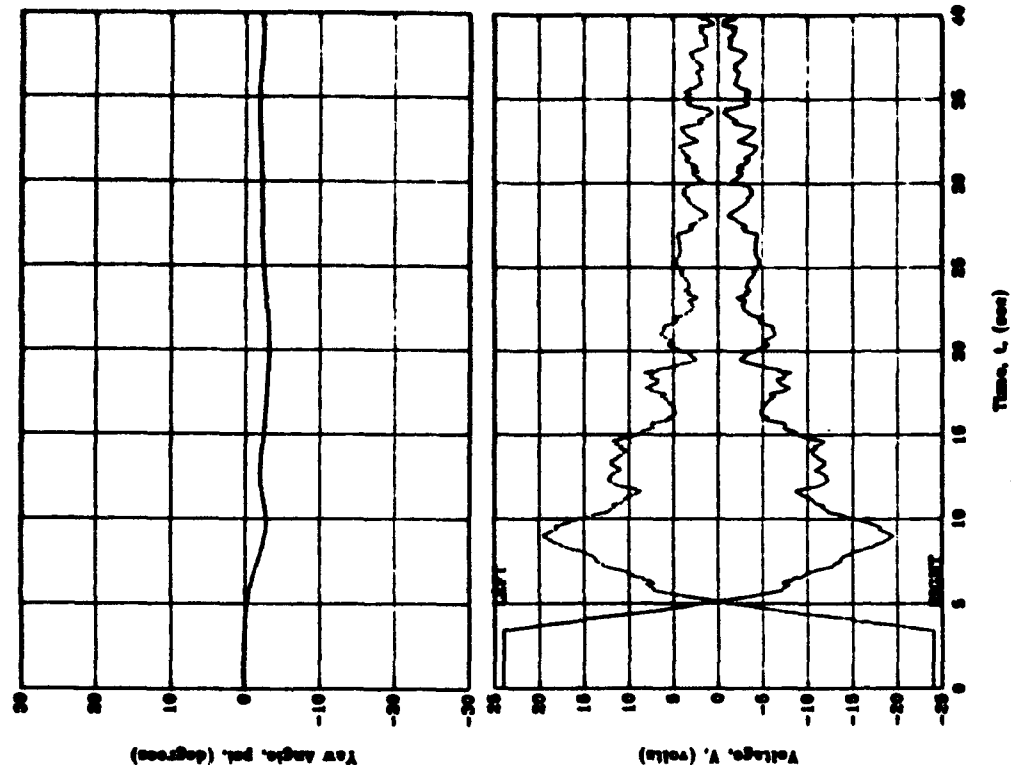


Figure 4.14 Longitudinal Position Experiment: Test 5

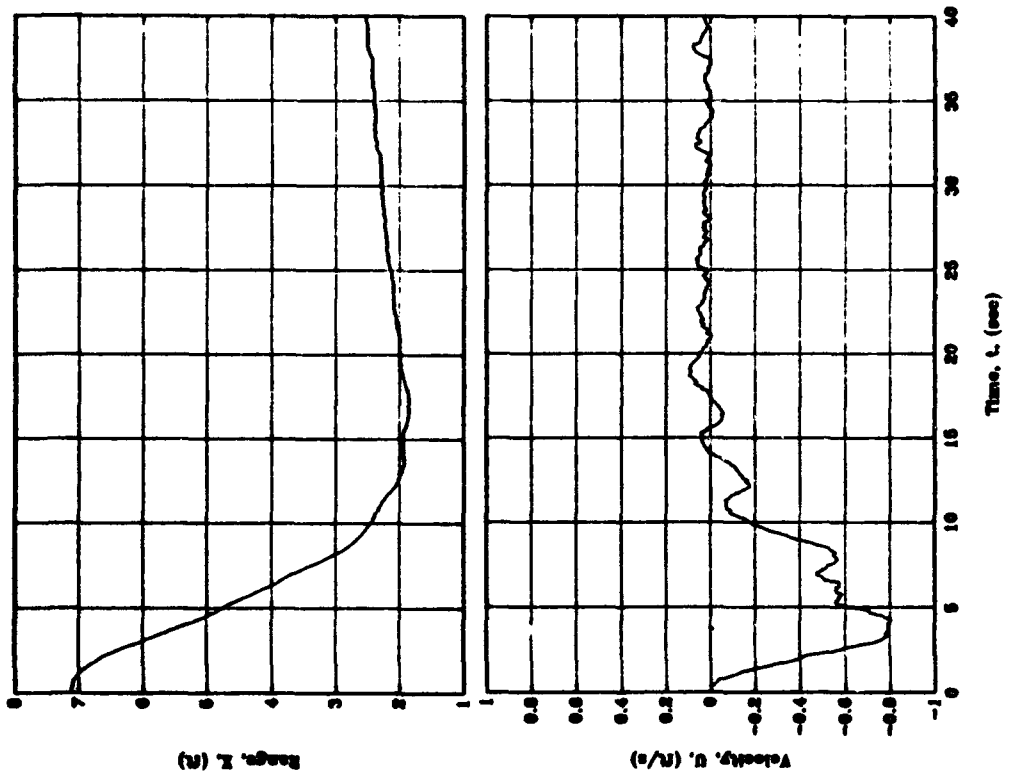
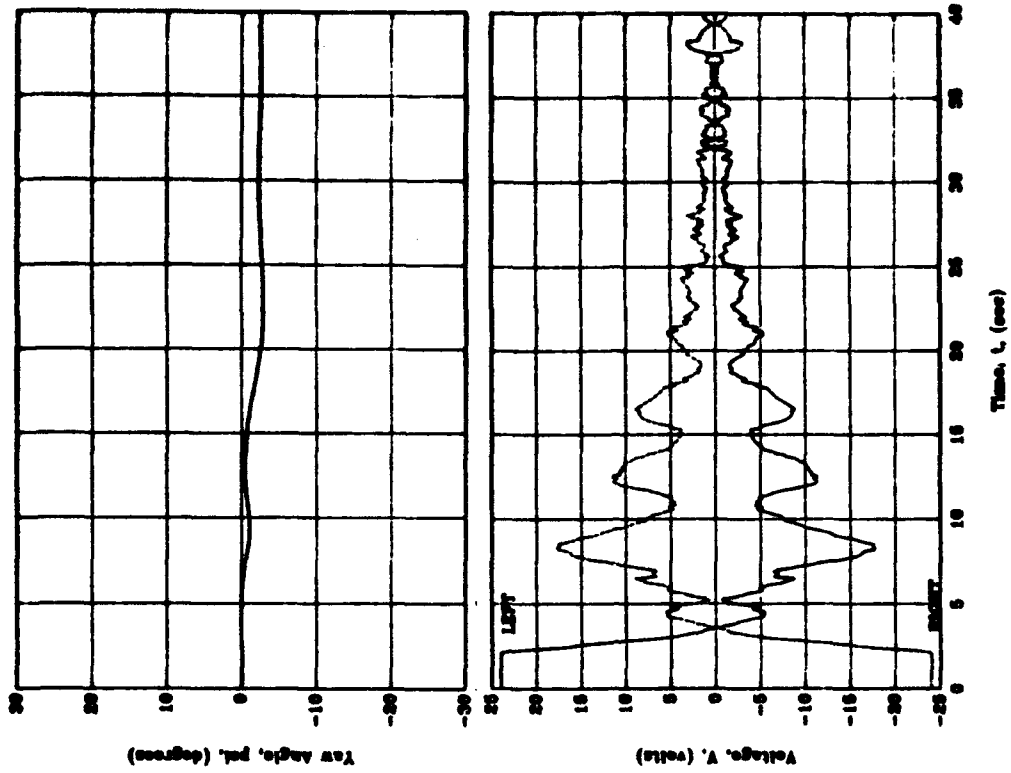


Figure 4.15 Longitudinal Position Experiment: Test 6

The largest range of motion (12.0 to 3.0 feet) was demonstrated for Test 7. Figure 4.16 shows a very good approach to the commanded steady state longitudinal position without the oscillations observed for Test 4.

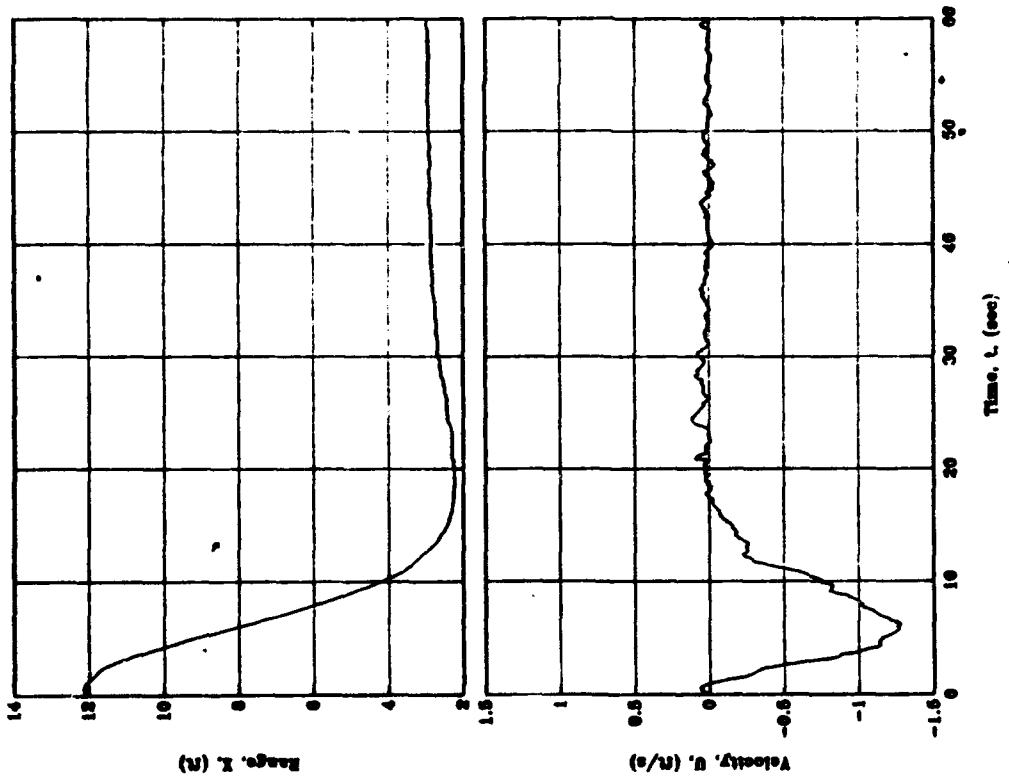
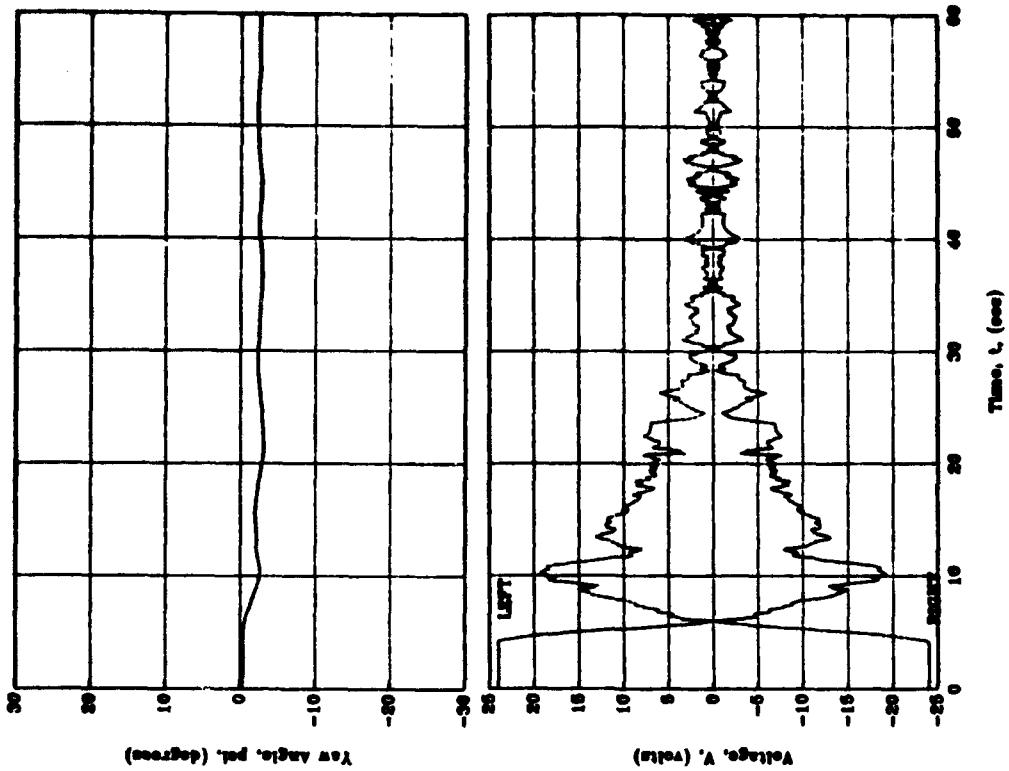


Figure 4.16 Longitudinal Position Experiment: Test 7

D. THEORETICAL MODEL

This section presents a theoretical model for the horizontal plane maneuvering of the AUV, during hover conditions. The development of the model is discussed in this section along with the results, which compare the actual motions of the AUV II, determined experimentally, with those predicted by the model.

1. Theoretical Model Development

The purpose of developing this theoretical model of the AUV, is to provide the capability to predict its motion under various maneuvering conditions. These results provide the basis for the development of a model based control system, whereby the predicted vehicle positions, velocities and accelerations during a particular maneuver are compared to the actual vehicle motions to produce an error signal which is then used to generate a corrective control signal. The model so developed is particular to the NPS AUV II vehicle although its structure may be generalized to other vehicles if specific coefficient values for those other vehicles were determined.

For the development of the AUV model, the simplified case of horizontal plane maneuvering is considered. Table 4.1 lists the symbols and variables used in the model development. The variables used are referenced to the global and body fixed coordinate systems of Figure 3.4. Only those variables applicable to two-dimensional, horizontal plane motion are shown. A dot over a variable indicates the time derivative of that variable.

In the case of horizontal plane maneuvering, the assumption was made that the center of mass of the vehicle is below its body fixed origin (so

TABLE 4.1 AUV MODEL: SYMBOLS AND VARIABLES

Symbol/Variable	Description
X, Y	Distance along global coordinate axis
x, y	Distance along body fixed coordinate axis
u, v	Velocity component (surge, sway) along body fixed coordinate (x, y) axis
r	Angular velocity component (yaw rate) about body fixed coordinate (z) axis
$X_, Y_$	Force component along body fixed coordinate axis
$N_$	Moment component about body fixed coordinate (z) axis
Ψ	Yaw angle
m	Mass of AUV II
I_{zz}	Moment of inertia about the body fixed coordinate (z) axis
$F_$	External force applied to the vehicle
$M_$	External moment applied to the vehicle
Subscripts	
f	External force or moment component due to net hydrodynamic loads on the vehicle
uu, vv, rr	Hydrodynamic force or moment component due to square law drag
$\dot{u}, \dot{v}, \dot{r}$	Hydrodynamic force or moment component due to added mass
Prop	Stern propulsion motor
Thrust	Thruster

that z_G is positive), while x_G and y_G are zero. Additionally, it was assumed that the inertial properties of the AUV are symmetric. Therefore, the motions of interest involve only the variables u , v and r (surge, sway and angular yaw velocities).

The equations of motion for the AUV were then written as follows:

$$m\dot{u} = mvr + X_r$$

$$m\dot{v} = -mur + Y_r$$

$$I_{zz}\dot{r} = N_r$$

$$\dot{\Psi} = r$$

$$\dot{X} = u \cos \Psi - v \sin \Psi$$

$$\dot{Y} = u \sin \Psi + v \cos \Psi$$

In the above equations, X_r , Y_r and N_r are changes in hydrodynamic forces on the vehicle body resulting from propulsor action and vehicle motion. They arise from hydrodynamic lift, drag and added mass origins. It was further assumed that for hover conditions, lift forces arising from small angles of drift, were minimal. The forces acting on the vehicle were then limited to added mass effects, drag and the maneuvering forces generated by the thrusters and stern propulsion motors.

The drag forces were modeled as being proportional to the square of the velocity using the absolute value to account for direction. Using dimensional hydrodynamic coefficients, the external force and moment equations were assumed to be simplified to the following expressions:

$$X_r = X_u \dot{u} + X_{uu} u |u| + F_{Prop}$$

$$Y_r = Y_v \dot{v} + Y_r \dot{r} + Y_{vv} v |v| + Y_{rv} r |r| + F_{Thrust}$$

$$N_r = N_r \dot{r} + N_v \dot{v} + N_{rv} r |r| + N_{vv} v |v| + M_{Thrust}$$

Substituting these expressions in to the equations of motion resulted in the following:

$$m\dot{u} = mvr + X_u \dot{u} + X_{uu} u |u| + F_{Prop}$$

$$m\dot{v} = -mur + Y_v \dot{v} + Y_r \dot{r} + Y_{vv} v |v| + Y_{rv} r |r| + F_{Thrust}$$

$$I_{zz} \dot{r} = N_r \dot{r} + N_v \dot{v} + N_{rv} r |r| + N_{vv} v |v| + M_{Thrust}$$

$$\dot{\Psi} = r$$

$$\dot{X} = u \cos \Psi - v \sin \Psi$$

$$\dot{Y} = u \sin \Psi + v \cos \Psi$$

Unlike standard maneuvering equations of motion, the square law drag terms do not nondimensionalize into a set of constant coefficient ordinary differential equations with definable stability limits independent of nominal forward speed.

2. Estimation of the Hydrodynamic Coefficients

Relatively accurate values for certain hydrodynamic coefficients ($X_u, X_{uu}, Y_v, Y_r, N_v$, and N_r) in the equations of motion have been developed and experimentally verified by Warner (1991), however these hydrodynamic coefficients were determined at much higher vehicle velocities than that which would occur during hover positioning. Additionally, no previous estimates were available for the remaining hydrodynamic coefficients for the square law drag (Y_{vv}, Y_{rv}, N_{vv} and N_{rv}).

To determine estimates of the hydrodynamic coefficients, comparisons between the theoretical model and the experimental data were made.

A computer program using Euler integration methods was written using the equations of motion to simulate the motion of the AUV in the horizontal plane. The code for the MATLAB (trademark of Math Works, Inc.) program is provided in Appendix G. As a starting point, the hydrodynamic coefficients determined by Warner (1991) were used. In addition, the hydrodynamic coefficients for the linear drag were used as first estimates for the square law drag hydrodynamic coefficients.

The program was run for each of the three positioning experiments, comparing the results for one particular test, from each experiment. The coefficients were adjusted so as to achieve the best agreement between the model and the experimental data, with the hydrodynamic coefficients common for all three types of positioning experiments. The hydrodynamic coefficients were adjusted to one significant digit. Table 4.2 lists the initial and final values for the hydrodynamic coefficients.

A large difference was noted between the initial and final values for X_{uu} . The initial value was derived for the case where the vehicle was moving at a nominal steady state, average speed of 1.5 feet per second (Warner, 1991). Under these conditions, the stern propulsion motors are operating with a thrust reduction effect due to the forward motion of the vehicle. This thrust reduction can be modeled, similarly to drag, by a square law force as follows:

**TABLE 4.2 AUV II HYDRODYNAMIC COEFFICIENTS:
HOVER CONDITIONS**

HYDROYNAMIC COEFFICIENTS	INITIAL VALUE	FINAL VALUE
Xuu	-0.4024	-3.0
Xudot	-0.00282*377.67	-0.06*377.67
Yvv	-0.10700*51.72	-0.5*51.72
Yrr	0.01187*377.67	0.01187*377.67
Yvdot	-0.03430*377.67	-0.04*377.67
Yrdot	-0.00178*2756.81	-0.00178*2756.81
Nvv	-0.00769*377.67	-0.00769*377.67
Nrr	-0.00390*2756.81	-0.04*2756.81
Nvdot	-0.00178*2756.81	-0.001*2756.81
Nrdot	-0.00047*20137.50	-0.002*20137.50

$$F_{Prop} = F_0 + X_{Reduct} u|u|$$

where F_0 is the nominal static force of the stern propulsion motor equal to five pounds (Saunders, 1990).

The final value of X_{uu} from Table 4.2 can be considered to be representative of the combined effects of drag and thrust reduction such that (to one decimal place):

$$X_{uu (Final)} = X_{uu (Drag)} + X_{uu (Reduct)}$$

$$X_{uu (Drag)} = -0.4$$

$$X_{uu (Reduct)} = -2.6$$

These results predict a steady state speed for the vehicle, at maximum voltage, of 1.3 feet per second.

3. Theoretical Model Results

Comparison between the experimental data and that predicted by the theoretical model, for the yaw positioning experiment is shown in Figure 4.17. The results for a 90 degree test are shown. The yaw position curve shows that less overshoot is predicted by the model than that measured experimentally, however the vehicle approached the final commanded position with less oscillation. Similar dynamic characteristics are seen in the yaw rate and thruster voltage curves.

The results for the lateral positioning experiment are shown in Figure 4.18. A comparison of Test 3 (see Table 3.2) is shown. The lateral position curve shows similar dynamic characteristics between the model and the

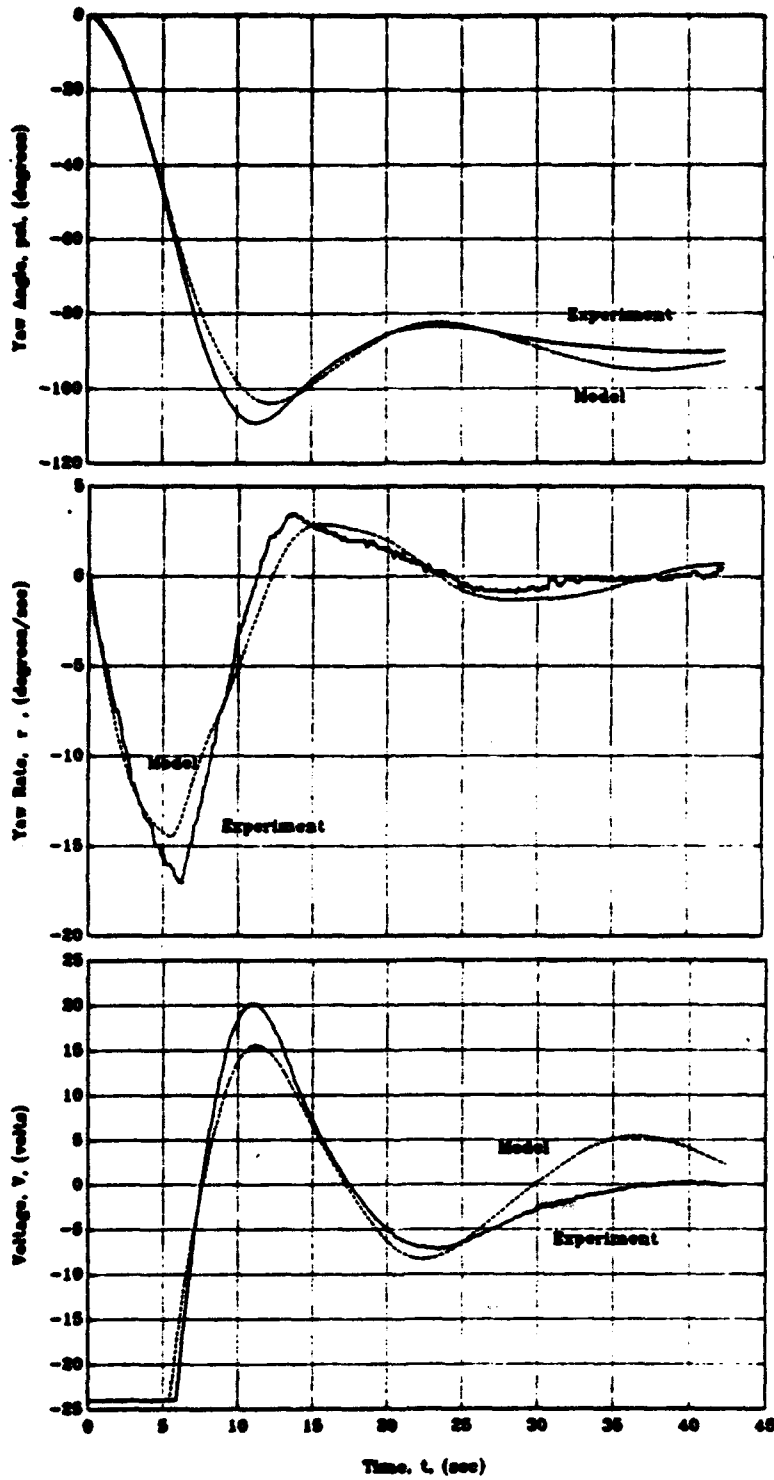


Figure 4.17 AUV Model: Yaw Position Experiment

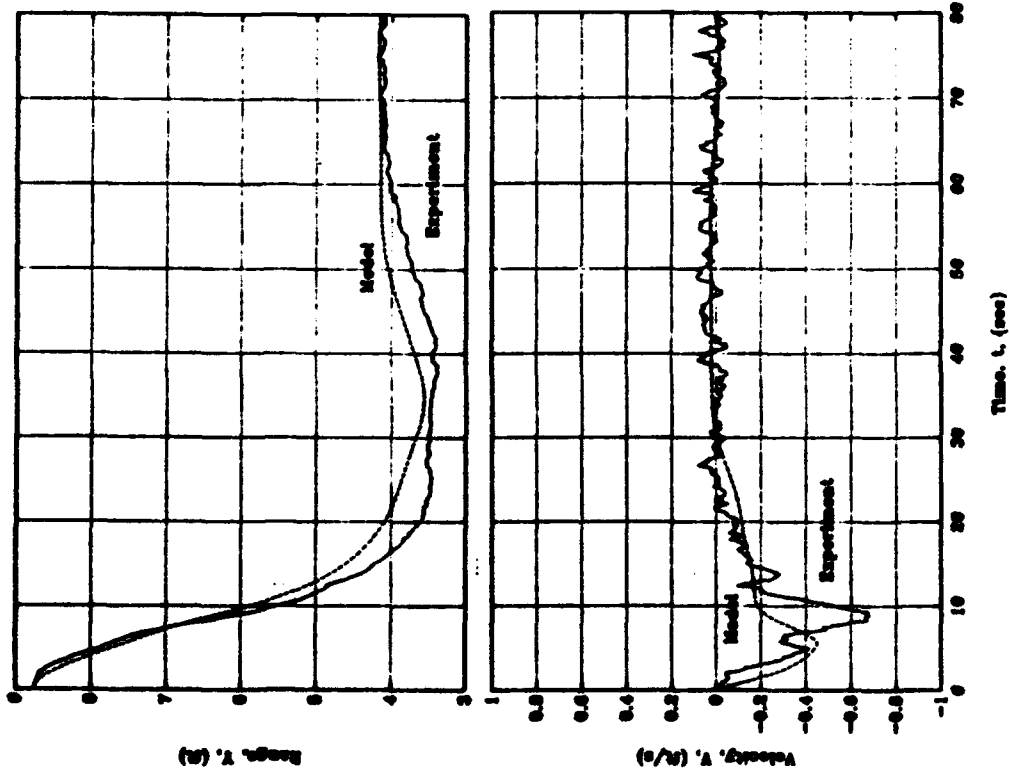
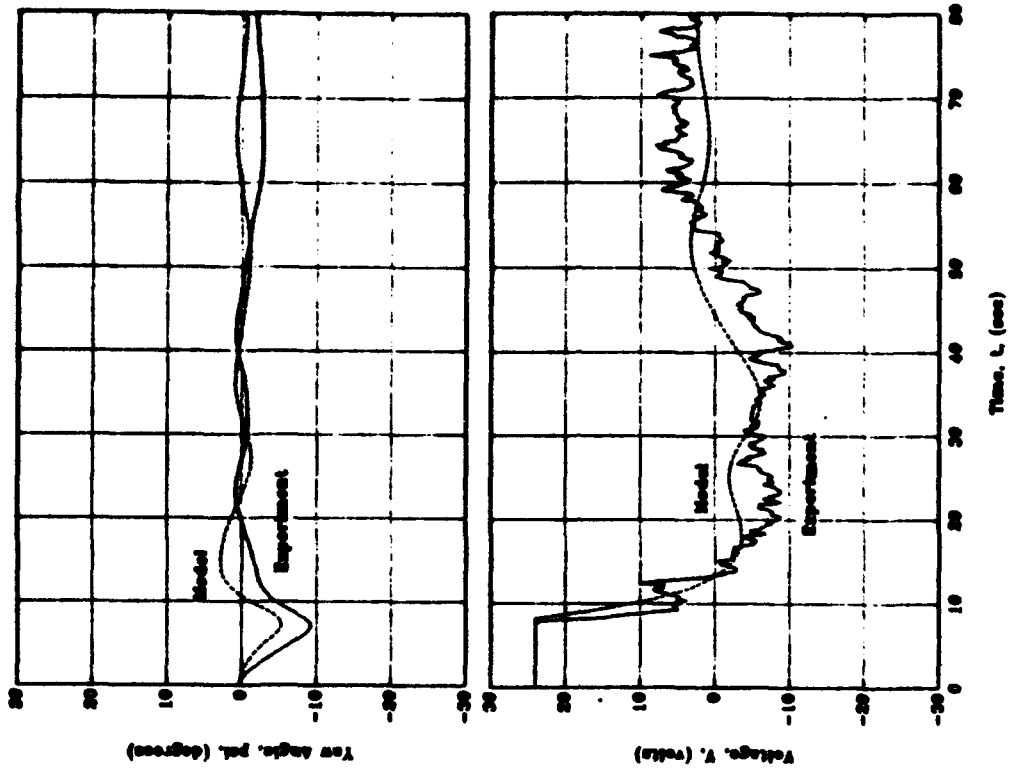


Figure 4.18 AUV Model: Lateral Position Experiment (Test 3)

experimental data, however the model reached a peak velocity, of smaller magnitude, sooner than the vehicle.

Similar dynamic characteristics are shown in the yaw position curve for the lateral positioning experiment as were observed for the yaw positioning experiment. The model shows less overshoot and a more oscillatory approach to the final commanded position than the data. The difference in the steady state positions, due to the stiction in the vehicle's thrusters is also shown. Similar features are shown in the thruster voltage curve.

Figure 4.19 shows the results for the longitudinal positioning experiment comparison. The comparison was made for Test 7 (see Table 3.2). Very good agreement is shown between the model and the data for the longitudinal range and surge velocity curves. The model shows the same overshoot as the data with only a slightly oscillatory approach to the final commanded position. A slight difference in peak value and time of occurrence is shown in the velocity curve. The same characteristics are shown in the stern propulsion voltage curve.

The stiction in the thrusters and stern propulsion motors is shown in the difference between the yaw position curves for the model and the data.

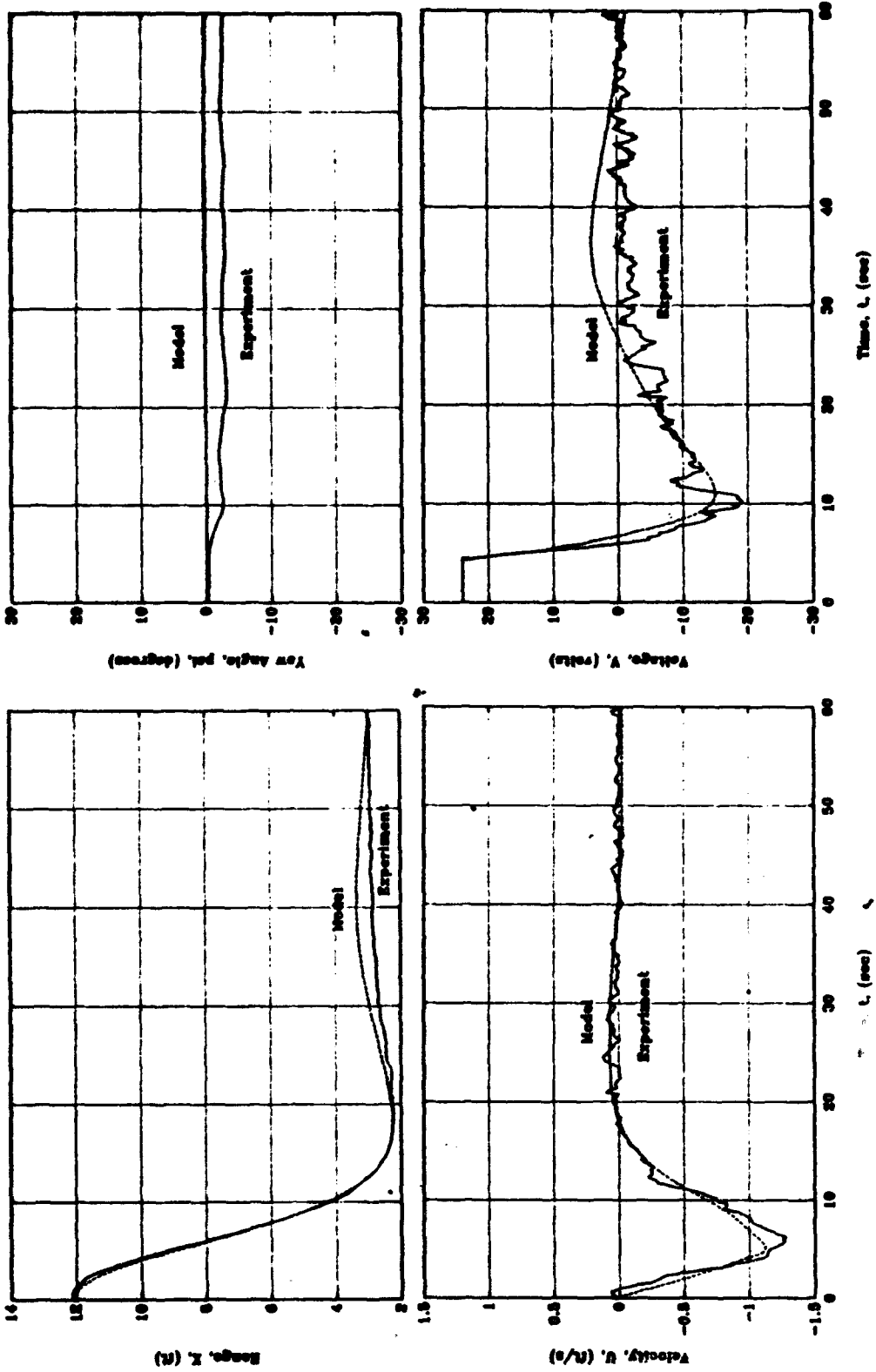


Figure 4.19 AUV Model: Longitudinal Position Experiment (Test 7)

V. SUMMARY

This chapter documents generalized conclusions of the results presented in Chapter IV. Specific comments regarding the level of success in meeting the objectives of this study are included. Recommendations for areas of further study, related to the concepts discussed in this thesis are made.

A. CONCLUSIONS

Through the course of this study, the ability to achieve accurate acoustic positioning capabilities of the NPS Autonomous Underwater Vehicle (AUV II) under hover conditions was demonstrated.

Use of an independent self-sonar which provided environmental imaging data without the aid of a transponder, along with the inputs from a free directional gyro system provided adequate data from which to base vehicle positioning commands.

Execution of the maneuvering commands through the use of stern propulsion motors and lateral tunnel thrusters, proved vital in achieving the ability to accurately position the vehicle, based on sensor data inputs.

The results of the yaw positioning experiment showed that an accurate final commanded angular position can be achieved using the yaw position inputs from the free directional gyro system and maneuvering commands executed by the thrusters.

Accurate lateral and longitudinal positioning, in the vicinity of a local target, was achieved through the combined input data from the gyro and the sonar systems, and the combined maneuvering efforts of the stern propulsion motors and the thrusters. The stability of the positioning data relative to the target, however was dependent on the gain of the sonar. Overdriving the sonar transducer resulted in unstable positioning data. This indicates that in future missions, an automatic "sonar supervisor" must be included in the control software.

The proportional derivative control law employed to generate the maneuvering commands produced the expected vehicle motion dynamics. The ability to change the dynamic motion characteristics (overshoot and oscillation), was achieved by adjusting the control law gains.

In the cases where the control effort was governed by a combination of position errors (yaw position and range) as seen in the lateral and longitudinal positioning experiments, the stability of the positioning ability was dependent on the coupling effects of the two directions of motion. The motion became particularly unstable in the situations where the position errors resulted in saturation of the thrusters.

Motor stiction affected the error in the final commanded positions, in all of the positioning experiments. The level of stiction in the thrusters limited the ability to achieve the final commanded yaw position and lateral range in both the yaw and lateral positioning experiments. The experimental results showed that the level of stiction was not identical for both thrusters, nor was it the same for either direction for one thruster.

The motor stiction effects were worsened in the case of the longitudinal positioning experiment where the stern propulsion motors generated a yaw moment on the vehicle, which was below the threshold of the lateral thruster response.

The results of the theoretical model provided adequate data to support a model based control effort, however, several effects which were beyond the scope of this study, were not included. Some of which include the following:

1. Motor stiction, as previously discussed.
2. Changes in thruster and stern propulsion force effects due to changes in the velocity of the vehicle.
3. Changes in effects of the hydrodynamic coefficients due to changes in vehicle velocity.

B. RECOMMENDATIONS FOR FURTHER STUDY

This thesis examined the first experiments conducted to study the ability of the NPS AUV II to achieve acoustic dynamic positioning during hover conditions. As a result, several related areas require further research.

Proportional derivative control laws were used to generate the positioning commands for the AUV with favorable results, however optimization of the control law gains is still required. In addition, other types of control methods which may be incorporated, should be studied. In particular, sliding mode control, using model based command generators, should be examined for its suitability to support dynamic positioning behaviors without driving thrusters into saturated conditions.

Further work is required in the area of modeling the motion of the AUV during hover conditions. Certain areas of concern, such as thruster and stern propulsion motor thrust effectiveness and hydrodynamic forces require further research if generalizations of the model were to be pursued.

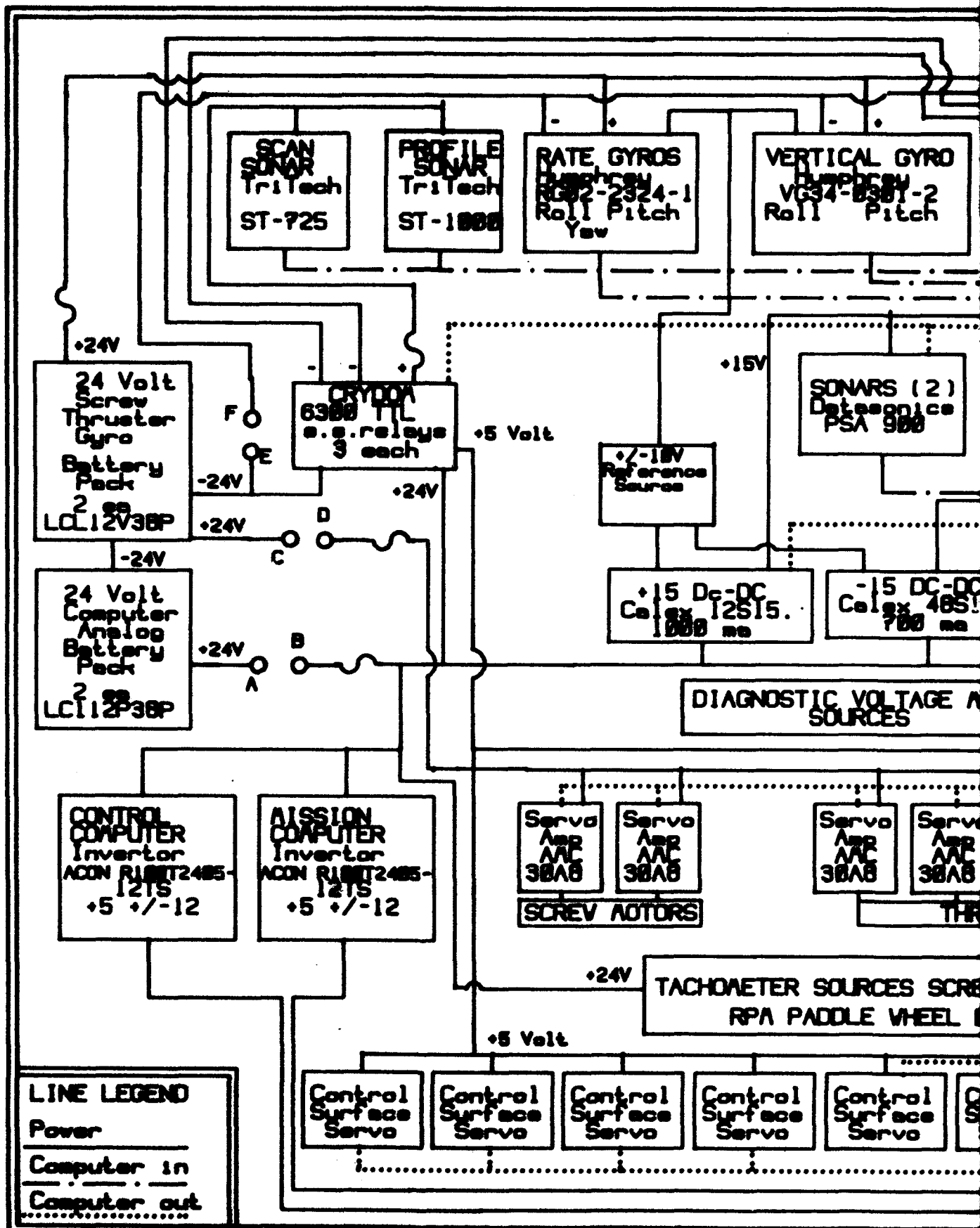
Experiments should be conducted, to verify higher levels of autonomous operation by examining more complex motion behaviors, including longer missions, combining motions commanded in sequence or simultaneously, using either timed based or sensory data based inputs as the basis for the selection of behaviors.

Using sonar to identify objects of interest within the field of view should be integrated into the capabilities of the robot submarine, although delays in the availability of position related information are likely to cause positional motion instability. A study and development of model based predictor/corrector control is likely to be a requirement for maintaining stable combined motion.

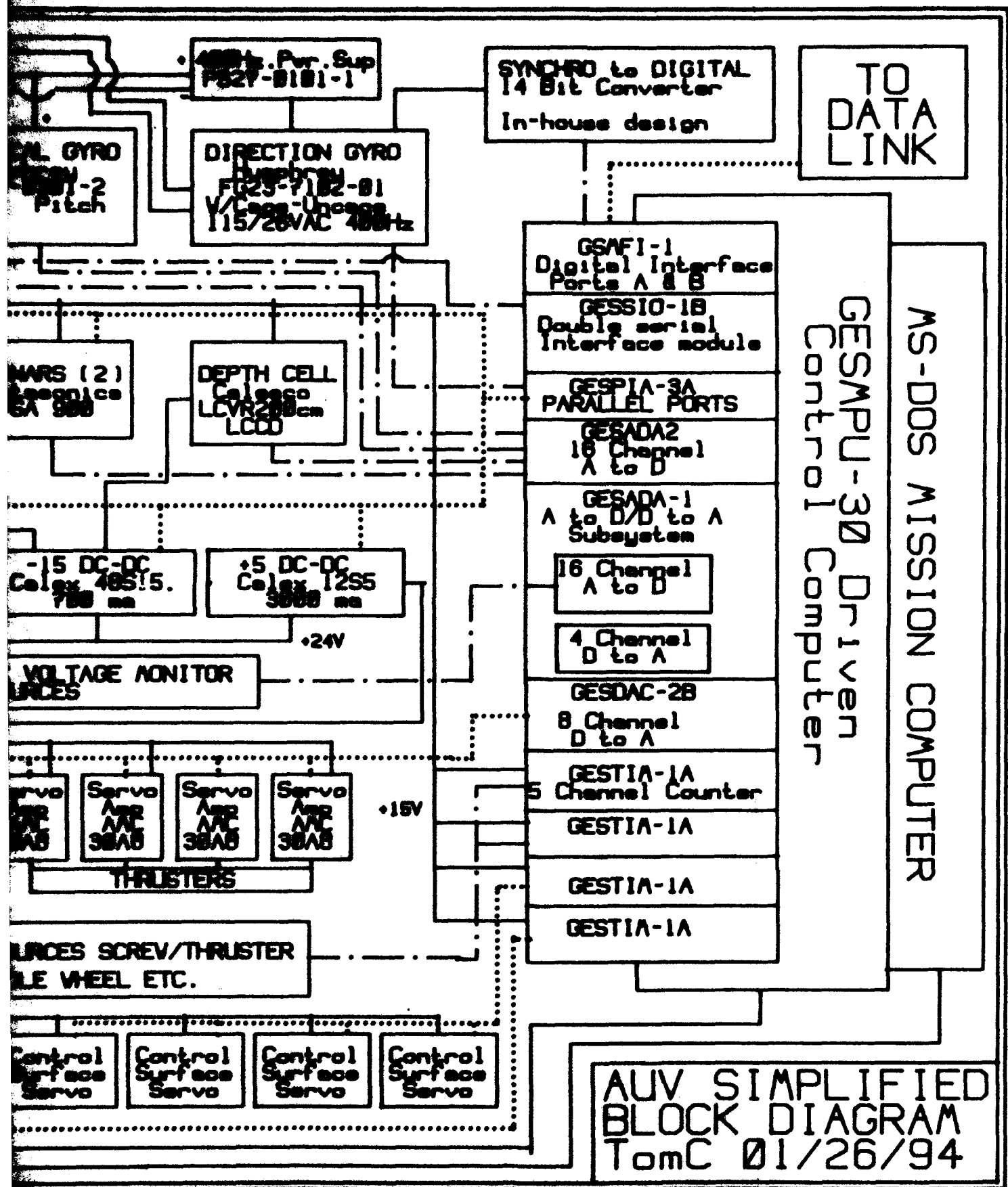
Investigations of disturbance response in the presence of water current could and should be conducted.

APPENDIX A AUV II CONFIGURATION BLOCK DIAGRAM

A simplified block diagram of the major equipment groups is provided on the following page. This diagram shows the basic system power paths and the computer data transfer paths between the components.



A



B

APPENDIX B AUV II WIRING LIST

The wiring list for the current configuration of the AUV II is presented on the following pages.

For each item shown, the type of signal carried or channel is listed along with the terminal pin assignment, color, voltage rating and description.

Further wiring details can be found in the manufacturer's technical manual for the individual component.

WIRING LIST FOR ADV 01/12/94

QUANTITY WIREAW

ITEM	SIG NAME/CONN	TERM	COLOR	TYPE	TO/FROM
BATT FWD, COMPUTER/ANALOG PS		POS NEG	WHT BLK	POM 24VDC GND	CIRC BRKR, PT. A GND/REF BUSS
BATT, AFT, GYRO/PROPS AND THRUSTERS		POS NEG	WHT BLK	POM 24VDC GND	CIRC BRKR, PT. C GND/REF BUSS
RELAY, MAIN POWER		PT A, HOT PT B PT C, HOT PT D ACTUAT + ACTUAT -	WHT RED RED WHT WHT RED WHT ORG ORG/GRN	POM 24VDC POM 24VDC POM 24VDC POM 24VDC POM 24VDC POM 24VDC POM 24VDC CNTL 24VDC GND	COMP/AM CIRC BRKR TERM A, POWER THRUHULL FUSE BLOCK 1, (TH A1) FUSE BLK 1, ANAL/COMP GYRO/SCREW CIRC BRKR TERM C, POWER THRUHULL FUSE BLK 3, SERVO AMP TERM B1, POM THRUHULL GND/REF BUSS
CIRC BRKR, ANALOG P.S. AND COMPUTERS		PT A 30 AMP	WHT WHT	POM 24VDC POM 24VDC	ANAL/COMP BATT TERM A, MASTER RELAY
CIRC BRKR, SERVO AMPS		PT C PT C 30 AMP	WHT WHT WHT	POM 24VDC POM 24VDC POM 24VDC	GYRO/SCREW BATT GYRO CIRC BRKR TERM C, MASTER RELAY
CIRC BRKR, GYROS		HOT 8 AMP	WHT WHT	POM 24VDC POM 24VDC	PT C (on SERVO CIR BRKR) FUSE BLK 2, GYROS
ANALOG POM SUPPLY BOARD	ANALOG DIG GND A/D GND A/D GND A/D GND A/D GND A/D GND A/D GND A/D GND 15 POM CNTRL 5 POM CNTRL POM SUPPLY POM RETURN +5 POM +5 +5 +15 POM +15 +15 -15 POM -15 -15 +10 POM +10 +10 -10 POM -10	AN/DIG GND A/D GND, P3 A/D GND, P3 A/D GND, P3 A/D GND, P3 A/D GND, P2 A/D GND, P2 P2-1 P1-3 P1-2 P1-1 P4 P4 P4 P5 P5 P5 P6 P6 P6 P7 P7 P7 P8 P8	BLK BLK GREY GREY BLK BLK BLK WHT WHT/DRN WHT BLK RED RED no conn RED/WHT RED RED/WHT BLK no conn RED/BLK GND/RED GND/RED GND/RED GND/BLK GND/RED GND/RED GND/RED GND/BLK GND/BLK	GND/REF GND/REF GND/REF GND/REF GND/REF GND/REF GND/REF TTL CNTRL TTL CNTRL 24 VDC POM RTN +5 VDC POM DIAGNOSTICS +15 VDC POM +15 VDC POM DIAG -15 VDC POM DIAG +10 VDC REF +10 VDC REF REF -10 VDC REF -10 VDC REF	CELESCO DEPTH CELL BOARD T15 DATASONICS SONAR BOARD T2 ICU-2A BRKOUT (ADC-1 SL5) T P2 ICU-2A BRKOUT (ADC-2 SL 6) T P2 SERVO FIN CONNECTION ACOM P.S. (BOTH), COM CONN. -24 VDC GND BUSS PIA-3A BRKOUT T35 PIA-3A BRKOUT T37 MASTER RELAY TERM B ANALOG -24 VDC GND BUSS FIN SERVO CONNECTOR ICU-2A BRKOUT (ADC-1), T2 DATASONICS SONAR BOARD T3 CELESCO DEPTH CELL, T13 ICU-2A BRKOUT (ADC-1), T0 CELESCO DEPTH CELL T12 ICU-2A BRKOUT (ADC-1), T1 RATE GYROS TERM F VERT GYROS TERM E & J ICU-2A BRKOUT (ADC-1), T3 RATE GYROS TERM E VERT GYROS TERM H & L

FB CABE	-10	P8	ORG/BLK	DIAG	ICU-2A BRKOUT (ABC-1), T4
FB UNCADE	RELAYED POW	P9-3	BLK	-24 VDC RTN	F6 DB25 T12
TRITECH SONAR	RELAYED POW	P9-2	WHT	-24 VDC RTN	F6 DB25 T11
FB CABE RELAY	RELAYED POW	P9-1	WHT	24 VDC	TRITECH CONN PIN 3
FB UNCADE RELAY	RELAY CNTRL TTL	P10-3	GRN/WHT	TTL CNTRL	PIA-3A BRKOUT T50
TRITECH SONAR RELAY	RELAY CNTRL TTL	P10-2	GRN/BLK	TTL CNTRL	PIA-3A BRKOUT T48
	RELAY CNTRL TTL	P10-1	GRN	TTL CNTRL	PIA-3A BRKOUT T46
TRANSPORT PLUG TO SPIN GYROS, CONN TO THRUHULL INSIDE/OUTSIDE	ORG	B1	RED		
	RED	A1	ORG		
	WHT	C	WHT		
	BLK	A	WHT/BLK		
	GRN, BAT GND BUS	E	BLU	GND	SPIN GYROS
	WHT/BLK, GYROS	F	BLK	POW, 24V	JUMPED TO E
RUN PLUG FOR NORMAL OPERATION					
MASTER RELAY SOLOMID	ORG	B1	RED	CNTL 24VDC	CLOSE MASTER RELAY
24VDC POW	RED	A1	ORG	POW 24VDC	JUMPED TO B1
INSIDE/OUTSIDE	WHT	C	WHT		
	BLK	A	WHT/BLK		
	GRN, BAT GND BUS	E	BLU	GND	SPIN GYROS
	WHT/BLK, GYROS	F	BLK	POW, 24V	JUMPED TO E
THRUHULL, POWER, AUV INSIDE PIGTAIL TO INSIDE CONNECTIONS	ORG	B1	ORG	CNTL 24VDC	PT B1, MASTER RELAY
	RED	A1	RED	POW 24VDC	FUSE BLOCK 1, 1 AMP
	WHT	C	RED	CHG GYRO BA	TERM C, MASTER RELAY
	BLK	A	RED	CHG COMP BA	TERM A, MASTER RELAY
	GRN	E	BLK	GND	GND/REF BUSS
	WHT/BLK	F	BLK	POW RTN	GYRO FUSE BLK 2
UMBILICAL/BENCH BOX THRU-HULL OUTSIDE PIGTAIL TO UMBILICAL	RED	B1	RED	CNTL 24VDC	TOGGLE SW., CONN A1
	ORG	A1	ORG	POW 24VDC	1 AMP FUSE/SWITCH
	WHT	C	WHT	CHARGE BATT	5 AMP FUSE, RED RECPT
	WHT/BLK	A	GRN	CHARGE BATT	5 AMP FUSE, RED RECPT
	BLU	E	BLU	GND	BLK BANANA RECEP.(2)
	BLK	F	BLK	POW RET	SN. TOGGLE, CONN E
FUSE BLOCK 1, FWD		IN	WHT	POW 24VDC	TERM B, MASTER RELAY
		5 AMP	WHT	POW 24VDC	ANALOG P.S.
		0.1 AMP	WHT	POW 24VDC	TURBO PROBE
		10 AMP	WHT	POW 24VDC	ACON P.S.(2) DS9, DS8
		IN	RED	POW 24VDC	PT A, MASTER RELAY
		1 AMP	RED	POW 24VDC	PT A1, POWER THRUHULL
FS BLOCK 2, AFT, GYRO		IN	WHT	POW 24VDC	GYRO CIRC BRKR
		5 AMP	RED	POW 24VDC	RATE GYROS (3)
		2 AMP	RED	POW 24VDC	VERTICAL GYROS (2)
		2 AMP	RED	POW 24VDC	FREE GYRO POW INVERT.
		RET	BLK	POW RTN	RATE GYROS (3)
		RET	BLK	POW RTN	VERT GYROS (2)
		RET	BLK	POW RTN	FREE GYRO POW INVERT.
		RET	BLK	POW RTN	TERM F, POW THRUHULL

PS BLOCK 3, SERVO AMP

THR	5 AMPS	WHT	POW 24VDC	TERM 9, MASTER RELAY
THR	5 AMPS	WHT	POW 24VDC	FOR/VERT THR SERVO T4
THR	5 AMPS	WHT	POW 24VDC	FOR/HOR THR SERVO T4
THR	5 AMPS	WHT	POW 24VDC	AFT/VERT THR SERVO T4
PROP	10 AMPS	WHT	POW 24VDC	AFT/HOR THR SERVO T4
PROP	10 AMPS	WHT	POW 24VDC	STBD MAIN SERVO T4
PROP	5 AMPS	RED	POW 24VDC	PORT MAIN SERVO T4
				FREE GYRO TERM 14

FREE GYRO (UN)CAGE

GND/REF BUSS

BUSS	BLK	GND/REF	ANALOG P.S. ANAL GND
BUSS	BLK	POW RTN	TRITEK PROF. SONAR
BUSS	BLK	POW RTN	TRITEK SCAN SONAR
BUSS	BLK	POW RTN	ACON P.S. (COMPUTERS)
BUSS	BLK	GND	COMP./ANALOG BATT.,-
BUSS	BLK	GND	GYRO/MOTOR BATT.,-
BUSS	BLK	POW RTN	TERM E, POW THRU MULL
BUSS	ORG/GRN	POW RTN	ACTUAT-, MASTER RELAY
BUSS	BLK	POW RTN	ANALOG P.S., 24V RET
BUSS	BLK	POW RTN	SERVO AMPS, FUSE BLK3

OS9 ACON P.S. INVERTER

GND	3	BLK	POW RTN	GND/REF BUSS
POW	5	WHT	POW 24VDC	FUSE BLK 1
SENS	8	BLK	SENS	JUMPED TO 9 & 13
		BLK	GND/REF	POW RTN RPM SENSORS
GND	9	BLK-WHT	GND/REF	OS9 COMPUTER GND
		BLK	GND/REF	JUMPED TO 8 & 13
GND	13	BLK	CONN/REF	ANAL P.S., ANAL GND
		BLK	GND/REF	JUMPED TO 8 & 9
POW	10	WHT	POW +5VDC	OS9 COMPUTER
		WHT	POW	JUMPED TO 11
POW	11	RED	POW +5VDC	RPM SENSORS
		WHT	SENS	JUMPED TO 10
POW	12	WHT	POW -12VDC	OS9 -12VDC SUPPLY
POW	14	WHT	POW +12VDC	OS9 +12VDC SUPPLY

OS9 COMPUTER

GND	BLK-WHT	GND/REF	TERM 9, OS9 ACON P.S.
+5VDC	WHT	POW +5VDC	TERM 10, OS9 ACON
+12VDC	WHT	POW +12VDC	TERM 14, OS9 ACON
-12VDC	WHT	POW -12VDC	TERM 12, OS9 ACON
RIBBON	GRY	CNTRL, I/O	BREAK OUT BOARDS (4)

OS9 COMPUTER BOARDS

OS9 ACON P.S. INVERTER

3	BLK	POW RTN	GND/REF BUSS
5	WHT		
8	BLK	SENS	JUMPED TO 9 & 13
9	BLK	GND/REF	JUMPED TO 8 & 13
13	BLK	GND/REF	JUMPED TO 8 & 9
10	WHT	POW	JUMPED TO 11
11	WHT	SENS	JUMPED TO 10
12			
13			
14			

OS9 COMPUTER

SERVO AMP PORT MAIN SCREEN

1 -H	BLK	POW RTN	PORT MAIN MOTOR, BLK
2 +H	WHT	VAR POW	PORT MAIN MOTOR, RED

	3 POW GND	BLK	POW RTN	FUSE BLOCK 3
	4 HI VOLT	WHT	POW 24VDC	FUSE BLOCK 3
	CONN 2	GREY	SIG GND	JUMPED TO PIN 5
	CONN 4	RED	+ REF IN	DAC-2B BKOUT SL11 T30
	CONN 5	GREY	- REF	DAC-2B BKOUT SL11 T27
	CONN 8	VIOL	CURR MON	ICU-2A, SL 6, T 00
	CONN 11	BLU	INHIB	PIA-3A, SL 4, T 26
SERVO AMP STDB MAIN SCREW	1 -M	BLK	POW RTN	STDB MAIN MOTOR, BLK
	2 +M	WHT	VAR POW	STDB MAIN MOTOR, RED
	3 POW GND	BLK	POW RTN	FUSE BLOCK 3
	4 HI VOLT	WHT	POW 24VDC	FUSE BLOCK 3
	CONN 2	GREY	SIG GND	JUMPED TO PIN 5
	CONN 4	ORANG	+ REF IN	DAC-2B BKOUT SL11 T32
	CONN 5	GREY	- REF	DAC-2B BKOUT SL11 T29
	CONN 8	BLU	CURR MON	ICU-2A, SL 6, T 1
	CONN 11	VIOL	INHIBIT	PIA-3A, SL 4, T 24
SERVO FOR/VERT THRUSTER	1 -M	BLK	POW RTN	FOR/VERT THRUSTER, BLK
	2 +M	WHT	VAR POW	FOR/VERT THRUSTER, RED
	3 POW GND	BLK	POW RTN	FUSE BLOCK 3
	4 HI VOLT	WHT	POW 24VDC	FUSE BLOCK 3
	CONN 2	GREY	SIG GND	JUMPED TO PIN 5
	CONN 4	BLU	+ REF IN	DAC-2B BKOUT SL11 T34
	CONN 5	GREY	- REF	DAC-2B BKOUT SL11 T31
	CONN 8	YEL	CURR MON	ICU-2A, SL 6, T 3
	CONN 11	BRN	INHIBIT	PIA-3A, SL 4, T 22
SERVO FOR/HOR THRUSTER	1 -M	BLK	POW RTN	FOR/HOR THRUSTER, BLK
	2 +M	WHT	VAR POW	FOR/HOR THRUSTER, RED
	3 POW GND	BLK	POW RTN	FUSE BLOCK 3
	4 HI VOLT	WHT	POW 24VDC	FUSE BLOCK 3
	CONN 2	GREY	SIG GND	JUMPED TO PIN 5
	CONN 4	BLK	+REF IN	DAC-2B BKOUT SL11 T36
	CONN 5	GREY	-REF	DAC-2B BKOUT SL11 T33
	CONN 8	WHT	CURR MON	ICU-2A, SL 6, T 4
	CONN 11	YEL	INHIBIT	PIA-3A, SL 4, T 20
SERVO AFT/VERT THRUSTER	1 -M	BLK	POW RTN	AFT/VERT THRUSTER, BLK
	2 +M	WHT	VAR POW	AFT/VERT THRUSTER, RED
	3 POW GND	BLK	POW RTN	FUSE BLOCK 3
	4 HI VOLT	WHT	POW 24VDC	FUSE BLOCK 3
	CONN 2	GREY	SIG GND	JUMPED TO PIN 5
	CONN 4	YEL	+REF IN	DAC-2B BKOUT SL11 T38
	CONN 5	GREY	-REF	DAC-2B BKOUT SL11 T35
	CONN 8	BLU	CURR MON	ICU-2A, SL 6, T 5
	CONN 11	GRN	INHIBIT	PIA-3A, SL 4, T 18
SERVO AFT/HOR THRUSTER	1 -M	BLK	POW RTN	AFT/HOR THRUSTER, BLK
	2 +M	WHT	VAR POW	AFT/HOR THRUSTER, RED
	3 POW GND	BLK	POW RTN	FUSE BLOCK 3
	4 HI VOLT	WHT	POW 24VDC	FUSE BLOCK 3
	CONN 2	GREY	SIG GND	JUMPED TO PIN 5
	CONN 4	WHT	+REF IN	DAC-2B BKOUT SL11 T40
	CONN 5	GREY	-REF	DAC-2B BKOUT SL11 T37
	CONN 8	ORG	CURR MON	ICU-2A, SL 6, T 6
	CONN 11	ORG	INHIBIT	PIA-3A, SL 4, T 16
PROP, STB MAIN SCREW	RED	WHT	VAR POW	STB MAIN SERVO, +M
	BLK	BLK	POW RTN	STB MAIN SERVO, -M
	OPN GND	BLK	GND/REF	OS9 ACORN P.S., T 8
	OPN 3 CHA	ORG	TACH	TIM-1A, SL 7, T 3

	RPN 4 Vcc	RED	POW 5VDC	059 ACON P.S., T 11
PROP, PORT MAIN SERVO	RED	WHT	VAR POW	PORT MAIN SERVO, +M
	BLK	BLK	POW RTN	PORT MAIN SERVO, -M
	RPN GND	BLK	GND/REF	059 ACON P.S., T 8
	RPN 3 CHA	YEL	TACH	TIM-1A, SL 7, T 6
	RPN 4 Vcc	RED	POW 5DC	059 ACON P.S., T 11
THRUSTER, FOR/VERT	RED	WHT	VAR POW	FOR/VERT SERVO, +M
	BLK	BLK	POW RTN	FOR/VERT SERVO, -M
	RPN GND	BLK	GND/REF	059 ACON P.S., T 8
	RPN 3 CHA	BRN/BLK	TACH	TIM-1A, SL 8, T 9
	RPN 4 Vcc	RED	POW 5VDC	059 ACON P.S., T 11
THRUSTER, FOR/HOR	SEE	FOR/VERT	TACH	TIM-1A, SL 8, T 10
	RPN 3 CHA	VIOL		
THRUSTER, AFT/VERT	SEE	FOR/VERT	TACH	TIM-1A, SL 8, T 7
	RPN 3 CHA	BLU/WHT		
THRUSTER, AFT/HOR	SEE	FOR/VERT	TACH	TIM-1A, SL 8, T 8
	RPN 3 CHA	WHT/BLK		
FIN SERVO CONN BOARD	SUPPLY	RED	POW 5 VDC	ANALOG P.S., 5 VDC
	OUT	RED	POW 5VDC	FIN SERVOS (8), T 3
	OUT	RED	5 VDC	FIN SIGNAL PULL-UP BOARD
	RET	BLK	GND	ANALOG P.S., GND/REF
	RET	BLK	GND	FIN SERVOS (8), T 2
	REF	GREY	GND/REF	TIM BRKOUT, T23 and T24
FIN SIGNAL BOARD inject 5VDC	SUPPLY	RED	POW 5VDC	FIN SERVO 5 VDC POW CONN
	OUT	WHT	5 VDC	TIM BRKOUT, T11
		WHT	5 VDC	TIM BRKOUT, T12
		WHT	5 VDC	TIM BRKOUT, T13
		WHT	5 VDC	TIM BRKOUT, T14
		WHT	5 VDC	TIM BRKOUT, T17
		WHT	5 VDC	TIM BRKOUT, T18
		WHT	5 VDC	TIM BRKOUT, T19
		WHT	5 VDC	TIM BRKOUT, T20
FIN, FOR/TOP	1	BLK-VIOL	SIG	TIM-1A BRKOUT T11
	2	BLK	GND/REF	FIN SERVO BOARD, GND
	3	RED	POW 5 VDC	FIN SERVO BOARD, POW
FIN, FOR/STDB	1	BLK-ORG	SIG	TIM-1A BRKOUT T14
	2	BLK	GND/REF	FIN SERVO BOARD, GND
	3	RED	POW 5 VDC	FIN SERVO BOARD, POW
FIN, FOR/PORT	1	BLK-RED	SIG	TIM-1A BRKOUT T13
	2	BLK	GND/REF	FIN SERVO BOARD, GND
	3	RED	POW 5 VDC	FIN SERVO BOARD, POW
FIN, FOR/BOT	1	BLK-YEL	SIG	TIM-1A BRKOUT T12
	2	BLK	GND/REF	FIN SERVO BOARD, GND
	3	RED	POW 5 VDC	FIN SERVO BOARD, POW
FIN, AFT/TOP	1	BLK-WHT	SIG	TIM-1A BRKOUT T17

		2	BLK	GND/REF	FIN SERVO BOARD, GND
		3	RED	POW 5 VDC	FIN SERVO BOARD, POW
FIN, AFT/STDB		1	BLK-BRN	SIG	TIM-1A BRKOUT T20
		2	BLK	GND/REF	FIN SERVO BOARD, GND
		3	RED	POW 5 VDC	FIN SERVO BOARD, POW
FIN, AFT/PORT		1	BLK-GRN	SIG	TIM-1A BRKOUT T19
		2	BLK	GND/REF	FIN SERVO BOARD, GND
		3	RED	POW 5 VDC	FIN SERVO BOARD, POW
FIN, AFT/BDT		1	BLK-BRN	SIG	TIM-1A BRKOUT T18
		2	BLK	GND/REF	FIN SERVO BOARD, GND
		3	RED	POW 5 VDC	FIN SERVO BOARD, POW
GYRO, PITCH RATE	P.S. REF	A	BLK	GND/REF	FUSE BLOCK 2, GND
	P.S. + DC	B	RED	24 VDC	FUSE BLOCK 2, COMMON 5 AMP FUSE
	SIGNAL +	D	BRN	ANALOG SIG	ICU-2A BRKOUT (ADC-2), T8
	SIG. -REF	E	GRN	-10 VDC REF	ANALOG P.S. BOARD, T P8
	SIG +REF	F	WHT	+10 VDC REF	ANALOG P.S. BOARD, T P7
GYRO, ROLL RATE	P.S. REF	A	BLK	GND/REF	FUSE BLOCK 2, GND
	P.S. + DC	B	RED	24 VDC	FUSE BLOCK 2, COMMON 5 AMP FUSE
	SIGNAL +	D	BLK	ANALOG SIG	ICU-2A BRKOUT (ADC-2), T9
	SIG. -REF	E	GRN	-10 VDC REF	ANALOG P.S. BOARD, T P8
	SIG +REF	F	WHT	+10 VDC REF	ANALOG P.S. BOARD, T P7
GYRO, YAW RATE	P.S. REF	A	BLK	GND/REF	FUSE BLOCK 2, GND
	P.S. + DC	B	RED	24 VDC	FUSE BLOCK 2, COMMON 5 AMP FUSE
	SIGNAL +	D	WHT	ANALOG SIG	ICU-2A BRKOUT (ADC-2), T10
	SIG. -REF	E	GRN	-10 VDC REF	ANALOG P.S. BOARD, T P8
	SIG +REF	F	WHT	+10 VDC REF	ANALOG P.S. BOARD, T P7
GYRO, VERTICAL PITCH & ROLL ANGLE	P.S. + DC	A	RED	24 VDC	FUSE BLOCK 2, COMMON 2 AMP FUSE
	P.S. REF	B	BLK	GND/REF	FUSE BLOCK 2, GND
	ERECT CUTOUT	C	WHT	CNTRL	JUMPED TO D
	ERECT CUTOUT	D	GRN	CNTRL	JUMPED TO C
	SIG. + REF, GRN	E	ORG/RED	+10 VDC REF	ANALOG P.S. BOARD, T P7
	SIG. + REF, YEL	J	ORG/RED	+10 VDC REF	SAME WIRE, T P7
	SIG. - REF, BLU	H	ORG/BLK	-10 VDC REF	ANALOG P.S. BOARD, T P8
	SIG. - REF, BLK	L	ORG/BLK	-10 VDC REF	SAME WIRE, T P8
	PITCH ANGLE, SIG	F	BRN	ANALOG SIG	ICU-2A BRKOUT (ADC-2), T11
	ROLL ANGLE, SIG	K	VIDL	ANALOG SIG	ICU-2A BRKOUT (ADC-2), T12
GYRO, FREE, P.S. INVERTER	AC OUTPUT	1A	RED	POW 115VAC	F8 88 25 CONN., T4
	AC COMMON	2B	WHT	AC GND/REF	F8 88 25 CONN., T7
	AC OUTPUT	3C	BLK	POW 24VAC	F8 88 25 CONN., T6
	DC INPUT	4D	RED twist pair	POW 12VDC	GYRO FUSE BOX (RED POW), F82

	DC GND	SE	BLK	DC GND/REF	GYRO FUSE BOX	BLK via Thru-Hu F-E
GYRO, FREE @ 25 conn	S3	1	RED	S16 S3	SYNCHRO P1:1 T5	
	AC COM/REF S2	2	ORG/GRN	GND/REF S2	SYNCHRO P1:1 T3	
		3	WHT	AC COM	P.S. T2B, SYNCHRO P1:1 T2	
	AC POW	4	RED	POW 115 VAC	P.S. T1	
	no conn	5				
	AC POW	6	BLK	POW 26 VAC	P.S. T3C, SYNCHRO P1:1 T1	
		7	WHT	AC COM	JUMPED TO T3	
	UNCAGE INDICATE	8	GRN	TTL LO TRUE	PIA-3A BRKOUT T23	
		9	WHT/RED	D16 GND	PIA-3A BRKOUT T3	
		10	WHT		JUMPED TO T9	
	UNCAGE (NOT)	11	WHT	POW	UNCAGE RELAY via ANAL BRD P9 T2	
	CAGE (NOT)	12	BLK	POW	CAGE RELAY via ANAL BRD P9 T3	
	no conn	13				
	POW FOR (UN)CAGE	14	RED	POW 24 VDC	SERVO AMP FUSE BLOCK, 5 AMP, F83	
	CAGE INDICATE	15	WHT	TTL LO TRUE	PIA-3A BRKOUT T26	
		16	WHT		JUMPED TO T14	
	no conn	17				
	S1	18	GRN	S16 S1	SYNCHRO P1:1 T4	
	no conn	19				

GYRO, FREE, SYNCHRO RESOLVER BOARD NOTE-takes power from computer, not gyro	OUTPUT	RIBBON	GRY	DIG/ANAL	HED 34 CONN TO MF1-1 SL 12
	OUTPUT SEE SCHEM. AND/OR T.C.				
	P1:1/J 1:1	1	BLK	IP REF HI	
		2	WHT	IP REF LO	
		3	ORG/GRN	S2	
		4	GRN	S1	
		5	RED	S3	

THRUMALL #2, RS232 TELE CABLE COLORS					
	WHT	GRN	RIBBON	OS9 MF1-1 SL12 T1	
	GRN	ORG	RIBBON	OS9 MF1-1 SL12 T3	
	BLK	BRN	RIBBON	OS9 MF1-1 SL12 T5	
	YEL	GRN	RIBBON	DOS MF1-1 SL T1	
	RED	ORG	RIBBON	DOS MF1-1 SL T3	
	BLU	BRN	RIBBON	DOS MF1-1 SL T5	

THRUMALL #1, RS232 FORWARD CS T80 USES					
	WHT	GRN	RIBBON		
	GRN	ORG	RIBBON		
	BLK	BRN	RIBBON		
	YEL	GRN	RIBBON		
	RED	ORG	RIBBON		
	BLU	BRN	RIBBON		

TRITEK PROFILER BOARD FLYING CONN + 10 PIN BULKH COLORS					
DATA OUT	A	RED	RS 232	FLYING CONN	
DATA IN	B	GRN	RS 232	"	
DC POW	C	WHT	+ 24 VDC	"	
GND/REF	D	BLK	GND/REF	"	
ANALOG OUT	E	ORG	ANALOG DC	"	
HOUSING EARTH	NO CONN				

TRITEK SCANNER SONAR FLYING CONN + 10 PIN BULGH COLORS	DATA OUT	A	RED/BLK	RS 232	FLYING CONN
	DATA IN	B	GRN/BLK	RS 232	"
	DC POW	C	WHT/BLK	+ 24 VDC	"
	GND/REF	D	BLU	GND/REF	"
	ANALOG OUT HOUSING EARTH	E NO CONN	ORG/BLK	ANALOG DC	"
FLYING OUTBOARD CONN. TRITECH PROFILER	DATA OUT	A	RED/4	RS 232 OUT	PIN 4, WHT INBOARD WIRE
	DATA IN	B	GRN/3	RS 232 IN	PIN 3, GRN INB
	DC POW	C	WHT/1	+24 VDC	PIN 1, WHT INB
	GND/REF	D	BLK/2	GND/REF	PIN 2, BLK & GRY INB
	ANALOG OUT	E	ORG/5	ANALOG DC	NO CONN
FLYING OUTBOARD CONN. TRITECH SCANNER	DATA OUT	A	RED/BLK/8	RS 232 OUT	PIN 8, RED INBOARD WIRE
	DATA IN	B	GRN/BLK/9	RS 232 IN	PIN 9, BLK INB
	DC POW	C	WHT/BLK/7	+24 VDC	PIN 7, WHT INB
	GND/REF	D	BLU/6	GND/REF	PIN 6, BLK & GREY INB
	ANALOG OUT	E	ORG/BLK/10	ANALOG DC	NO CONN
FORWARD 10 PIN THRU-HULL INBOARD CONN. (TRITECH SONARS)	DC POW	1/C	WHT	+24 VDC	ANALOG P.S. T P9-1
	POW GND	2/D	BLK	GND/REF	-24 VDC GND BUSS
		2/D	GRY	GND/REF	SIO-1B CARD, PIN 13, PROF PORT
	DATA IN	3/B	GRN	RS 232	SIO-1B CARD, PIN 3, PROF PORT
	DATA OUT	4/A	WHT	RS 232	SIO-1B CARD, PIN 5, PROF PORT
	ANALOG SIG	5/E	NO CONN		
	POW GND	6/D	BLK	GND/REF	COMMONED TO PIN 2
		6/D	GRY	GND/REF	SIO-1B, PIN 13, SCAN PORT
	DC POW	7/C	WHT	+ 24 VDC	COMMONED TO PIN 1
	DATA OUT	8/A	RED	RS 232	SIO-1B CARD, PIN 5, SCAN PORT
DATA IN	9/B	BLK	RS 232	SIO-1B CARD, PIN 3, SCAN PORT	
ANALOG SIG	10/E	NO CONN			
FORWARD 4 PIN THRU-HULL OUTBRD via FLYING CONN (A,B,C,D)		1 (C)	WHT	SIG +	TURBO PROBE PULSE + (RED)
		2 (B)	BLK	GND/REF	DATASONICS SONAR REF (BLK)
		3 (D)	GRN	GND/REF	TURBO PROBE REF (BLK)
		4 (A)	RED	SIG +	DATASONIC SONAR SIG + (RED)
FORWARD 4 PIN THRU-HULL INBOARD		1 (C)	WHT	SIG +	T PROBE CIRCUIT BOARD T5
		2 (B)	BLK	GND/REF	DATASONICS CIRCUIT BOARD INPUT T1
		3 (D)	GRN	GND/REF	T PROBE CIRCUIT BOARD T6
		4 (A)	RED	SIG +	DATASONICS CIRCUIT BOARD INPUT T4
DATASONICS SONAR TRANS. (FLYING CONN)	SIG+	A	RED	SIG +	TO 4-PIN BULKHEAD CONN
	SIG REF	B	BLK	SIG REF	TO 4-PIN BULKHEAD CONN
DATASONICS SONAR BOARD THERMISTER	INPUT CONN.	4	RED	SIG +	SONAR SIG, via FWARD BULH CONN P4
	INPUT CONN.	1	BLK	SIG REF	SONAR SIG, via FWARD BULH CONN P2
	THERM INPUT		RED		THERMISTER
	THERM INPUT		GRN		THERMISTER
12 PIN	1	BLU/BLK	NO CONN	EXT. KEY INPUT	

2	BLK	POW GND	ANALOG P.S. GND
3	RED/WHT	POW 15 VDC	ANALOG P.S. +15 VDC SUPPLY
4	BLK	ANAL GND	JUMPED TO T2
5	BLK/WHT-RED	NO CONN	ERROR SIG
6	NO CONN		
7	NO CONN		
8	NO CONN		
9	NO CONN		
10	NO CONN		
11	WHT/BLK-RED	SIG +	ICU-2A BRKOUT T13
12	NO CONN		

DEPTH CELL BOARD
DEPTH CELL TRANSD

TURBO PROBE BOARD

	POW	1	no conn		
	GND/REF	2	WHT	POW 24 VDC	FUSE BLK 1 (MASTER RELAY)
	SIG OUT	3	BLK	GND/REF	GNR REF BUSS
	SIG IN	4	WHT	PULSE SIG	TIN BRKOUT T4
	SIG REF	5	WHT	SIG + IMP	PROBE via 4 PIN THR-H T1 + RED (C)
		6	GRN	SIG IMP REF	PROBE via 4 PIN THR-H T3 + BLK (D)

TURBO PROBE TRANSD

	SIG +	WHT IN AUV	RED (C)	+ SIG	TURBO P CARD via FLY CONN + 4 PIN
	SIG REF	GRN IN AUV	BLK (D)	SIG REF	TURBO P CARD via FLY CONN + 4 PIN

GPS RECEIVER
GPS DIFF. RECEIVER
GPS ANTENNA

TIN-1A slot 7
620 HEX (A9,B,3)
INCL. BRKOUT
(INPUT)

10	gate 1	6	YELL	RPH SIG	PT SCREW RPH T3
8	gate 2	3	ORG	RPH SIG	STDD SCREW RPH T3
6	gate 3	4	WHT	RPH SIG	TURBO PROBE T4
4	gate 4	1			
3	gate 5	2			
19	GND	23	GRY	GND	FIN SERVO BOARD, GND
20	GND	24	GRY	GND	FIN SERVO BOARD, GND
1,2	+15 VDC		RED-ORG	POW	TERN 0 SL 5 BRKOUT

TIN-1A slot 8
620 HEX (A9,B,4)
INCL. BRKOUT
(INPUT)

10	gate 1	9	GRN/BLK	RPH sig	F.V. THR RPH T3
8	gate 2	10	VTOL	RPH sig	F.H. THR RPH T3
6	gate 3	7	BLU/WHT	RPH sig	A.V. THR RPH T3
4	gate 4	8	WHT/BLK	RPH sig	A.H. THR RPH T3
3	gate 5	5			
19	GND	23	GRY	GND	FIN SERVO BOARD, GND
20	GND	24	GRY	GND	FIN SERVO BOARD, GND
1,2	+15 VDC		RED-ORG	POW	TERN 0 SL 5 BRKOUT

TIN-1A SLOT 9
640 HEX (A9,8,5)
INCL. BRKOUT
(OUTPUT)
5 VDC INJECTION

7 out 1 11
5 out 2 12
9 out 3 14
11 out 4 13
17,18,19,20
13 out 5 16
17 GNC1 15
19 GND 23
20 GND 24
1,2 +12 VDC

VIOL
YEL
ORG
RED
WHT
GND
GND
POW
GRY
GRY
RED-ORG

CNTRL
CNTRL
CNTRL
CNTRL
5 VDC
FWD TOP FIN, T 1
FWD BOT FIN, T 1
FWD STBD FIN, T 1
FWD PORT FIN, T 1
FIN SERVO INJECTION BOARD

FIN SERVO BOARD, GND
FIN SERVO BOARD, GND
TERM 0 SL 5 BRKOUT

TIN-1A SLOT 10
600 HEX (A9,8,6)
INCL. BRKOUT
(OUTPUT)
5 VDC INJECTION

7 out 1 17
5 out 2 18
9 out 3 20
11 out 4 19
17,18,19,20
13 out 5 22
15 Fout 21
19 GND 23
20 GND 24
25
26
1,2 +12VDC

WHT
BRN
GRN
ORG
WHT
GND/REF
GND/REF
GND/REF
GND/REF
POW
GRY
GRY
RED-ORG

CNTRL
CNTRL
CNTRL
CNTRL
5 VDC
Aft. FIN, Top
Aft. FIN, Bottom
Aft.Fin, STBD
Aft.Fin, Port
FIN SERVO INJECTION BOARD

INTERN GND + FIN SERVO BOARD GND
INTERN GND + FIN SERVO BOARD GND
JUMPED TO T23
JUMPED TO T24
TERM 0 SL 5 BRKOUT

BAC-2B SLOT 11
40 HEX (A5)
INCL BRKOUT
ANALOG SIG. OUT

1 27
2 30
3 29
4 32
5 31
6 34
7 33
8 36
9 35
10 38
11 37
12 40
13 39
14 42
15 41
16 44
17 +15 VDC 43
18 +15 VDC 46
19 -15 VDC 45
20 -15 VDC 48

GREY
RED
GREY
ORG
GREY
BLUE
GREY
BLK
GREY
YEL
GREY
WHT
GND/REF
Ch.1
GND/REF
Ch.2
GND/REF
Ch.3
Ch.4
GND/REF
Ch.4
GND/REF
Ch.6
GND/REF
Ch.7
GND/REF
Ch.8
+15 DC PWR
+15 DC PWR
-15 DC PWR
-15 DC PWR

PORT S SERV T5
PORT S SERV T4
STBD S SERV T5
STBD S SERV T4
F V TH SERV T5
F V TH SERV T4
F H TH SERV T5
F H TH SERV T4
A V TH SERV T5
A V TH SERV T4
A H TH SERV T5
A H TH SERV T4
Internal DC-DC Pwr
" " "
" " "
" " "

ABC-2 (ICU-2B) SLT 6
20 HEX (A4)
INCL BRKOUT
ANALOG INPUTS
DEPTH SIGNAL

CURRENT NON 0
CURRENT NON 1
2
CURRENT NON 3
CURRENT NON 4
CURRENT NON 5
CURRENT NON 6
DEPTH 7

VIOL
BLU
YEL
WHT
BLU
ORG
YEL
ANAL. SIG
ANAL. SIG
ANAL. SIG
ANAL. SIG
ANAL. SIG
ANAL. SIG

PORT SCREW SERVO A T8
STBD SCREW SERVO A T8
F V TH SERVO AMP T8
F H TH SERVO AMP T8
A V TH SERVO AMP T8
A V TH SERVO AMP T8
DEPTH CELL CARD T10

RATE GYRO	PITCH RATE	8	BRN-BLU	ANAL. SIG	Ptch Rate Gyro, PIN D
RATE GYRO	ROLL RATE	9	BLK-BLU	ANAL. SIG	Roll Rate Gyro, PIN D
RATE GYRO	YAW RATE	10	WHT-BLU	ANAL. SIG	Yaw Rate Gyro, PIN D
VERTICAL GYRO	PITCH ANGLE	11	BRN	ANAL. SIG	Ptch Ang. Gyro, PIN F
VERTICAL GYRO	ROLL ANGLE	12	VIOL	ANAL. SIG	Roll Ang. Gyro, PIN K
SOMAR	DATASOMICS	13	WHT/BLK/RED	ANAL. SIG	DATAS SOMAR CARD, T11
	TRIT PRDF?	14			
	TRIT SCANNER?	15			
GND, JUMPED	ANAL/DIG	P2	GREY	GND/REF	AN/DIG GND ANAL P.S.

ADC-1 (ICU-2A), SL 5 10 HEX, ANALOG P.S. INCL. BKOUT DIAGNOSTICS	+15 VDC SUPPLY	0	RED/WHT	ANAL DIAGN	+ 15V TERM ANAL. P.S.
		0	RED/ORG	POW +15VDC	TIM CARDS PIN 1,2 (4)
	-15 VDC SUPPLY	1	RED/BLK	ANAL DIAGN	- 15V TERM ANAL P.S.
	+5 VDC SUPPLY	2	RED	ANAL DIAGN	+ 5V TERM ANAL P.S.
	+10 VDC SUPPLY	3	ORG/RED	ANAL DIAGN	+ 10V TERM ANAL P.S.
	-10VDC SUPPLY	4	ORG/BLK	ANAL DIAGN	- 10V TERM ANAL P.S.
		5			
		6			
		7			
		8			
	9				
	10				
		P2	GREY	GND/REF	AN/DIG GND ANAL P.S.

PIA-3A, 80 HEX, SL 4 TTL INPUTS P2 VIA1 INCL. BKOUT	1	+12	not conn	NC			
	2	-12	not conn	02			
	3	+5		01	WHT	+ 5VDC	TO SERVO AMP INVERTOR CHIP
	4	+5		04			
	5	GND		03	WHT/RED	DIG GND	FROM FR GYRO PIN 9
				03	WHT	DIG GND	TO SERVO AMP INVERTOR CHIP
	6	GND		06			
	7	CB2		05			
	8	CA2		08			
	9	CB1		07			
	10	CA1		10			
	11	PB7		09			
	12	PA7		12			
	13	PA6		11			
	14	PA6		14			
	15	PB5		13			
	16	PA5		16			
	17	PA4		15			
	18	PA4		18			
	19	PB3		17			
	20	PA3		20			
	21	PB2		19			
	22	PA2		22			
	23	PB1		21			
	24	PA1		24			
	25	PB0		23	grn	TTL LO/TRUE	FREE BY D825, PIN 8
26	PA0		26	wht	TTL LO/TRUE	FREE GR D825, PIN 15	

PIA-2A can't, slot 4	1 +12	Not conn			
TTL OUTPUTS P2 V200	2 -12	Not conn			
INCL BRKOUT	3 +5		28		
	4 +5		27		
	5 GND		30		
	6 GND		29		
	7 CDE		32		
	8 CA21		31		
	9 CA1		34		
	10 CA1		33		
	11 PB7		36		
P.S. ON/OFF	12 PA7 +/- 13V		35	wht	TTL HI/TRU ANAL P.S. T P2-1
	13 PB6		38		
P.S. ON/OFF	14 PA6 + 3V		37	wht/brn	TTL HI/TRU ANAL P.S. T P1-3
	15 PB5		40		
THRUSTER SERVO INHIBIT	16 PA5 A.H.Thr		39	wht-39	TTL INIT HI INVERTER BOARD T 8
	17 PB4		42		
THRUSTER SERVO INHIBIT	18 PA4 A.V.Thr		41	wht-41	TTL INIT HI INVERTER BRD T 6
	19 PB3		44		
THRUSTER SERVO INHIBIT	20 PA3 F.H.Thr		43	wht-43	TTL INIT HI INV BRD T 45
TRITEC SONAR ON/OFF	21 PB2 Trittech		46	green	TTL LO/TRU ANAL P.S. P10-1
THRUSTER SERVO INHIBIT	22 PA2 F.V.Thr		45	wht-45	TTL INIT HI INV BRD T 2
FREE GYRO	23 PB1 Uncage		48	grn/blk	TTL LO/TRU ANAL P.S. P10-2
SCREW SERVO INHIBIT	24 PA1 Stb Screw		47	wht-47	TTL INIT HI INV BRD T 17
FREE GYRO	25 PB0 Cage		50	grn/wht	TTL LO/TRU ANAL P.S. P10-3
SCREW SERVO INHIBIT	26 PA0 Port screw		49	wht-49	TTL INIT HI INV BRD T 15

TTL INVERTER FOR
PIA-3A TTL OUTPUTS
TO SERVO AMPS

A.H. THR INHIB	T39	8-12	ORG	TTL LO/TRU	A.H.TH SERVO AMP T-11
A.V. THR INHIB	T41	6-14	GRN	TTL LO/TRU	A.V.TH SERVO AMP T-11
F.H. THR INHIB	T43	4-16	YEL	TTL LO/TRU	F.H.TH SERVO AMP T-11
F.V. THR INHIB	T45	2-18	BRN	TTL LO/TRU	F.V.TH SERVO AMP T-11
STB SCREW INHIB	T47	17-3	VIOLE	TTL LO/TRU	STB SCRW SERV AMP T11
PRT SCREW INHIB	T49	15-5	BLUE	TTL LO/TRU	PT SCRW SERVO AMP T11
+5VDC PMR, BRKOUT	T1	1,10,19	WHT	PMR	PIA-3A BRKOUT T1
GND, PIA BRKOUT	T3	20	WHT	DIG GND	PIA-3A BRKOUT T3

WFI-1 address 700 hex slot (A9,8,7) slot 12

NO BRKOUT, DIRECT FLAT RIBBON CONN.

ASSIGN ON 24 PIN CONN. ON WFI-1 BOARD FROM SYNCHRO DEMOD.

All signals to/from P2 to Synchro to Digital Board from DG

P2	Function	Signal	P2	Function	Signal
1	+12		2	-12	
3	+5		4	+5	
5	GND		6	GND	
7	CDE		8	CA2	
9	CA1		10	CA1	
11	PB7	Not Inhibit	12	PB7	Bit 7
13	PB6	Busy	14	PA6	Bit 6
15	PB5	Bit 13	16	PA5	Bit 5
17	PB4	Bit 12	18	PA4	Bit 4
19	PB3	Bit 11	20	PA3	Bit 3
21	PB2	Bit 10	22	PA2	Bit 2
23	PB1	Bit 9	24	PA1	Bit 1
25	PB0	Bit 8	26	PA0	Bit 0
27	No connection		28	No connection	
29	Timer Gate	NC	30	Timer Gate	NC

26	:	Out1	NC	32	:	Get1	NC
28	:	Out2	NC	34	:	Cate2	NC

WFI-1 con't, slot 12 CTR 10 pin conn. 009 RS232 conn. NO BREAKOUT, DIRECT CONN	GND	PIN 1	RIB-GRN	GND	THRU-HULL 02, WMT
	NC	PIN 2			
	TID	PIN 3	RIB-ORG	CONN	THRU-HULL 02, GRN
	NC	PIN 4			
	RIB	PIN 5	RIB-BRN	CONN	THRU-HULL 02, BLK
	BTR	PIN 6			
	RTS	PIN 7			
	DCD	PIN 8			
	CTS	PIN 9			
	NC	PIN 10			

BESS10-10 BOARD RS232, TRITECH PROFILER	DATA IN	PIN 3	RIBGN, ORG	RS 232	10 PIN FWARD THRU-HULL CONN, PIN 3
	DATA OUT	PIN 5	RIB, GRN	RS 232	10 PIN FWARD THRU-HULL CONN, PIN 4
	GND/REF	PIN 13	RIB, ORG	RS 232	10 PIN FWARD THRU-HULL CONN, PIN 2
RS 232, TRITECH SCANNER	DATA IN	PIN 3	RIB, ORG	RS 232	10 PIN FWARD THRU-HULL CONN, PIN 9
	DATA OUT	PIN 5	RIB, GRN	RS 232	10 PIN FWARD THRU-HULL CONN, PIN 8
	GND/REF	PIN 13	RIB, ORG	RS 232	10 PIN FWARD THRU-HULL CONN, PIN 6

APPENDIX C CENTER OF GRAVITY CALCULATION

The calculation of the center of gravity for the AUV is provided on the following page.

For each item shown, the location of its individual center of gravity, relative to the X and Y datum, is listed, along with its weight and first moments in the X and Y directions. The location of the center of gravity is shown at the bottom of the page.

BUOYANCY TEST 02/04/94

ITEM	Xin	Yin	Wt(lb)	Mx	My
FWD VERT THRUSTER ASSY	14.0	10.0	5.0	70.0	50.0
FWD HORIZ. THRUSTER ASSY	6.3	7.0	5.5	34.4	38.5
AFT VERT. THRUSTER ASSY	49.0	8.5	5.0	245.0	42.5
AFT HORIZ THRUSTER ASSY	56.0	6.5	5.5	308.0	35.8
MASTER RELAY	10.0	11.0	0.5	5.0	5.5
BATT. COMPUTER, ANALOG, 2 FWD	20.5	8.0	54.0	1107.0	432.0
BATT. MOTORS, SONAR, 2 AFT	41.8	7.6	54.0	2254.5	410.4
BILGE PLATES, 2 FWD	9.5	8.0	3.2	30.4	25.6
BILGE PLATES, 2 MID	31.3	7.8	4.0	123.4	30.8
BILGE PLATES, 2 AFT	50.0	7.6	2.5	125.0	19.0
HULL 8 SERVOS, MPROP, 4 PLATES	33.3	7.9	150.6	5007.4	1189.7
NOSE, EMPTY LESS 1LB BUOY.	-7.5	8.0	1.3	-9.8	10.4
FINS, 8, META CENTER AT CG	31.3	7.8	5.1	159.4	39.8
THRUSTER P.S., 4 Midship	31.3	8.0	6.4	200.0	51.2
MAIN PROP P.S., 2 fwd	14.5	8.0	3.2	46.4	25.6
COMPUTER/ANALOG P.S. (2)	21.0	8.0	4.2	88.2	33.6
VERT. GYRO w/BRACKET	14.0	13.0	2.0	28.0	26.0
RATE GYRO(s)	13.0	3.0	3.9	50.7	11.7
FREE GYRO + MOUNT	49.0	2.3	3.3	159.3	7.5
INVERTER FOR F. GYRO	47.5	12.8	1.4	66.5	17.9
NUT PLATE	33.0	7.8	4.5	148.5	35.1
OS 9 CAGE (right)	31.3	5.0	4.2	129.7	20.8
OS 9 CARDS (0.45lb x) 12	31.3	5.0	5.4	168.8	27.0
486 CAGE (left) -lead	31.3	10.0	3.6	114.1	36.5
486 CARDS (0.45lb x) 3 -lead	31.3	10.0	1.4	42.2	13.5
RIBBON CABLE INTERFACE (4)	41.0	7.8	1.5	61.5	11.7
TURBO-PROBE INCL. MOUNT	-2.0	4.0	3.4	-6.8	13.6
WIRING, MISC.	31.3	7.8	3.0	93.8	23.4
DIFF. GPS REC.+ANT. (0.9LBS)			0.0	0.0	0.0
GPS RECEIVER				0.0	0.0
GPS ANTENNA + MOUNT	10.5	4.5	1.0	10.5	4.5
TOPSIDE THRU-HULLS	14.0	8.0	3.0	42.0	24.0
T725 SCANNING SONAR	-8.0	10.0	2.6	-20.8	26.0
T1000 PROFILING SONAR	-5.0	10.0	2.6	-13.0	26.0
TRITECH SONAR MOUNT, WIRES	-7.0	10.0	3.0	-21.0	30.0
DATASONICS SONAR + MOUNT, WIRE	-4.0	6.0	2.4	-9.6	14.4
BUOYANCY, SONARS	-6.0	9.5	-2.0	12.0	-19.0
BUOYANCY, SUPP'S, T PROBE	-4.0	8.0	-0.6	2.4	-4.8
TRIM LEAD by F.GYRO INV.	51.0	12.8	4.5	229.5	57.6
TRIM LEAD, aft	63.0	8.3	5.9	371.7	49.0
TRIM LEAD, aft of computers	38.0	7.8	8.9	338.2	69.4
TRIM LEAD	51.0	4.0	5.0	255.0	20.0
TRIM LEAD, fwd of computers	24.5	6.5	4.4	107.8	28.6
TRIM LEAD, tweak	38.0	8.3	0.3	13.3	2.9

TOTALS lbs-TOT 388.5 12155.2 3010.7

C.G., X,Y INCHES FROM DATUM 31.29 7.75
 EST. RESERVE BUOYANCY (FRESH) - LBS. 0.5

NOTE: X DATUM IS FORWARD OUTER HULL EDGE, POSITIVE AFT
 Y DATUM IS INNER STBD HULL SIDE, POSITIVE TO PORT
 DRY C.G.(in) X,Y 31.25, 7.75

APPENDIX D CENTER OF BUOYANCY CALCULATION

The calculation of the center of buoyancy for the AUV is provided on the following page.

For each item shown, the location of its individual center of gravity, relative to the X, Y and Z datum, is listed, along with its weight and first moment in the Z direction. The location of the center of buoyancy is shown at the bottom of the page.

ITEM	Xin	Yin	Zin	Wt(lb)	Mz
FWD VERT THRUSTER ASSY	14.0	10.0	4.8	5.0	23.8
FWD HORIZ. THRUSTER ASSY	6.3	7.0	4.8	5.5	26.1
AFT VERT. THRUSTER ASSY	48.0	8.5	4.8	5.0	23.8
AFT HORIZ THRUSTER ASSY	56.0	6.5	4.8	5.5	26.1
MASTER RELAY	10.0	11.0	1.0	0.5	0.5
NUT PLATE	33.0	7.8	9.5	4.5	42.8
DIFF GPS REC.+ ANT					0.0
GPS RECEIVER	0.0	0.0	0.0	0.0	0.0
GPS ANTENNA, MOUNT, WIRING	10.5	4.5	13.0	1.0	13.0
BATT. COMPUTER, ANALOG, 2 FWD	20.5	8.0	3.5	54.0	189.0
BATT. MOTORS, SONAR, 2 AFT	41.8	7.6	3.5	54.0	189.0
BILGE PLATES, 2 FWD	9.5	8.0	0.4	3.2	1.3
BILGE PLATES, 2 MID	31.3	7.8	0.4	4.0	1.6
BILGE PLATES, 2 AFT	50.0	7.6	0.4	2.5	1.0
HULL 8 SERVOS, MPROP, 4 PLATES	33.3	7.9	4.8	150.6	715.4
NOSE, EMPTY, less 1 lb. buoy	-7.5	8.0	4.8	1.3	6.2
FINS, 8, META CENTER AT CG	31.3	7.8	4.8	5.1	24.2
THRUSTER P.S., 4 midship	31.3	8.0	4.5	6.4	28.8
MAIN PROP P.S., 2 fwd	14.5	8.0	4.5	3.2	14.4
COMPUTER/ANALOG P.S. (2)	21.0	8.0	8.0	4.2	33.6
VERT. GYRO w/BRACKET	14.0	13.0	3.0	2.0	6.0
RATE GYRO(s)	13.0	3.0	2.5	3.9	9.8
FREE GYRO + MOUNT	49.0	2.3	4.0	3.3	13.0
INVERTER FOR D.G.	47.5	12.8	3.0	1.4	4.2
TOPSIDE THRU-HULLS	14.0	8.0	10.0	3.0	30.0
OS 9 CAGE (right)	31.3	5.0	5.5	4.2	22.8
OS 9 CARDS (@.4 lb x) 12	31.3	5.0	5.5	5.4	29.7
486 CAGE (left)	31.3	10.0	5.5	3.6	20.1
486 CARDS (@.4 lb x) 3	31.3	10.0	5.5	1.4	7.4
RIBBON CABLE INTERFACE (4)	41.0	7.8	7.0	1.5	10.5
WIRING, MISC.	31.3	7.8	8.0	3.0	24.0
TURBO-PROBE INCL. MOUNT	-2.0	4.0	4.0	3.4	13.6
DATASONICS SONAR, MOUNT, WIRES	-4.0	6.0	2.5	2.4	6.0
T725 SCANNING SONAR	-8.0	10.0	5.5	2.6	14.3
T1000 PROFILING SONAR	-5.0	10.0	5.5	2.6	14.3
TRITECH SONAR MOUNT, WIRES	-7.0	10.0	5.5	3.0	16.5
BUOYANCY, SONARS	-6.0	9.5	5.5	-2.0	-11.0
BUOYANCY, SUPP'S, T-PROBE	-4.0	8.0	5.0	-0.6	-3.0
					0.0
TRIM LEAD, by fr gyro inv	51.0	12.8	1.0	4.5	4.5
TRIM LEAD, AFT	63.0	8.3	3.0	5.9	17.7
TRIM LEAD, aft of computer	38.0	7.8	2.5	7.2	18.0
TRIM LEAD, by fr gyro	51.0	4.0	1.0	5.0	5.0
TRIM LEAD, forw of computer	24.5	6.5	2.5	6.1	15.3
TRIM LEAD, tweak	38.0	8.3	8.0	0.3	2.8

TOTALS

lbs-TOT

388.5

1651.8

BG=CTR-BUOYz - CGz, INCHES

0.50

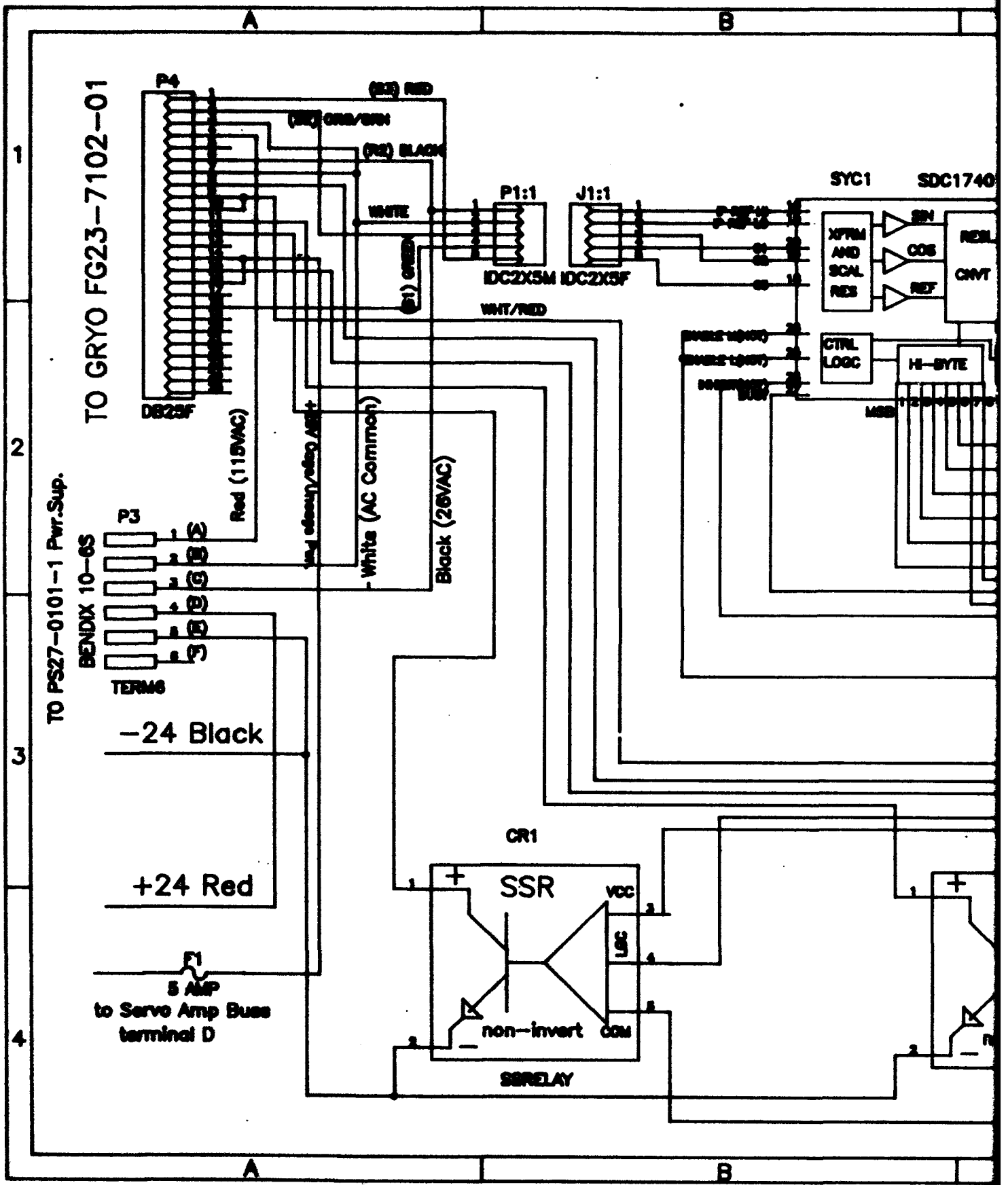
RESERVE BUOYANCY (FRESH) LBS.-est.

0.5

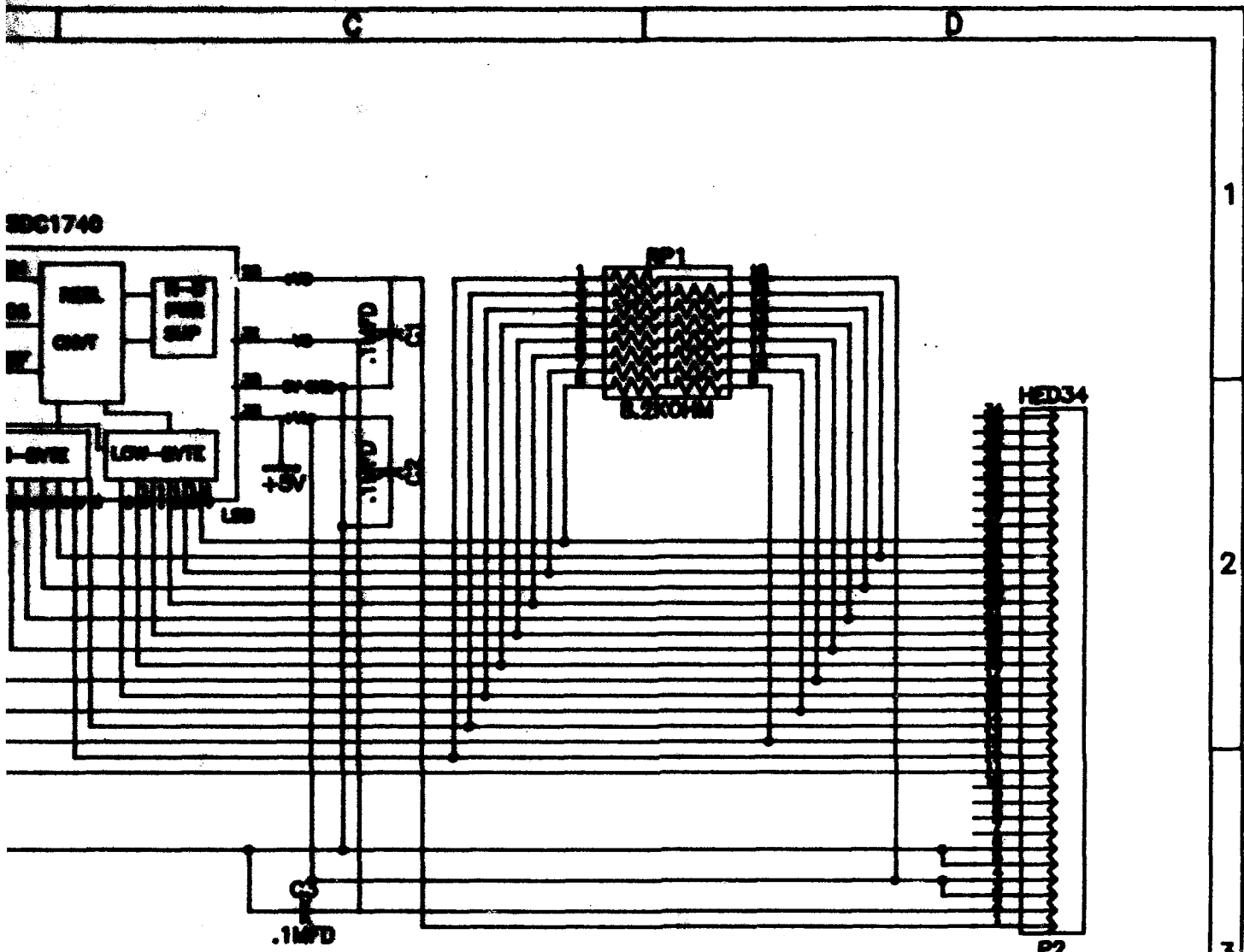
NOTE: X DATUM IS FORWARD OUTER HULL EDGE, POSITIVE AFT
 Y DATUM IS INNER STBD HULL SIDE, POSITIVE TO PORT
 Z DATUM IS INNER HULL BOTTOM, POSITIVE UP
 CTR-BUOY(in) X,Y,Z 31.25, 7.75, 4.75

APPENDIX E FREE GYROSYNCHRO BOARD WIRING DIAGRAM

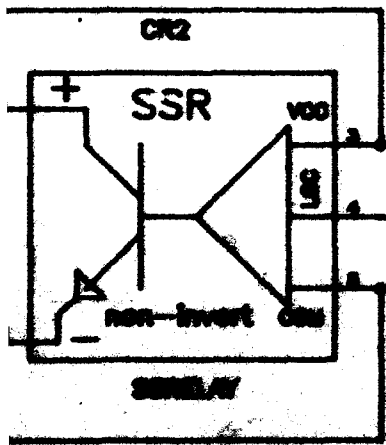
The wiring diagram for the free directional gyro and the synchro to digital converter is provided on the following page.



A



- Digital Ground PIA Terminal 3
- Uncege indicate Lo True PIA Terminal 23
- Cege indicate Lo True PIA Terminal 28
- Cege Control Lo True PIA Terminal 50
- VCC +5V
- Uncege Control Lo True PIA Terminal 48
- COMMON (Digital Ground)



Title: SYNCRO BOARD/DG SYSTEM		
Shee	Number	Rev
B	Design: T. Christian	2.0
Date: August 11, 1984	Drawn by: T. Christian	Sheet 1 of 1

B

108

APPENDIX F KALMAN FILTER SUBPROGRAM

The subprogram for the Kalman filter, in C source code, is provided on the following pages. Velocity and acceleration data is obtained by extracting an estimate of the derivative, and second derivative, of sonar range data using the subprogram. The filter also provides a smooth position estimate.

```
/* KALMAN FILTER FOR SONAR RANGE */
Kalman(yk,xk_0,xk_1,xk_2)
```

```
double yk,*xk_0,*xk_1,*xk_2;
```

```
double xk1_0,xk1_1,xk1_2;
double phiI[3][3],h[3],b[3],lk[3],res,q,rv;
```

```
/* a=[0 1 0;0 0 1;0 0 0]; phiI=expm(a*0.1); where dt = 0.1 */
b[0] = 0.0;
b[1] = 0.0;
b[2] = 1.0;
```

```
/* phiI = [1.0    0.1    0.005
           0.0    1.0    0.1
           0.0    0.0    1.0] */
```

```
phiI[0][0] = 1.0;
phiI[0][1] = 0.1;
phiI[0][2] = 0.005;
phiI[1][0] = 0.0;
phiI[1][1] = 1.0;
phiI[1][2] = 0.1;
phiI[2][0] = 0.0;
phiI[2][1] = 0.0;
phiI[2][2] = 1.0;
```

```
rv = 0.1;
q = 0.01;
/*thres = 2.0; Global Now */
```

```
/* h = [1 0 0]; */
h[0] = 1.0;
h[1] = 0.0;
h[2] = 0.0;
```

```
if(kal_init == 1)
{
    *xk_0 = yk;
    *xk_1 = 0.0;
    *xk_2 = 0.0;
```

```
/* xk1=xk; */
xk1_0 = *xk_0;
xk1_1 = *xk_1;
xk1_2 = *xk_2;
}
```

```
/* set lk = const. */
lk[0] = 0.2544;
lk[1] = 0.3727;
lk[2] = 0.2731;
```

```

/* xk1(:,i)=phi1*xk(:,i); */
xk1_0 = phi1[0][0]*(*xk_0) + phi1[0][1]*(*xk_1) + phi1[0][2]*(*xk_2);
xk1_1 = phi1[1][0]*(*xk_0) + phi1[1][1]*(*xk_1) + phi1[1][2]*(*xk_2);
xk1_2 = phi1[2][0]*(*xk_0) + phi1[2][1]*(*xk_1) + phi1[2][2]*(*xk_2);

/* res=(yk(i)-h*xk1(:,i)); */
res = yk - (h[0]*xk1_0 + h[1]*xk1_1 + h[2]*xk1_2);

/* Set res = 0.0 if larger than threshold */
if(fabs(res) > thres)
{
    res = 0.0;
}

/*xk(:,i+1)=xk1(:,i) + lk*res; */
*xk_0 = xk1_0 + lk[0]*res;
*xk_1 = xk1_1 + lk[1]*res;
*xk_2 = xk1_2 + lk[2]*res;

```

APPENDIX G AUV SIMULATION MODEL

The program, in MATLAB source code, which simulates the AUV maneuvering in a horizontal plane is provided on the following pages.

AUV SIMULATION MODEL: MANEUVERING IN HORIZONTAL PLANE

clear;

LOAD DATA FROM TEST

**load ser1256;
load d1256;
s = ser1256;
h = d1256;
NP = 800;
dt = 0.1;
t = [0:dt:dt*NP];**

DERIV OF YAW;

**hd(1) = (h(2,2)-h(1,2))/0.1;
for I = 2:NP,
 hd(I) = (h(I+1,2)-h(I-1,2))/0.2;
end;**

FIND SCALE AND BIAS

**hr = h(1:NP,3)';
P = polyfit(hr,hd,1);**

INIT CONDS

**Xs(1) = 0.0;
Ys(1) = s(1,3);
u(1) = 0.0;
v(1) = 0.0;
r(1) = h(1,3);
rdot = 0.0;
Ydots(1) = 0.0;
Xdot(1) = 0.0;
GF = pi; % for RW, FW, GF = pi;
PSI(1) = GF+h(1,2);**

POSITION ORDERS

**PSIcom = GF*180/pi-0.0; % give PSIcom in degrees
Xcom = 0.0;
Ycom = 4.0;**

CONTROL LAW GAINS

**RW = -1.0; % for RW, RW = -1.0;
FW = 1.0; % for FW, FW = -1.0;
Kpsi = 80.0;
Tdr = 1.0;
Kr = Kpsi*Tdr;
Kx = 0.0; % for YAW, LAT test, Kx = 0.0;
Tdx = 3.0;
Ku = Kx*Tdx;
Ky = 12.0; % for YAW, LONG test, Ky = 0.0;
Tdy = 3.0;
Kv = Ky*Tdy;**

AVV DIMENSIONS

```
NMV = 24.0;
NSF = 5.0;
TF = 2.0;
a = 13.52;
DF = 23.0/12.0;
Xg = 0.125/12.0;
xs = 3.0;
X(1) = Xs(1)-xs*cos(PSI(1));
Y(1) = Ys(1)-xs*sin(PSI(1));
Ydot(1) = Ydots(1)-xs*r(1);
```

HYDRODYNAMIC COEFFS;

```
Xuu = -3.0;
Xudot = -0.06*377.67;
Yvv = -0.5*51.72;
Yrr = 0.01187*377.67;
Yvdot = -0.04*377.67;
Yrdot = -0.00178*2756.81;
Nvv = -0.00769*377.67;
Nrr = -0.04*2756.81;
Nvdot = -0.001*2756.81;
IssNrdot = 45.0-(-0.002*20137.50);
```

for I = 1:NP,

CALCULATE VOLTAGES

```
VPTH(I) = -(Kpsi*(PSI(I)-PSIcom*pi/180)+Kr*r(I)...
           +RW*(Ky*(Ys(I)-Ycom)+Kv*Ydot(I)));
if VPTH(I) > NMV, VPTH(I) = NMV; end;
if VPTH(I) < -NMV, VPTH(I) = -NMV; end;
```

```
VATH(I) = (Kpsi*(PSI(I)-PSIcom*pi/180)+Kr*r(I)...
           -RW*(Ky*(Ys(I)-Ycom)+Kv*Ydot(I)));
if VATH(I) > NMV, VATH(I) = NMV; end;
if VATH(I) < -NMV, VATH(I) = -NMV; end;
```

```
VLS(I) = -FW*(Kx*(Xs(I)-Xcom)+Ku*Xdot(I));
if VLS(I) > NMV, VLS(I) = NMV; end;
if VLS(I) < -NMV, VLS(I) = -NMV; end;
```

```
VRS(I) = -FW*(Kx*(Xs(I)-Xcom)+Ku*Xdot(I));
if VRS(I) > NMV, VRS(I) = NMV; end;
if VRS(I) < -NMV, VRS(I) = -NMV; end;
```

CALCULATE FORCES

```
FPTH(I) = TF/(NMV^2)*VPTH(I)*abs(VPTH(I));
FATH(I) = TF/(NMV^2)*VATH(I)*abs(VATH(I));
FTTH(I) = FPTH(I)+FATH(I);
MTH(I) = (FPTH(I)-FATH(I))*DF;
FLS(I) = NSF/(NMV^2)*VLS(I)*abs(VLS(I));
FRS(I) = NSF/(NMV^2)*VRS(I)*abs(VRS(I));
```

EQUATIONS OF MOTION

```
udot = (m*v(I)*r(I)+Xuu*u(I)*abs(u(I))...  
        +PLS(I)+PRS(I))/(m-Xudot);  
vdot = (Yvv*v(I)*abs(v(I))+Yrr*r(I)*abs(r(I))-m*u(I)*r(I)...  
        +Yrdot*rdot+PTH(I))/(m-Yvdot);  
rdot = (Nvdot*vdot+Nvv*v(I)*abs(v(I))+Nrr*r(I)*abs(r(I))...  
        +NTH(I))/(IssNrdot);  
Xdot(I+1) = u(I)*cos(PHI(I))-v(I)*sin(PHI(I));  
Ydot(I+1) = u(I)*sin(PHI(I))+v(I)*cos(PHI(I));  
Ydots(I+1) = Ydot(I+1)+xs*r(I);
```

EULER INTEGRATION

```
u(I+1) = u(I)+udot*dt;  
v(I+1) = v(I)+vdot*dt;  
r(I+1) = r(I)+rdot*dt;  
PHI(I+1) = PHI(I)+r(I)*dt;  
X(I+1) = X(I)+Xdot(I+1)*dt;  
Y(I+1) = Y(I)+Ydot(I+1)*dt;  
Xs(I+1) = X(I+1)+xs*cos(PHI(I+1));  
Ys(I+1) = Y(I+1)+xs*sin(PHI(I+1));
```

end

LIST OF REFERENCES

Brown, J. P., "Four Quadrant Dynamic Model of the AUV II Thruster," Master's Thesis, Naval Postgraduate School, Monterey, California, September 1988.

Cody, S. E., "An Experimental Study of the Response of Small Tunnel Thrusters to Triangular and Square Wave Inputs," Master's Thesis, Naval Postgraduate School, Monterey, California, December 1992.

Good, M. R., "Design and Construction of a Second Generation Autonomous Underwater Vehicle," Master's Thesis, Naval Postgraduate School, Monterey, California, December 1989.

Healey, A. J., Marco, D. B., "Experimental Verification of Mission Planning by Autonomous Mission Execution and Data Visualization using the NPS AUV II," *Proceedings of the IEEE Oceanic Engineering Society Symposium on Autonomous Underwater Vehicles*, AUV-92 Washington, D. C., June 1992.

Ingold, B. W., "Key Feature Identification from Image Profile Segments using a High Frequency Sonar," Master's Thesis, Naval Postgraduate School, Monterey, California, December 1992.

Marco, D. B., Doctoral Dissertation, Naval Postgraduate School, Monterey, California, forthcoming.

Saunders, T. E., "Performance of Small Thrusters and Propulsion Systems," Master's Thesis, Naval Postgraduate School, Monterey, California, March 1990.

Warner, D. C., "Design, Simulation and Experimental Verification of a Computer Model and Enhanced Position Estimator for the NPS AUV II," Master's Thesis, Naval Postgraduate School, Monterey, California, December 1991.

INITIAL DISTRIBUTION LIST

- | | | |
|-----------|--|----------|
| 1. | Defense Technical Information Center
Cameron Station
Alexandria, VA 22304-6145 | 2 |
| 2. | Library, Code 53
Naval Postgraduate School
Monterey, CA 93943-5002 | 2 |
| 3. | Chairman, Code ME/KK
Department of Mechanical Engineering
Naval Postgraduate School
Monterey, CA 93943-5000 | 1 |
| 4. | Dr. Anthony J. Healey, Code ME/HY
Department of Mechanical Engineering
Naval Postgraduate School
Monterey, CA 93943-5000 | 1 |
| 5. | Naval Engineering Curricular Office, Code 34
Naval Postgraduate School
Monterey, CA 93943-5000 | 1 |
| 6. | Donald P. Brutzman, LCDR, USN, Code OR/BR
Department of Operations Research
Naval Postgraduate School
Monterey, CA 93943-5000 | 1 |
| 7. | Mr. Chris O'Donnell
Commander, Naval Explosive Ordnance Disposal
Technology Division
Indian Head, MD 20640-5070 | 1 |

8. **Charles N. Calvano, CAPT, USN (Ret), Code ME/CA** 1
Department of Mechanical Engineering
Naval Postgraduate School
Monterey, CA 93943-5000

9. **Walter A. Ericson, CAPT, USN (Ret)** 1
9980 Cummins Place
San Diego, CA 92131

10. **Richard E. Pearsall, CAPT, USN (Ret)** 1
1228 Sotheby Court
Virginia Beach, VA 23464

11. **David E. Woodbury, CAPT, USN (Ret)** 1
7126 Red Horse Tavern Lane
Springfield, VA 22153

12. **Kevin A. Torsiello, LT, USN** 1
Operations Department, Code 300
Norfolk Naval Shipyard
Portsmouth, VA 23709-5000